

**AN INVESTIGATION INTO THE INTRODUCTION OF
PROCESS ANALYTICAL TECHNOLOGY, USING NEAR
INFRARED ANALYSIS, TO SELECTED
PHARMACEUTICAL PROCESSES**

K. Naicker

**AN INVESTIGATION INTO THE INTRODUCTION OF PROCESS
ANALYTICAL TECHNOLOGY, USING NEAR INFRARED ANALYSIS, TO
SELECTED PHARMACEUTICAL PROCESSES**

K. Naicker

**Submitted in fulfilment of
the requirements for the degree of**

MAGISTER SCIENTIAE

in the

FACULTY OF HEALTH SCIENCES

at the

NELSON MANDELA METROPOLITAN UNIVERSITY

November 2006

Supervisor: Mr G. Kilian

Co-Supervisor: Dr J. Olivier

DECLARATION

I hereby declare that the work on which this dissertation is based is original (except where acknowledgements have been made) and that neither the whole work nor any part thereof has been, is being, or is to be submitted for another degree at this or any other university.

K Naicker

On this _____ day of _____ at the University of Port Elizabeth.

TABLE OF CONTENTS

Table of contents	i
Acknowledgements	v
List of key abbreviations	vi
List of figures	vii
List of tables	x
Summary	xi
Chapter 1	1
1. Introduction to the study	1
1.1 Background to the study	1
1.2 Motivation for the study	1
1.3 Aim and objectives	2
1.3.1 Aim	2
1.3.2 Objectives	2
Chapter 2	3
2. Literature review	3
2.1 Process analytical technology (PAT)	3
2.1.1 Definition of PAT	3
2.1.2 Drug quality	3
2.1.3 Tools available for PAT implementation	4
2.1.4 PAT and risk analysis	6
2.1.5 Selecting a process analytical technology	7
2.2 Near infrared spectroscopy (NIR) as a PAT tool	8
2.2.1 Background to infrared spectroscopy	8
2.2.2 Theory and principles of NIR spectroscopy	9
2.2.3 Measurements	12
2.2.4 Factors affecting spectral response	13
2.2.5 Instrumentation	13
2.2.6 NIR as a PAT initiative	16
2.3 NIR application to selected processes	16
2.3.1 Incoming raw material analysis	16
2.3.2 Blend Uniformity	18

2.3.3	Granule moisture determination	21
2.4	Summary	25
Chapter 3		26
3.	Incoming raw material analysis	26
3.1	Introduction	26
3.2	NIR instrument	27
3.2.1	Rapid Content TM Analyzer Hardware	27
3.2.2	Rapid Content TM Analyzer Software	28
3.2.3	Instrument Diagnostics	29
3.3	Methodology	31
3.3.1	Overview of methodology	31
3.3.2	Materials used	32
3.3.3	Sample selection for library calibration	32
3.3.4	External library validation (positive and negative challenges)	33
3.3.5	Experimental	33
3.3.6	Data analysis	34
3.4	NIR method development	35
3.4.1	Visual inspection and mathematical pre-treatment of spectra	35
3.4.2	Library calibration	42
3.4.3	Qualification of products	51
3.4.4	Identification method	51
3.4.5	Internal validation	52
3.4.6	Positive challenge	53
3.4.7	Negative challenge	53
3.4.8	Robustness	56
3.5	Discussion	57
3.6	Summary	58
Chapter 4		60
4.	Blend uniformity analysis	60
4.1	Introduction	60
4.2	Equipment	61
4.3	Methodology	62
4.3.1	Materials used	62

4.3.2	Software method development for blend monitoring	63
4.3.3	Spectral data from blends	64
4.3.4	Methods of sampling and analysis	65
4.3.5	Analytical methods	66
4.3.6	Statistical analysis	68
4.3.7	Experimental	68
4.4	Results and discussion	70
4.4.1	Lactose monohydrate and magnesium stearate blends	70
4.4.1.1	Software method	70
4.4.1.2	Lactose monohydrate and magnesium stearate blends conducted	73
4.4.2	Ridaq® granule and magnesium stearate blends	80
4.4.2.1	Software method	80
4.4.2.2	Ridaq® granule and magnesium stearate blends conducted	84
4.5	Summary	94
Chapter 5		95
5.	Moisture determination in the fluid bed dryer	95
5.1	Introduction	95
5.2	Product temperature as a monitoring tool	95
5.3	Near infrared as a monitoring tool	99
5.4	Statistical evaluation of moisture values	101
5.4.1	Statistical evaluation of Product A	102
5.4.2	Statistical evaluation of Product B	103
5.5	Summary	104
Chapter 6		106
6.	Conclusion and recommendations	106
6.1	Raw material identification and qualification	106
6.2	Blend uniformity analysis	107
6.3	Moisture determination in the FBD	108
6.4	PAT implementation – The way forward	109
Reference list		112

Appendices		
Appendix A	Raw material analysis	119
	A.1 Spectral library validation report	120
	A.2 Positive challenge - starch maize	121
	A.3 Positive challenge - lactose monohydrate	122
	A.4 Negative challenge - pregelatinised starch	123
	A.5 Negative challenge – tablettose	124
Appendix B	Moisture determination in the fluid bed dryer	125
	B.1 Moisture values for Product A	126
	B.2 Moisture values for Product B	127
	B.3 Example of recipe used for the drying of product in the FBD	128
Appendix C	Concept Article	134

ACKNOWLEDGEMENTS

I extend my sincere appreciation and thanks to the following people and institutions:

- My supervisors, Dr Johan Olivier and Mr Gareth Kilian for their support, assistance and encouragement during the year.
- Aspen Pharmacare for allowing me the use of their analytical equipment as well as providing the materials and equipment to conduct the experimentation.
- The technical transfer department of Aspen Pharmacare for their assistance.
- The Nelson Mandela Metropolitan University for the opportunity to fulfil a lifelong ambition.
- A special thank you to my husband Diren and my family for their unconditional love, support and encouragement.

“Dedicated to my spiritual guide – Sri Sathya Sai Baba for divine inspiration”

LIST OF KEY ABBREVIATIONS

AA	Atomic Absorption
CE	Capillary Electrophoresis
CDER	Centre for Drug Evaluation and Research
CFR	Code of Federal Regulations
CVM	Centre for Veterinary Medicine
DCM	Data collection Method
EMC	Equilibrium moisture content
FBD	Fluid bed dryer
GC	Gas Chromatography
HPLC	High Performance Liquid Chromatography
IBC	Intermediate Bulk Container
IR	Infrared
LCL	Lower control Limit
LIF	Light induced Fluorescence
MCC	Medicines Control Council
MHRA	Medicines and Healthcare Regulatory Authority
NIR	Near infrared
NMR	Nuclear Magnetic Resonance
ORA	Office of Regulatory Affairs
PAT	Process analytical technology
PC	Principle Components
RCA	Rapid Content TM Analyser
RSD	Relative Standard Deviation
rpm	revolutions per minute
SD	Standard Deviation
UCL	Upper control Limit
US DHHS	United States Department of Health and Human services
US FDA	United States Food and Drug Administration
UV	Ultraviolet
XDS	Off-axis digital synchronous

LIST OF FIGURES

2.1	Second derivative of starch maize showing overtones and combination bands	10
2.2	Three common forms of assessing NIR data from varied samples	13
2.3	Schematic representation of a filter-based spectrometer	14
2.4	Schematic representation of a scanning grating based spectrometer	14
2.5	Schematic representation of an interference-type spectrometer	15
2.6	Schematic representation of a diode-array spectrometer	16
3.1	Rapid Content TM Analyzer	27
3.2	Spectra from instrument noise test	30
3.3	NIR calibration flow chart	31
3.4.a	Untreated spectra of 31 batches of ac-di-sol USNF	36
3.4.b	Second derivative of 31 batches of ac-di-sol USNF	36
3.5.a	Untreated spectra of 30 batches of lactose monohydrate	37
3.5.b	Second derivative of 30 batches of lactose monohydrate	37
3.6.a	Untreated spectra of 34 batches of microcrystalline cellulose	38
3.6.b	Second derivative of 34 batches of microcrystalline cellulose	38
3.7.a	Untreated spectra of 37 batches of povidone K25	39
3.7.b	Second derivative of 37 batches of povidone K25	39
3.8.a	Untreated spectra of 34 batches of purified talc	40
3.8.b	Second derivative of 34 batches of purified talc	40
3.9.a	Untreated spectra of 42 batches of starch maize	41
3.9.b	Second derivative of 42 batches of starch maize	41
3.10.a	Spectra of samples of ac-di-sol USNF	44
3.10.b	Explained variance within the samples of ac-di-sol USNF	44
3.10.c	3-D cluster plot of ac-di-sol USNF	44
3.10.d	Frequency vs. probability of the samples of ac-di-sol USNF	44
3.11.a	Spectra of samples of lactose monohydrate	45
3.11.b	Explained variance within the samples of lactose monohydrate	45
3.11.c	3-D cluster plot of lactose monohydrate	45
3.11.d	Frequency vs. probability of the samples of lactose monohydrate	45
3.12.a	Spectra of samples of lactose monohydrate	46
3.12.b	Explained variance within the samples of lactose monohydrate	46

3.12.c	3-D cluster plot of lactose monohydrate	46
3.12.d	Frequency vs. distance of the samples of lactose monohydrate	46
3.13.a	Spectra of samples of microcrystalline cellulose	47
3.13.b	Explained variance within the samples of microcrystalline cellulose	47
3.13.c	3-D cluster plot of microcrystalline cellulose	47
3.13.d	Frequency vs. distance of the samples of microcrystalline cellulose	47
3.14.a	Spectra of samples of povidone K25	48
3.14.b	Explained variance within the samples of povidone K25	48
3.14.c	3-D cluster plot of povidone K25	48
3.14.d	Frequency vs. distance of the samples of povidone K25	48
3.15.a	Spectra of samples of purified talc	49
3.15.b	Explained variance within the samples of purified talc	49
3.15.c	3-D cluster plot of purified talc	49
3.15.d	Frequency vs. probability of the samples of purified talc	49
3.16.a	Spectra of samples of starch maize	50
3.16.b	Explained variance within the samples of starch maize	50
3.16.c	3-D cluster plot of starch maize	50
3.16.d	Frequency vs. distance of the samples of starch maize	50
3.17	Overlay of starch maize and pregelatinized starch in the second derivative	54
3.18	Overlay of lactose monohydrate and tablettose in the second derivative	55
4.1	SP15 NIR Laboratory Blender	61
4.2	Schematic of IBC and gravity trigger switches	62
4.3	Moving variance calculation – Block 1 representing the first 8 spectra and block 2 and 3 representing the spectra as the blend progresses	64
4.4	Areas of sample removal in the pilot scale blender	66
4.5	Second derivative of 4 scans of lactose monohydrate	70
4.6	Second derivative of 4 scans of magnesium stearate	71
4.7.a	Overlay of lactose monohydrate and magnesium stearate showing the minimum peaks for magnesium stearate (green)	72
4.7.b	Overlay of lactose monohydrate and magnesium stearate showing the minimum peaks for lactose monohydrate (red)	72
4.8	Standard deviation across the three blends at 1213 nm	74

4.9	Standard deviation across the three blends at 1448 nm	74
4.10	Standard deviation across the three blends at 1213 nm	76
4.11	Standard deviation across the three blends at 1448 nm	76
4.12	Standard deviation across the three blends at 1213 nm	78
4.13	Standard deviation across the three blends at 1448 nm	78
4.14	Mean standard deviation of absorbance at 1213 nm \pm SD for the three blends (error bars indicate standard deviation of the mean standard deviation of absorbance calculated for the 3 blends)	79
4.15	Second derivative of the 6 scans of Ridaq® granule	80
4.16	Second derivative of 4 scans of magnesium stearate	81
4.17.a	Overlay of Ridaq® granule and magnesium stearate showing the minimum peaks for magnesium stearate (red)	82
4.17.b	Overlay of Ridaq® granule and magnesium stearate showing the minimum peaks for Ridaq® granule (green)	82
4.18	Standard deviation across the three blends at 1213 nm	84
4.19	Standard deviation across the three blends at 1591 nm	84
4.20	Standard deviation across the three blends at 1213 nm	86
4.21	Standard deviation across the three blends at 1591 nm	86
4.22	Standard deviation across the three blends at 1213 nm	87
4.23	Standard deviation across the three blends at 1591 nm	88
4.24	Mean of standard deviation of absorbance at 1213 nm (error bars indicate standard deviation of the mean standard deviation of absorbance calculated for the 3 blends)	89
4.25	Standard deviation across the six blends at 1213 nm	91
4.26	Standard deviation across the six blends at 1591 nm	92
5.1	Schematic of a FBD	96
5.2	Temperature vs time in the FBD during drying	98
5.3	FBD fitted with CORONA NIR device	101
5.4	Capability histogram and Normal probability plot for Product A	102
5.5	Capability plot of Product A	103
5.6	Capability histogram and Normal probability plot for Product B	104
5.7	Capability Plot of Product B	104

LIST OF TABLES

2.1	The electromagnetic spectrum	9
3.1	Raw materials for the development of the spectral library	32
3.2	Recommended sample selection options	42
3.3	Qualification method used for the raw materials in the library	51
3.4	Identification method used for the raw materials in the library	52
3.5	Summary of internal library validation	52
3.6	Positive and negative challenges to the library	56
4.1	NIR absorption peaks identified for magnesium stearate	72
4.2	NIR absorption peaks identified for lactose monohydrate	73
4.3	AA results for magnesium stearate per 102.2 mg sample mass for blends run for 1 minute and 40 seconds	75
4.4	AA results for magnesium stearate per 102.2 mg sample mass for blends run for 8 minutes	77
4.5	AA results for magnesium stearate per 102.2 mg sample mass for blends run for 16 minutes	79
4.6	NIR absorption peaks identified for magnesium stearate	82
4.7	NIR absorption peaks identified for Ridaq® granule	83
4.8	AA results for magnesium stearate per 102.2 mg sample mass for blends run for 1.5 minutes	85
4.9	AA results for magnesium stearate per 102.2 mg sample mass for blends run for 6 minutes	87
4.10	AA results for magnesium stearate per 102.2 mg sample mass for blends run for 17 minutes	88
4.11	AA results for magnesium stearate per 102.2 mg sample mass	92
4.12	Last four data points at 1591 nm for blends that were run to real-time endpoints	93
B.1	Moisture values for Product A	126
B.2	Moisture values for Product B	127

SUMMARY

Introduction: Process analytical technologies are systems for the analysis and control of manufacturing processes to assure acceptable end-product quality. This is achieved by timely measurements of critical parameters and performance attributes of raw material and in-process material and processes. The introduction of process analytical technology using near infrared analysis was investigated in three areas, namely incoming raw material analysis, blend uniformity analysis and moisture determination in the fluid bed dryer. **Methodology:** *Incoming raw material identification* - The FOSS XDS rapid content analyzer was used for the development of a NIR method for the identification and material qualification of starch maize and lactose monohydrate. *Blend uniformity analysis* – The SP15 Laboratory Blender fitted with near infrared probe was utilized for the study. Two types of blend experiments were designed to monitor the distribution of magnesium stearate (lubricant) in the blend, namely, a powder blend utilizing lactose monohydrate and a granule blend utilizing Ridaq® granule. Software methods were developed to monitor the standard deviation of the absorbance at the wavelengths that were specific for lactose monohydrate, Ridaq® granule and magnesium stearate. To confirm the prediction of end-point using near infrared, results were verified using an atomic absorption method for magnesium stearate. The blends were sampled at the selected time intervals corresponding to three states of the blend, namely, before end-point, at end-point and after end-point using a sampling plan. An additional six blends were conducted for the granule blend and sampled when the standard deviation had reached a value below 3×10^{-6} at the magnesium stearate wavelength at four consecutive data points (standard deviation value extrapolated from blends carried out to predetermined time intervals). *Moisture determination in the fluid bed dryer* – Moisture values for two products (Product A and Product B) were retrospectively collected from past production batches. A process capability study was conducted on the moisture values to determine if the current process was in a state of control. **Results and Discussion:** *Incoming raw material identification* – The algorithms used for the spectral library were able to distinguish between the raw materials selected. The spectral library positively identified the starch maize and lactose monohydrate samples that were not present in the library. The negative challenge with pregelatinised starch and tablettose demonstrated that the spectral library was able to differentiate between closely related

compounds. *Blend uniformity analysis* – Blends sampled at the predetermined time intervals demonstrated a homogeneous state when the standard deviation of the absorbance was low and a non-homogeneous state when the standard deviation of the absorbance was high, thus near infrared prediction on the state of the blend was confirmed by the standard analytical methods. The series of Ridaq® granule and magnesium stearate blends sampled when the standard deviation was below 3×10^{-6} were homogeneous with the exception of one blend that was marginally out of specification. Blend durations were significantly lower than the standard blend durations used in the facility and ranged from 112 to 198 seconds. *Moisture determination in the fluid bed dryer* – From the process capability study of the two products it was noted that Product A is stable but can still be optimized while Product B is at a desirable state. The statistical evaluation of the moisture values for Product A and Product B demonstrated that the use of the product temperature to monitor the moisture gave consistent results. The current process is stable and capable of producing repeatable results although near infrared provides a means for continuously monitoring the product moisture and allows one to take action to prevent over-drying or under-drying. **Conclusion:** From the investigations conducted, it can be seen that there is definitely a niche for process analytical technology at this pharmaceutical company. The implementation is a gradual process of change, which may take time, probably several years (Heinze & Hansen 2005).

Key words: process analytical technology, near infrared spectroscopy, raw material identification, blend monitoring and fluid bed dryer.

CHAPTER 1

INTRODUCTION TO THE STUDY

1.1 BACKGROUND TO THE STUDY

One of South Africa's largest generic pharmaceutical companies has recently launched an oral solid dosage (OSD) facility boasting state of the art manufacturing equipment. This facility has also received approval from the United States Food and Drug Administration (US FDA) and the Medicines and Healthcare products Regulatory Agency (MHRA) for the manufacture of a range of pharmaceuticals.

This company is contemplating the introduction of process analytical technology (PAT) using near infrared (NIR) analysis to selected pharmaceutical processes at the OSD facility. Process analytical technologies are systems for the analysis and control of manufacturing processes to assure acceptable end-product quality. This is achieved by timely measurements of critical parameters and performance attributes of raw material and in-process material and processes. (US FDA, United States Department of Health and Human services (US DHHS), Centre for Drug Evaluation and Research (CDER), Centre for Veterinary Medicine (CVM), & Office of Regulatory Affairs (ORA) 2004)

The desired goal of the PAT framework is to design and develop processes that can consistently ensure a predefined quality at the end of the manufacturing process. To "build quality" into a product requires a product design that lends itself to quality and the manufacturing process to be monitored and controlled as opposed to only testing the product at the end of the manufacturing process to assure quality. (Afnan 2004)

1.2 MOTIVATION FOR THE STUDY

Kourti (2004) states that PAT can assure acceptable end-product quality, reduce or eliminate end-product testing, reduce manufacturing cost through increased efficiency, reduce production cycle times and reduce rejects and re-processing. The initiative also has the potential of reducing raw material cost by precise formulation, thereby increasing automation to improve operator safety and reducing human errors, improving efficiency and managing variability. The outcomes of the PAT initiative

are therefore desirable to this pharmaceutical company. It is envisaged that adoption and implementation of this paradigm shift from end-product testing to real-time testing will provide an advantage over competitors.

The pharmaceutical manufacturing environment is very competitive and requires manufacturers to strive to improve product quality while reducing manufacturing costs. The US FDA's initiative on PAT aims to facilitate the introduction of new technologies to pharmaceutical manufacturers. PAT systems are encouraged as they provide timely analysis of critical quality parameters with the goal of improving final product quality and reducing manufacturing costs. (US FDA *et al.* 2004)

1.3 AIMS AND OBJECTIVES

1.3.1 Aim

To investigate the potential influence of the introduction of PAT using NIR analysis on the manufacturing processes of solid dosage forms with respect to incoming raw material identification, blend uniformity prediction and granule moisture determination.

1.3.2 Objectives

The aim of the study is to be achieved through the realisation of the following objectives:

- To investigate the application of NIR analysis to incoming raw material identification.
- To predict blend uniformity using NIR technology.
- To evaluate the feasibility of a blender fitted with a NIR device for blend monitoring.
- To retrospectively determine the accuracy of the current method for moisture content determination in the fluid bed dryer (FBD) using statistical analysis of past production batches.
- To evaluate the feasibility of installing a NIR device to continuously monitor the drying process in a FBD.

CHAPTER 2

LITERATURE REVIEW

2.1 PROCESS ANALYTICAL TECHNOLOGY

2.1.1 Definition of PAT

PAT is defined by the US FDA *et al.* (2004) as “a system for designing, analyzing and controlling manufacturing through timely measurements (that is, during processing) of critical quality and performance attributes of raw and in-process material and processes with the goal of ensuring final product quality”. The goal of PAT is to understand the manufacturing process. This encompasses chemical, physical, microbiological, mathematical and risk analysis conducted in an integrated manner.

2.1.2 Drug quality

The US FDA’s current approach to drug quality is that quality cannot be tested into products; it should be built-in or should be by design (US FDA *et al.* 2004). End-product testing is based on statistical sampling and testing to confirm the conformance of a batch to a specification standard. It often requires a destructive test. The risk of out-of-specification scenarios is higher with end-product testing as the testing is only conducted when the batch is complete. (Erni 2005)

Quality can be built into pharmaceutical products through a comprehensive understanding of the intended therapeutic outcome; patient population; route of administration; and pharmacological, toxicological, and pharmacokinetic drug characteristics. An understanding of the chemical, physical and biopharmaceutic characteristics of the drug, design of product and optimum packaging design and design of manufacturing processes to ensure acceptable and reproducible product quality and performance throughout a product’s life is also regarded as key areas of focus. (US FDA *et al.* 2004)

2.1.3 Tools available for PAT implementation

The establishment of effective processes for managing physical attributes of raw and in-process materials requires an understanding of the properties that are critical to quality. Examples of these attributes include particle size and shape variations within a sample of raw and in-process material. These variations may not be detected by the analytical methods for chemical attributes (e.g., identity and purity) and may manifest itself in the final product thus compromising the quality of the product. Thus the inherent undetected variability of raw materials and in-process materials is a critical focus area in PAT. Appropriate use of PAT tools and principles can provide relevant information relating to physical, chemical and biological attributes. This enables process control, process optimization and addresses the limitations of time defined end-points, thereby, improving efficiency. (US FDA *et al.* 2004)

In the PAT draft guidance, the US FDA *et al.* (2004) characterizes the tools for PAT as multivariate tools for design, data acquisition and analysis; process analyzers; process control tools; and continuous improvement and knowledge management tools. An appropriate combination of some or all of these tools may be applicable to a single unit operation or to an entire manufacturing process.

2.1.3.1 Multivariate tools for design, data acquisition and analysis

It is evident that pharmaceutical processes are complex multi-factorial systems. Developmental strategies are used to identify optimal formulations and processes. Knowledge acquired in these developmental programs is the foundation for product and process design. (Kourti 2004)

Brereton (2005) states that this involves the use of multivariate mathematical approaches, such as statistical design of experiments, response surface methodologies, process simulation and pattern recognition tools, in conjunction with knowledge management systems. Statistical approaches exist that are effective for identifying and studying the effect and interaction of product and process variables (Brereton 2005).

These tools enable the identification and evaluation of product and process variables that may be critical to product quality and performance and may identify potential failure modes and mechanisms, the effects of which can be quantified by the product quality (Kourti 2004).

2.1.3.2 Process analyzers

Ciurczak and Drennen III (2002b) recognize that the available tools for process analysis have advanced from those that take predominately univariate process measurements such as pH, temperature and pressure to those that measure biological, chemical and physical attributes. The measurements are classified as at-line, where the sample is removed, isolated from, and analyzed in close proximity to the process stream; on-line, where the sample is diverted from the manufacturing process and may be returned to the process stream and in-line, where the sample is not removed from the process stream and can be invasive or noninvasive (Ciurczak & Drennen III 2002b).

Process analyzers have advanced, making real-time control and quality assurance during manufacture possible. Often these tools must be used in combination with multivariate methods to extract critical process knowledge for real-time control and quality assurance. Statistical and risk analyses of the process are necessary to assess the reliability of predictive mathematical relationships. A sensor based “process signature” can be useful in relating the underlying steps or transformations. These signatures may also be useful for process monitoring, control and end-point determination depending on the level of process understanding. The process equipment, analyzer and their interfaces must be robust, reliable and have ease of operation. (US FDA *et al.* 2004)

2.1.3.3 Process control tools

Process monitoring and control strategies are aimed to monitor the state of a process and manipulate it to maintain a desired state. Factors to take into consideration are properties of input materials, the capability of the process analyzer to measure critical steps and reliable end-points to ensure consistent quality of output material and final product. (Ciurczak & Drennen III 2002b)

The US FDA *et al.* (2004) recommend the following to design and optimize drug formulations and manufacturing processes:

- Critical material and process characteristics must be identified and measured.
- A process measurement system that allows real-time or near real-time measurements must exist.
- Process controls that provide adjustments to ensure control of critical steps must be in place.
- Mathematical relationships between product quality characteristics and measurement of critical material and process characteristics must be understood.

2.1.3.4 Continuous improvement and knowledge management tools

Data collection over the life cycle of a product can be helpful in justifying proposals for post approval changes. Scientific understanding of relevant multi-factorial relationships can aid regulatory decisions. (US FDA *et al.* 2004)

2.1.4 PAT and risk analysis

Risk can be defined as the probability of harm multiplied by the severity of harm (US DHHS & US FDA 2004). The US DHHS and US FDA (2004) state that risk analysis is an important part of any PAT initiative and recognizes the various sources of risk as follows:

- Chemical risks such as incorrect concentrations of constituents in the formulation or incorrect compounds in formulation (mistake or reaction).
- Physical risks such as incorrect particle size distribution, crystal form, disintegration or solubility.
- Biological risks such as microbial contamination.
- Engineering risks that could be as a result of a process run at incorrect conditions.
- Analytical risks due to inadequate data measured on process or product.
- Mathematical-statistical risk due to data inadequately analyzed in development phase or the mathematical model is not working during on-line operation.
- Interpretation risks due to incorrect decisions as data or data analysis is not understood.

The US DHHS and US FDA (2004) have employed a risk-based approach, where the intensity of the regulatory oversight needed will be related to several factors, including the degree of the manufacturer's product and process understanding and the robustness of the quality system controlling the process. These regulatory bodies state that changes to complex products (e.g. proteins or naturally derived products) made with complex manufacturing processes or products that are less understood from a manufacturing or quality attribute perspective may need more regulatory control and on the other hand, changes in well-understood processes could be managed with less intervention from the regulatory authorities. The new assessment system proposed has the potential to reduce the regulatory burden in proportion to the manufacturer's effort to achieve continuous improvement and manufacturing process optimization.

2.1.5 Selecting a process analytical technology

Selecting the appropriate technology for the process is crucial to the success of the initiative. Geoffroy (2004) states that the technology should be easy to use and maintain, highly accurate and precise, must be transferable from instrument to instrument, must be capable of being validated and demonstrate ruggedness and reliability. The system must be user proof or system proof and be innovative.

The commonly used analytical tools for PAT are separation methods, such as high performance liquid chromatography (HPLC), gas chromatography (GC), capillary electrophoresis (CE); spectroscopic methods such as NIR, infrared (IR), ultraviolet (UV), nuclear magnetic resonance (NMR); physicochemical methods such as pH, dissolved oxygen, conductivity, effusivity and biosensors (Palermo 2001).

Acoustics resonance spectrometry can be used for the determination of granulation end-point in real-time. The mixing emits energy in the form of mechanical vibrations (acoustic emission), as a result of change such as particle size change, compound mixing or wetting. Electronic listening to these acoustic emissions can be used to detect process transitions and end-points. (Rudd 2004)

Light induced fluorescence (LIF) can be used for the rapid and non-destructive analysis of active pharmaceutical ingredients on tablet surfaces. LIF is beginning to be used for blend uniformity monitoring but is still not the conventional approach. (Ciurczak 2006)

NIR spectroscopy is widely used as a PAT tool. The popularity of NIR spectroscopy began in the agricultural environment when it became necessary to analyse compounds in their natural state, as sample preparation was not possible due to the nature of the compounds. NIR offered the ability to measure any form of sample; liquid, solid or semi-solid, which is one of the greatest advantages of the method. Based on this, the popularity of the technique has significantly grown. (Ciurczak 2006)

2.2 NEAR INFRARED SPECTROSCOPY AS A P.A.T. TOOL

2.2.1 Background to infrared spectroscopy

Light travels through space in the form of waves made up of successive crests and troughs. Waves have three primary characteristics, two of these are discussed below:

- Wavelength (λ): this is the distance between two consecutive crests or troughs often measured in meters or nanometers ($1 \text{ nm} = 10^{-9} \text{ m}$).
- Frequency (ν): the number of successive crests or troughs that pass a given point in unit time. The unit for frequency is hertz (Hz), which represents one cycle per second. (Masterton & Hurley 1993)

Table 2.1 shows the electromagnetic spectrum. The infrared part of the spectrum covers the wavelength range from approximately 700 nm to 1000 μm . The term "infrared" refers to a broad range of wavelengths, beginning at the top end of those wavelengths used for communication and extending to the lower wavelength (red) at the end of the visible spectrum. (Drennen III & Lodder 1993)

The infrared spectrum can be divided into three parts, namely far infrared (50 - 1000 μm) which are longer wavelengths, mid-infrared (3 - 50 μm) and near infrared (700 - 3000 nm) which is adjacent to the visible spectrum.

Table 2.1 The electromagnetic spectrum (adapted Drennen III & Lodder 1993)

The Electromagnetic Spectrum	
Designation	Wavelength Range
Gamma Ray	< 0.05 Angstroms
X-Ray	0.05 - 100 Angstroms
Far-ultraviolet	10 - 180 nm
Near-ultraviolet	180 - 350 nm
Visible	350 - 700 nm
Near infrared	700 - 3000 nm
Middle infrared	3 - 50 μm
Far infrared	50 - 1000 μm
Microwave	1 - 300 mm
Radio Wave	> 300 mm

2.2.2 Theory and principles of NIR spectroscopy

Vibrational spectroscopy is based on the concept that atom-to-atom bonds within molecules vibrate with frequencies that may be described by the laws of physics and are therefore subject to calculation (Ciurczak 2001).

When a photon with certain energy hits a bond, it is absorbed, the molecule becomes excited and the size (amplitude) of the motion increases. Different frequencies of vibration absorb different energies of photons. (Masterton & Hurley 1993)

At room temperature, most molecules are vibrating at the least energetic state; the lowest frequencies of any two atoms connected by a chemical bond may be roughly calculated by assuming that the band energies arise from the vibration of a diatomic harmonic oscillator and obey Hooke's Law: $\nu = \frac{1}{2} \pi (k/\mu)^{1/2}$

where ν = the vibrational frequency

k = the classical force constant

μ = the reduced mass of the two atoms

Hooke's Law works well for the fundamental vibrational frequency of simple diatomic molecules and polyatomic molecules, however this approximation only gives the average frequency of the diatomic bond. The electron withdrawing or donating properties of neighboring atoms and groups greatly influence the bond strength and length and thus the frequency of the X-H bonds. While an average wavelength value is not significant in structural determination or chemical analyses, these species' specific differences gives rise to a substance's spectrum. The "k" values vary and create energy differences that can be calculated and utilized for spectral interpretation. (Ciurczak 2001; Masterton & Hurley 1993)

The NIR region contains absorption bands corresponding to overtones and combinations of fundamental C-H, O-H and N-H vibrations involving the light hydrogen atoms. Figure 2.1 illustrates the overtones and combination bands. An overtone is a multiple of a fundamental vibration and occurs at about twice the frequency. A combination band occurs when two vibrations close in energy combine. (Workman 2001)

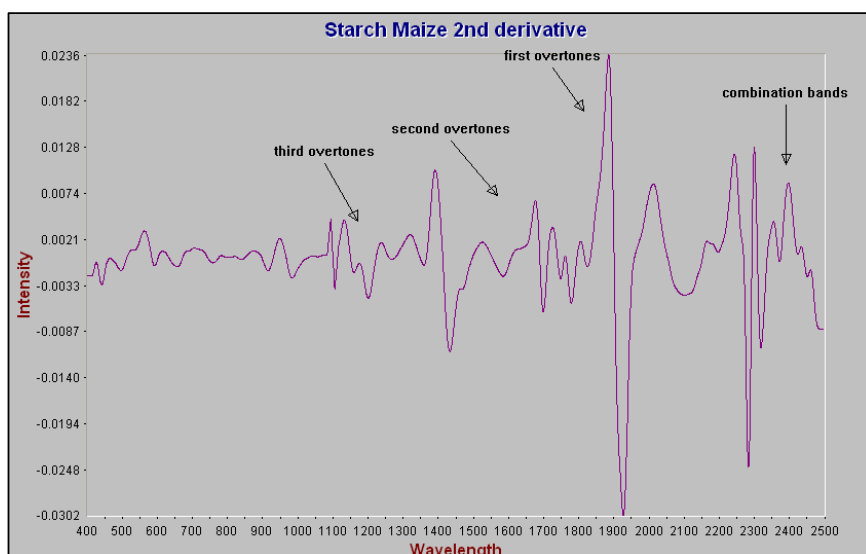


Figure 2.1 Second derivative of starch maize showing overtones and combination bands

NIR spectroscopy is therefore very useful for qualitative and quantitative analyses of water, alcohols, amines, and any compounds containing C-H, N-H and/or O-H groups (Drennen III & Lodder 1993).

The interpretation of NIR spectra depends on statistical methods to obtain qualitative and quantitative information from the spectra. The reason for this is that the NIR spectra often contain broad bands that are the result of many individual overlapped peaks. The physical or chemical property of the investigated sample is related to the absorption of radiation in the NIR wavelength range. Chemometrics, which is the extraction of chemical information from NIR spectra using computers and mathematics, is used to build a mathematical relationship to the spectra. The second derivative is used for the removal of baseline shifts and for the resolution of overlapping peaks. (Bokobza 1998)

A calibration experiment is very important in quantitative NIR spectroscopy, which involves collecting a set of reference samples that contain all physical and chemical variations to be expected in the unknown sample. The calibration experiment is to establish a mathematical relationship between the NIR spectrum and the physical parameters under investigation previously determined by an independent technique. The mathematical model enables the analysis of unknown samples based on their NIR spectra with reference to chemical or physical properties of interest. (Bokobza 1998)

The light in the NIR portion of the spectrum features long sample path lengths and relative insensitivity to glass allowing analysis of materials through containers or windows in their natural form without sample preparation. NIR analysis is non-destructive and speedy, allowing the tested material to be used for other purposes and provides real-time process monitoring. The NIR spectral range is sensitive to optical properties of typical pharmaceutical samples, which means that the spectra contain information relating to physical and chemical properties of the sample. (Ellis & Davies 2005)

NIR spectroscopy has proved to be a powerful tool for research in agriculture, food, pharmaceutical, chemical, polymer and petroleum industries (Bokobza 1998).

2.2.3 Measurements

The Pharmacopoeial Forum (1997) acknowledges the three different measurements commonly performed in the NIR spectral region as follows:

2.2.3.1 Reflectance

Reflectance (R) measures the ratio of the intensity of light reflected from the sample (I), to that reflected from a background or reference reflective surface, (I_r). NIR radiation can penetrate a substantial distance into the sample, where vibrational combinations and overtone resonance of the analyte species present in the sample, can absorb it. The radiation that is not absorbed is reflected back from the sample to the detector. This spectrum is obtained by calculating and plotting $\log(1/R)$ versus wavelength (commonly called absorbance). This can be expressed as $R = I/I_r$. (Pharmacopoeial Forum 1997)

2.2.3.2 Transmittance

Transmittance (T) measures the decrease in radiation intensity as a function of wavelength when radiation is passed through the sample. This involves the sample being placed in the optical beam between the source and the detector and the results being presented directly in terms of transmittance and/or absorbance. This can be expressed as $T = I/I_0$ where I is the intensity of the transmitted radiation and I_0 is the intensity of the incident radiation. (Pharmacopoeial Forum 1997)

2.2.3.3 Transflectance

This mode is a combination of transmission and reflectance. The measurement of transflectance is obtained by placing a mirror or a diffuse reflectance surface to reflect the radiation transmitted through a sample a second time, thus doubling the path-length. Non-absorbed radiation is reflected back from the sample to the detector. Transflectance (T^*) can be expressed as $T^* = I/I_T$ where I is the intensity of transmitted and reflected radiation measured with the sample and I_T is the intensity of transflected radiation without sample. (Pharmacopoeial Forum 1997)

Figure 2.2 illustrates the three types of measurements. The basis for all NIR measurements is light radiation passing through or into a sample and measuring the emerging beams (Ciurczak 2006).

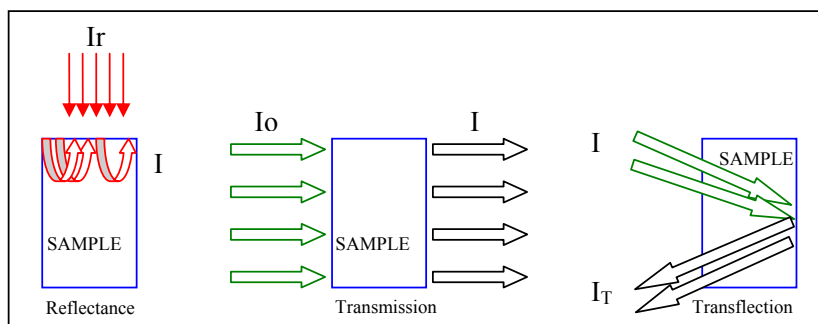


Figure 2.2 Three common forms of assessing NIR data from varied samples (adapted Ciurczak 2006).

2.2.4 Factors affecting spectral response

The Pharmacopoeial Forum (1997) identifies several factors to be considered that may affect the spectral response such as the temperature of the sample, the moisture and/or solvent residues of the sample, the sample thickness, the optical properties of the sample, polymorphism that may be exhibited by the sample and the age of the sample. It is important to consider these factors when calibrations are conducted.

2.2.5 Instrumentation

Ciurczak and Drennen III (2002b) describe the various types of NIR instrumentation as follows:

2.2.5.1 Filter-based instruments

A filter allows a particular portion of the spectrum to pass through (a bandpass filter) or blocks all wavelengths below or above a certain frequency (edge and cut-off filters). An interference filter consists of a transparent dielectric spacing material separating two partially reflective windows, allowing a specific set of wavelengths to pass. The outer windows have a higher refractive index than the center spacer, which determines the central wavelength via its thickness. A filter instrument can run many applications using a few select wavelengths. Figure 2.3 shows a schematic representation of filter-based instruments.

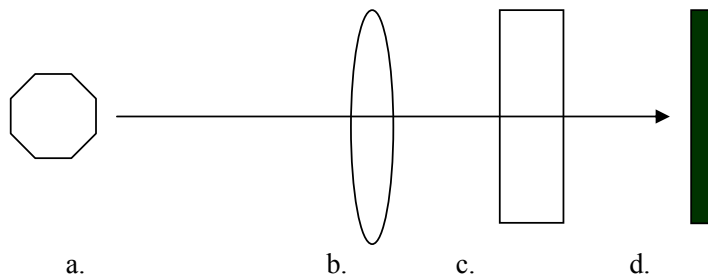


Figure 2.3 Schematic representation of a filter-based spectrometer; a. source, b. interference filter, c. sample, d. detector (adapted from Ciurczak & Drennen III 2002b).

2.2.5.2 Scanning grating monochromators

Gratings are interference based and are manufactured by the interference pattern of two lasers striking a photosensitive surface. This creates lines of very specific spacing on a reflective surface. When the polychromatic light from a source strikes on the surface, it behaves like a thousand prisms, dispersing light. The angle of rotation of the grating determines what wavelength is emitted from the exit slit. Cut-off filters are placed in a configuration such that only the required wavelength is allowed through. Figure 2.4 shows a schematic representation of scanning grating monochromators.

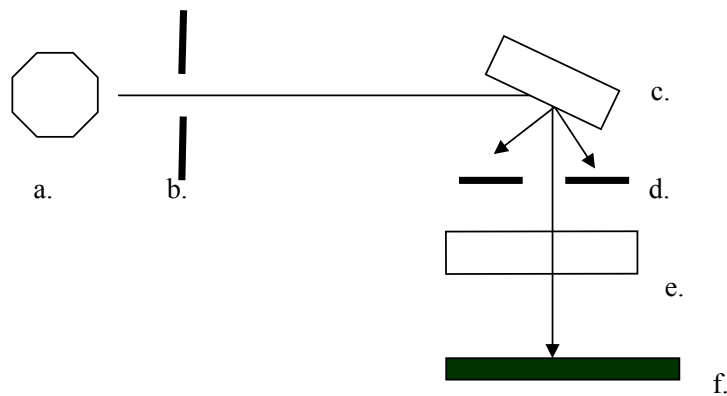


Figure 2.4 Schematic representation of a scanning grating based spectrometer; a. source, b. entrance slit, c. grating, d. exit slit, e. sample, f. detector (adapted from Ciurczak & Drennen III 2002b).

2.2.5.3 Interferometer-based instruments

The interferometer works on the principle whereby light from the source is split into two segments by the beam-splitter. One portion travels to a fixed mirror and is reflected back to the splitter. The second portion strikes on a moving mirror and returns to be recombined with the first portion of light. The pattern of peaks/troughs is called an interferogram and by applying mathematical calculations to these, a spectrum evolves. Interferometers are popular in both mid-range infrared and NIR. Figure 2.5 shows a schematic representation of interferometer-based instruments.

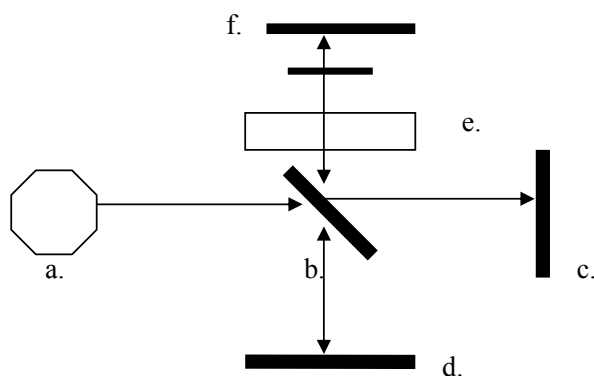


Figure 2.5 Schematic representation of an interference-type spectrometer; a. source, b. beam splitter, c. fixed mirror, d. moving mirror, e. sample, f. detector (adapted from Ciurczak & Drennen III 2002b).

2.2.5.4 Photo-diode arrays

This instrument utilizes a fixed monochromator, usually a holographic grating and an array of many small detectors. The light is collimated onto the grating and is thereafter dispersed into component wavelengths. The wavelengths are then directed to a series of photo-diodes. Photo-diode arrays are more commonly used for process control. Figure 2.6 shows a schematic representation of photo-diode array instruments.

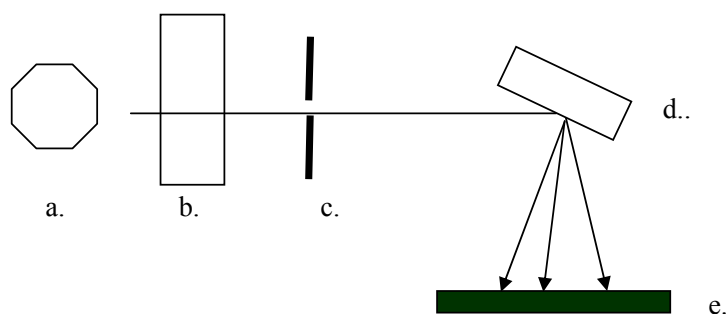


Figure 2.6 Schematic representation of a diode-array spectrometer; a. source, b. sample, c. slit, d. fixed monochromator, e. detector (adapted from Ciurczak & Drennen III 2002b).

2.2.6 NIR as a PAT initiative

Palermo (2001) states that NIR techniques can be applied to incoming raw material analysis, granulation, moisture determination, coating, blend uniformity determinations, assay and content uniformity testing of finished products in a pharmaceutical manufacturing facility.

The implementation of PAT to these areas ensures real-time monitoring of process end-points instead of conventional time determined end-points. This initiative offers greater understanding of manufacturing processes and better control over variables (US FDA *et al.* 2004). Rapid testing by NIR analysis at all stages of the manufacturing process can reduce production time and provide assurances at all stages of the manufacturing process that the product quality is being maintained (Bakeev 2003).

2.3 NIR APPLICATION TO SELECTED PROCESSES

2.3.1 Incoming raw material analysis

Raw materials can be divided into two categories, namely the active pharmaceutical ingredients (APIs) and the inactive pharmaceutical ingredients (IPIs). APIs bring about the pharmacological activity of the drug design while IPIs are inert materials, i.e. they do not have pharmacological activity related to the intended use of the

product, but are included in the formulation for other functions. Depending on the characteristics of the IPI, it may act as a diluent, disintegrant, preservative, colouring agent, flavouring agent, antioxidant, binder, lubricant or glidant in the context of oral solid dosage forms. IPIs play an important role in the formulation by aiding pharmaceutical drug manufacture, stability and activity.

Incoming raw material analysis is a critical step in the pharmaceutical manufacturing environment to ensure safe and efficacious pharmaceuticals. The quality of the raw materials can influence the manufacture, activity and stability of the finished pharmaceutical product (International Conference on Harmonization (ICH) 2004). The Medicines Control Council (MCC) (2003) requires the application of stringent standards to raw materials ensuring that the specified quality standards are satisfied prior to release. This entails that the incoming raw materials meet the specifications stated in terms of qualitative (identification) and quantitative (purity, particle size, moisture, hardness) analysis.

Raw materials are the starting blocks to pharmaceutical products. An effective way to avoid problems with products that involve a number of materials is to check the quality of the raw material. Avoiding the use of problematic raw material is an economic way to avoid costly waste. (Cinier & Guilmant 1998)

Currently the primary use of NIR analysis is in the identification of raw material. Some regulatory authorities have mandated a 100 % verification of materials before release to production, instead of the use of traditional statistical sampling. (Palermo 2001)

Cinier and Guilmant (1998) agree that HPLC is a popular technique for raw material analysis however NIR spectroscopy can be used as an alternate. The cost of an HPLC and NIR instrument is similar, but the HPLC method takes about 20 minutes, requires costly consumables such as solvents and stationary phases, while the NIR method takes approximately 1-2 minutes, and requires no sample preparation, which would save time and money. The HPLC technique can also have other problems associated with it for example, the column can age; the injection is with a syringe or an injection loop thus if there is a bubble, there could be inaccurate results and sample preparation

involves dissolving the sample in a solvent, which can give less accurate results. (Cinier & Guilmant 1998)

Bakeev (2003) states that the identification of raw materials using NIR involves the scanning of numerous lots of raw materials and discriminate analysis to qualitatively identify the materials. As a routine test procedure, the spectrum of a new sample is scanned and compared to the mean spectrum of each product in the library to obtain a rapid identification.

2.3.2 Blend Uniformity

2.3.2.1 Overview of the blending process

Travers (1988) differentiates between the words “mix” and “blend” in that blending is a way of mixing. Mixing is defined as putting together of substances in one mass or assemblage with more or less thorough diffusion of the constituent elements among one another whereas blending is defined as mixing homogeneously and inseparably.

The aim of mixing in the pharmaceutical context is to attain a mixture that will provide uniform unit doses. Homogeneity of a mixture is critical to ensure safe and efficacious delivery of pharmaceuticals. The most prevalent type of mixing used in the pharmaceutical industry is batch type mixing, that mixes a sub lot or total lot of a formula at one time. A well-designed manufacturing process should provide optimum mixing of substances throughout the different stages e.g. a wet granulation method provides mixing of powder prior to granulation, mixing during granulating, mixing in the FBD and finally blending. (Lantz & Schwartz 1989)

2.3.2.2 Tumble Blenders

Tumble blending equipment operate by the rotation of the entire mixer shell or body with no agitator or mixing blade. The different types of tumble blenders are barrel blenders, cube blenders, octagonal blenders, V-shaped blenders, double cone blenders and slant double cone blenders. The latter three types of blenders are extensively used for blending. The process of blending using this equipment imparts a minimum amount of energy to the product bed. These blenders operate by adding material to be blended to a volume of approximately 50 to 60 % of the blenders' total volume as

blending efficiency is affected by the load volume. Blending speed is also another factor to consider concerning efficiency in that the slower the blender, the lower the shear forces. Although higher blending speeds may provide more shear; more dusting may be prevalent causing segregation of fines. (Lantz & Schwartz 1989)

2.3.2.3 Problems associated with insufficient blending

Prior to the blending stage lubricants, antiadherents and glidants are added to the granule. Lubricants function to reduce friction between the granules and die wall during compression and ejection; antiadherents prevent sticking to the punch and die wall and glidants improve flow properties of the granule. (Gilbert & Anderson 1986)

Gilbert and Anderson (1986) describe lubrication used in tablet manufacture as boundary lubrication, which results from the adherence of polar portions of molecules with long carbon chains to the metal surfaces of the die wall. The common problems associated with poor lubrication are binding where tablets have vertically scratched edges, lack smoothness or gloss and are often fractured at the top edges; sticking where tablet faces appear dull; filming which is the early stages of sticking; picking which represents the advanced stages of sticking and capping and lamination which is normally associated with poor bonding and can also be a result of a system that is over lubricated (Gilbert & Anderson 1986).

2.3.2.4 Problems associated with over-blending

Granule and powder mixes are made up of particles that vary in size and shape, due to this, certain factors may operate to cause segregation (de-mixing) at the same rate as mixing occurs. The main factors promoting segregation are differences in particle size, shape and density. Smaller particles or more dense particles may fall to the bottom of the mass during blending leading to de-mixing. (Travers 1988)

Mixes that are not prone to segregation will continue to improve with an extended mixing times but segregating mixes may worsen after extended periods of blending. This is because the factors promoting segregation require a longer time to be established than those required to produce a reasonable blend. It is therefore disadvantageous to blend beyond the optimum point. (Travers 1988)

In addition to segregation, over-blending can lead to physical degradation of the material properties, and occurs in instances such as when a waxy lubricant is excessively deformed, causing it to coat the granule. This reduces the bioavailability of the granule. Coated granules are also damaged through abrasion and fracture. (Muzzio, Alexander, Goodridge, Shen, & Shinbrot 2003)

Over-blending especially with a hydrophobic lubricant such as magnesium stearate can lead to extended disintegration times and low hardness, which is due to intimate contact between granule, lubricant(s) and some inter-granular disintegrants. The blending times can influence the final granule with respect to active/excipient homogeneity and compressibility. (Kanfer, Walker, & Persicaner 2005)

In the case of direct compression formulations, over-blending can result in de-mixing of the active, prolonged disintegration time and soft tablets (Kanfer *et al.* 2005).

2.3.2.5 Monitoring blend uniformity using current methods

Conventional methods to determine blend uniformity include sampling from the bulk container and performing laboratory tests such as HPLC. A common approach to sampling is to use a thief probe. The drawbacks associated with a sample thief probe is that as the thief is inserted into the powder bed, some compaction takes place around the thief and flow into the thief may be poor. The sample representation of the blend may be inaccurate due to the fact that as the thief is inserted into the powder bed it may carry material from the surface of the mixture into the mixture depending on the diameter of the thief. A “bottom sample” may therefore be contaminated with a “top sample”. (Lantz & Schwartz 1989)

2.3.2.6 Monitoring blend uniformity using NIR analysis

Blend homogeneity can be determined in real-time using NIR spectral images. This can be very useful as a process-monitoring step to ensure uniform distribution of the active pharmaceutical ingredients, uniform distribution of lubricants and to determine the optimum blend time in scale up batches. (Palermo 2001)

NIR monitoring is a noninvasive technique that minimizes analysis times and sample preparation. It also eliminates the sampling errors associated with the removal of

samples from the blender by a sample thief. (El-Hagrasy, Morris, Damico, Lodder, & Drennen III 2001)

NIR methods provide a means of determining the homogeneity of all components in the blend as almost all pharmaceutically important compounds exhibit some NIR spectrum (El-Hagrasy *et al.* 2001).

2.3.3 Granule moisture determination

2.3.3.1 The drying process

Wet granulation is commonly used as a method of tablet manufacture, and serves to increase the particle size, supply a binder to the formulation, improve flow and compression characteristics and improve content uniformity. Wet granulations utilize drying to obtain the optimum moisture content of the granule. Drying refers to the removal of water (or other liquid) from a solid or semi-solid mass by an evaporative process. The moisture content of dried granule varies from product to product, thus drying is a relative term and refers to the process where the moisture content has been reduced from some initial value to a set point moisture. (Van Scoik, Zoglio, & Carstensen 1989)

The drying of granules involves two processes; heat is transferred to the granule to evaporate liquid and mass is transferred as a liquid or vapour within the solid and as a vapour from the surface into the surrounding gas phase (Van Scoik *et al.* 1989).

Van Scoik *et al.* (1989) describe the three means of heat transfer that apply to the drying processes as follows:

- Convection, which involves the transfer of heat from one point to another within a fluid by mixing one portion of the fluid with another e.g. the use of hot air in tray drying and fluid bed drying.
- Conduction, which is the transfer of heat from one body to another part of the same body, or from one body to another body in direct physical contact with it e.g. heat supplied to a granule bed via a metal shelf in the case of vacuum drying.

- Radiation, which is the transfer of heat energy between separate bodies not in contact with each other by means of electromagnetic waves e.g. microwave and infrared drying.

Van Scoik *et al.* (1989) state further that all three types of heat transfer may occur at the same time or in combinations. They give the following example to illustrate this point: In convection drying, there is a flow of hot gas past the wet surface of the granule. At the immediate surface of the granule, there is layer of gas known as the film layer or stagnant layer. Heat is transferred from the bulk gas through the film of the granule via molecular conduction. The resistance of this stagnant layer to heat flow depends primarily on its thickness. It is therefore evident that increasing the velocity of the drying air will increase the heat transfer coefficient, therefore as the velocity of the drying air increases, the stagnant layer becomes thinner.

Van Scoik *et al.* (1989) state that the total moisture content can be divided into two types namely bound moisture and unbound moisture. Bound moisture refers to water (or other solvent in non-aqueous systems) held by material in such a manner that it exerts a lower vapour pressure than that of the pure liquid at the same temperature. Water may be chemically or physically bound. Unbound moisture refers to moisture in association with a solid, which exerts the same vapour pressure as the pure liquid.

The free moisture content of a substance is the amount of moisture that can be removed from the material by drying at a specified temperature and humidity. The equilibrium moisture content (EMC) can therefore be described as the amount of moisture that remains associated with the material under the drying conditions. (Van Scoik *et al.* 1989)

2.3.3.2 Drying methods

The three most common drying methods for pharmaceutical granulations are oven drying, fluid bed drying and vacuum drying (Van Scoik *et al.* 1989). For the purposes of this project the FBD will be discussed in more detail.

2.3.3.2.1 Fluid bed drying

Fluid bed drying is a process in which filtered air is forced through a granule bed at a velocity sufficient to partially suspend the granule. The particles are continually lifted by drag forces from the air and fall back down under the influence of gravity. Fluidized drying techniques are efficient for the drying of solids due to their efficacy of promoting heat and mass transfer. Each granule is surrounded by a layer of dry air, which is constantly exchanged thus creating a high surface area for evaporation that aids to maintain the concentration gradient necessary for evaporation to occur. The humidity of the drying air has the greatest impact on the drying rate of aqueous based granulations as a result of the vapour pressure difference between moist solid and drying air. The fluidizing action of the bed promotes efficient mixing between the gas and solid phases, which helps maintain a uniform temperature throughout the fluid bed. (Van Scoik *et al.* 1989)

The fluid bed system allows material to be dried with a temperature profile. Moisture evaporating from the granule will cool the drying air. The energy consumed by evaporating moisture will be reflected in the constant temperature difference between the incoming warm, dry air and the cooler more humid exhaust air. As drying proceeds the increase in temperature of the exhaust air can be detected and the temperature of the drying air can be reduced to prevent overheating and over-drying. The monitoring of the granule temperature is usually used to determine the set point for specific moisture values. (Van Scoik *et al.* 1989)

2.3.3.3 Conventional moisture determination in the FBD

Traditional methods of monitoring the moisture content includes either off-line monitoring with Karl Fischer volumetric titrimetry or at-line with thermogravimetric loss-on-drying (LOD) methods (Mattes, Schroeder, Dhopeswarker, Kowal, & Randolph 2005).

The LOD method of moisture content determination of a solid can be expressed on a wet-weight or dry-weight basis. On a wet-weight and dry-weight basis the water content is expressed as a percentage of the wet solid or the dry solid respectively. LOD is an expression of the moisture content on a wet-weight basis and is expressed as a percentage of the weight of water in a sample divided by the total weight of the wet sample. The LOD of a wet sample is often determined by the use of a moisture balance, which has a heat source for rapid heating and a scale calibrated in percent LOD. A weighed sample is placed on the balance and allowed to dry until it reaches a constant weight. The moisture lost by evaporation is obtained directly from the percent LOD on the balance. (Rankell, Liberman, & Schiffmann 1986)

Moisture content (MC) refers to the moisture content on a dry-weight basis and is calculated as a percentage of the weight of water in a sample divided by the weight of dry sample (Rankell *et al* 1986).

The calculations for LOD and MC differ thus variations in moisture content will occur depending on which method is used and Rankell *et al.* (1986) state that the MC method is more reliable than the LOD method.

Both the Karl Fischer and LOD analyses require the process to be stopped, samples to be collected using a sample thief followed by analysis of the sample before the drying process continues (Mattes *et al.* 2005).

2.3.3.4 Moisture determination in the FBD using NIR analysis

In-line NIR spectroscopy would provide a means of continuously monitoring the drying process in the FBD. This can be very useful in achieving the optimum product moisture levels in real-time. LOD methods may result in over-drying or under-drying. (Ciurczak & Drennen III 2002b)

Water is a very strong absorber in the NIR region, making it a good candidate for quantitative analysis by NIR. The strong combination O-H band at approximately 1930 nm and first overtone O-H stretching from approximately 1450 nm can be used to measure the moisture content. (Bakeev 2003)

2.4 SUMMARY

There is a niche for the application of PAT using NIR technology within the pharmaceutical environment. This technology, if successfully implemented, has the potential to improve manufacturing efficiency, assure product quality and reduce cost due to greater efficiency. These outcomes are eagerly sought after especially at this pharmaceutical manufacturing company.

The aim of this project is the investigation of the potential benefits of adopting a PAT approach. The three pharmaceutical areas selected, namely incoming raw material identification, blend monitoring and moisture monitoring in the FBD, represent the areas where time and cost saving will have tremendous benefits to the company.

CHAPTER 3

INCOMING RAW MATERIAL ANALYSIS

3.1 INTRODUCTION

NIR technology is widely used by polymer and chemical companies while pharmaceutical companies are now uncovering the tremendous advantages of NIR techniques for raw material identification (Kemper & Luchetta 2003).

In the NIR context, NIR identification tests are to ensure the identity of the analyte in a sample or the identity of the sample matrix. Material identification is often associated with material qualification. Material qualification provides information on how well the material compares to material that has been accepted in the past and provides the assurance that the material is of the same grade and quality. (Kemper & Luchetta 2003)

Material qualification is important in a pharmaceutical environment as minor changes in the raw material can influence the final product (Cinier & Guilmant 1998). Variations in the raw material include the moisture content, impurities and other potentially unfavorable deviations. It can also be used to discriminate between closely related materials that may be indistinguishable by identification tests. (Kemper & Luchetta 2003)

Material identification and qualification is achieved by the comparison of the NIR spectrum (or a mathematical transformation of it) of the test sample to that of a reference library set up using approved samples of the relevant materials. If the batch of material that is being tested closely matches the spectral properties of that same material that has been approved for use in the past by conventional methods, then the test batch should be suitable. (Kemper & Luchetta 2003)

Mathematical techniques are generally used to extract information from NIR data. A training set is developed which represents the chemical and physical characteristics of the material ('process signature') and if the spectral signature of a material falls within

predefined statistical boundaries, there will be a high degree of confidence that the material conforms to the specification. (Boysworth & Booksh 2001)

The focus of this portion of the project is the development of a NIR method for the identification and qualification of starch maize and lactose monohydrate.

3.2 NIR INSTRUMENT

The Rapid Content™ Analyzer (RCA) - off-axis digital synchronous (XDS) series, manufactured by FOSS-NIRSystems (seen in Figure 3.1) was utilized for the development of the NIR method.

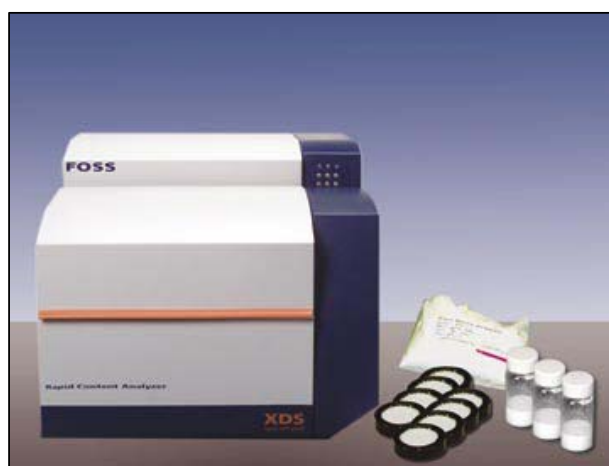


Figure 3.1 Rapid Content™ Analyzer (FOSS NIRSystems 2005)

3.2.1 Rapid Content™ Analyzer Hardware

The energy source for the RCA instrument is a 50-watt tungsten halogen lamp with an axial filament. The white light from the energy source is directed at concave holographic grating that behaves like a prism and separates the light into its individual wavelengths. The concave holographic grating is offset on the axis to ensure an even spread of the emerging beams of light. The emerging beams are first directed at the reference. The energy received by the detectors is displayed as a spectrum of the energy absorbed at the wavelengths of the absorption by the reference. The reference for reflectance is a ceramic plate. The assumption is that the reference does not absorb any energy and is therefore a measure of the instrument output. After obtaining a reference scan the light is then directed to the sample, where it interacts with the sample molecules. The energy that is not absorbed by the molecules in the sample is

returned to the detectors. The absorbance of the sample is the difference in absorbance of the reference scan and energy that is returned by the sample to the detector. During normal operation, a reference scan should be done every 10 samples or 30 minutes. (FOSS NIRSystems 2005)

The order-sorter filters keep out unwanted beams of light from the instrument beam. This allows scanning of 400 – 2500 nm. The RCA has four lead sulphide detectors for detection in the NIR region and four silicon detectors for detection in the visible region. The detectors alternate in a 45 degree circular orientation in the detector block which elevates specular reflection. (FOSS NIRSystems 2005)

3.2.2 Rapid Content™ Analyzer Software

The RCA operates on Vision® (version 3.2) software. Vision® is compliant to section 21, part 11 of the Code of Federal Regulations (CFR). Title 21 of the CFR contains regulations for good clinical practices, good laboratory practices and good manufacturing practices for the pharmaceutical and health care industries. Part 11 applies to the US FDA regulations providing criteria for the acceptance of electronic records and electronic signatures to be equivalent to paper records and hand written signatures. Audit trails are available that stores all activity and changes made on projects, calibrations, libraries, operation methods and security. When a change is made to raw data or a method, 21 CFR part 11 requires that a reason for the change of input be documented. Due to the regulations governing the pharmaceutical industry, CFR part 11 compliance is necessary. (FOSS NIRSystems 2005)

In Vision®, the basic unit of data storage is the project. Each project represents a separate database, which includes spectra, constituent values (if available) and the instrument configuration for the collection of spectra. A project requires a data collection method (DCM). This defines the instrument parameters for data acquisition (model, module, detector, scans). A DCM has to be defined every time a new project is created. DCM's cannot be shared between projects but are copied with spectra when copied between projects. (FOSS NIRSystems 2005)

A library represents samples of spectra or samples of product that have been selected from a project. The collections of spectra in a library are generally mathematically

pre-treated to remove baseline shifts and reduce the noise (Bokobza 1998). Thereafter the spectra of the different products in the library are mathematically treated with chemometric algorithms to ensure that there is differentiation between the spectra of the different products within the library (Kemper & Luchetta 2003).

Vision® contains four databases, namely a security database, a project database, a library database and a diagnostic database. The security database contains user identifications, passwords, security access levels and user preferences while the project database contains all spectral and constituent data needed for qualitative and quantitative model development, data collection methods, calibrations, equations and operations methods. The library database contains qualitative methods/models, pointers to spectra in the project database as well as validation results, and the diagnostic database contains the results of all instrument diagnostic tests and evaluations. (FOSS NIRSystems 2005)

3.2.3 Instrument Diagnostics

The diagnostics option is used to test and monitor the performance of the instrument. The daily diagnostic for the instrument is the performance test, which is for routine instrument maintenance and monitoring. This is a comprehensive test of the instrument operation and is therefore the final assurance that the instrument is ready to scan the sample. This includes the wavelength accuracy and precision, which compares the known peak positions of the internal reference materials to the peak position measurements of the instrument. This information is not downloaded to the instrument and is presented as a report. (FOSS NIRSystems 2005)

Instrument noise and amplifier gain also form part of the performance test. The instrument performs the noise test by scanning the internal ceramic as a reference and as a sample. The difference in the scans represents the noise which in theory, should be zero. The scanning is repeated ten times and the results are assessed to determine if they are within specification. Figure 3.2 represents spectra from a noise test that complies with specifications. (FOSS NIRSystems 2005)

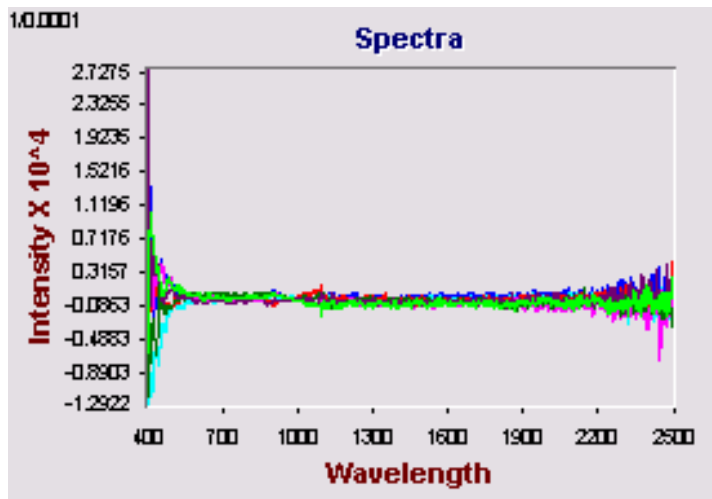


Figure 3.2 Spectra from instrument noise test (FOSS NIRSystems 2005)

The instrument performance verification (IPV) setup test provides the initial instrument response to calibrated photometric standards. This process verifies the photometric response of the instrument at 2 %, 10 %, 20 %, 40 % and 99 % reflectance using external certified standards. The responses to the external standards are compared to the standards on file. These responses should not be outside the acceptable tolerance limits. Following the IPV setup, routine photometric tests are conducted to monitor the photometric performance of the instrument. The photometric test compares current spectra of each standard to those stored during IPV setup. (FOSS NIRSystems 2005)

Wavelength certification tests are also conducted to confirm the peak positions of the instrument to a defined external standard. No adjustments are made. These diagnostics tests are critical to ensure that the instrument is performing within the required specifications. (FOSS NIRSystems 2005)

3.3 METHODOLOGY

3.3.1 Overview of methodology

An overview of the activities for the development and validation of the library is shown in Figure 3.3.

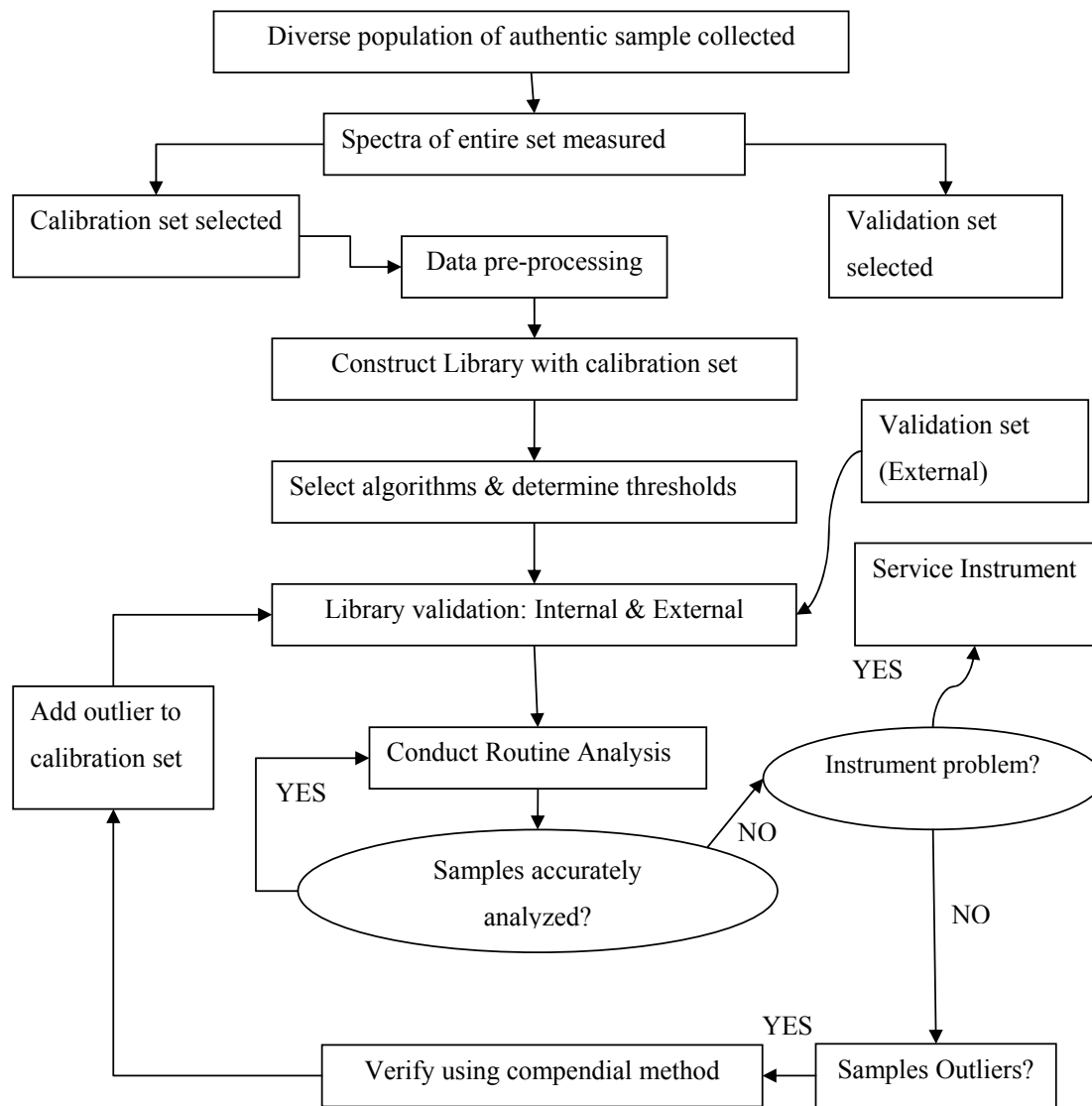


Figure 3.3 NIR calibration flow chart (adapted Workman 2001)

3.3.2 Materials used

The intended use of this library is for the identification and qualification of starch maize EP 2002 and lactose monohydrate EP 2004. Excipients commonly used by the facility in the powder form were chosen for the development of the spectral library.

Material usage printouts were obtained in order to select the raw materials for the development of the spectral library. The top 50 products were obtained in terms of use by volume and cost. The six raw materials chosen were based on high volume usage. Table 3.1 shows the raw materials chosen for the development of the spectral library. The item number refers to specific numbers that is used by the facility to differentiate between materials.

Table 3.1 Raw materials for the development of the spectral library

Item number	Raw material
103310	Lactose monohydrate EP 2004
115260	Microcrystalline cellulose PH101 EP 2002
103190	Povidone K25 EP 1997
106320	Purified talc EP 5.01
122420	Aci-di-sol USNF 22 Supp 2 (Crosscarmellose Sodium)
105880	Starch maize EP 2002

The facility stores retention samples of all batches of raw materials. Authentic retention samples were chosen for the calibration (“training”) of the NIR system. These raw materials are from the approved suppliers to the facility and have been approved by the quality control laboratory as acceptable for use.

3.3.3 Sample selection for library calibration

A spectral library represents samples of spectra or samples of product that have been selected from a project. Kemper and Luchetta (2003) recommend twenty batches or more of each raw material to represent statistically the batch-to-batch variability for most products as it is important to build the acceptable batch-to-batch variability into the library.

The chosen six raw materials with a minimum of twenty batches per raw material were used to train the system. The batches were chosen from the most recent batches to ensure that the age of the sample did not affect the spectral response. (Kemper & Luchetta 2003)

3.3.4 External library validation (positive and negative challenges)

In order to use the spectral library for identification of starch maize and lactose monohydrate, a second set of samples was used for the positive challenge of the library. Samples of starch maize and lactose monohydrate that were not present in the spectral library were used to run a routine analysis and assess the spectral response to these samples. The rationale for doing this is to verify that the library and the set chemometrics were capable of recognizing these samples and that there were no mismatches. (Kemper & Luchetta 2003)

In addition, negative challenges to the library were performed, the purpose being to ensure that the spectral library could differentiate between similar materials (Kemper & Luchetta 2003). These could be structural similarities or nomenclature similarities. To confirm the specificity of the spectral library to starch maize and lactose monohydrate, pregelatinized starch and tablettose were used as the negative challenge to the library. (Section 3.4.7 provides the rationale for the choice of these materials as the negative challenge).

3.3.5 Experimental

The NIR spectra of the selected samples were collected using the Vision ® software and the RCA instrument. The data collection parameters were set to measure the full range (400 – 2500 nm). Reflection was used as the detector type as all the samples are solids. The instrument was set to measure 32 scans per sample with an analysis time of approximately 30 seconds per sample.

The effective sample size in NIR methodology is significantly smaller than in conventional methods, and is often less than a unit dose size. This is due to the area of sample that is illuminated by the NIR beam. (Pharmaceutical Analytical Science Group (PASG) 2001)

Retention samples are stored in 50 ml glass bottles with a diameter of 30 mm and contain approximately 100 g of sample. The samples were presented to the instrument in this manner. The powders in the glass bottles were placed directly on the RCA window of the instrument. The iris adapter was used to centralize the bottle. The spectra of the material were then measured through the bottom of the bottles. Care was taken to ensure consistent packing against the optical surface as sample presentation is a potential source of variation during sample measurements (Kemper & Luchetta 2003).

3.3.6 Data analysis

Chemometrics is defined as the application of mathematical procedures for processing, evaluating and interpreting large amounts of data. It is applied to find statistical correlation between spectral data and known properties of a sample. Prior to processing the data, preprocessing is usually performed to determine any baseline drift or slope in the spectrum. (Ciurczak & Drennen III 2002b)

A project for the calibration was created using the selected six raw materials. The measured spectra were visually examined for the presence of anomalies or outliers. Potential outliers were investigated and documented.

A library was then constructed using the spectra from the project. All spectra in the library were qualified mathematically and an “Identification Method Development” was created. The library was validated (internal validation) by running the internal validation available on the Vision® software. The positive challenges to the library were then carried out with the authentic samples of starch maize and lactose monohydrate. Pregelatinized starch and tablettose were used to conduct the negative challenges to the library.

The chemometric algorithms available on the Vision® software are as follows:

- Mathematical pre-treatments and scatter corrections (N-Point Smooth, Derivatives, Standard Normal Variate (SNV), Baseline Correction, Detrend, Savitsky-Golay, Multiple Scatter Correction)
- Sample selection- population structuring (Random, Maximum Distance in Wavelength Space, Mahalanobis Distance in Principle Component Space)

These chemometric algorithms were used to extract information from the spectra in order to relate physical or chemical properties of the investigated samples to the absorption of radiation in the NIR wavelength (Bokobza 1998).

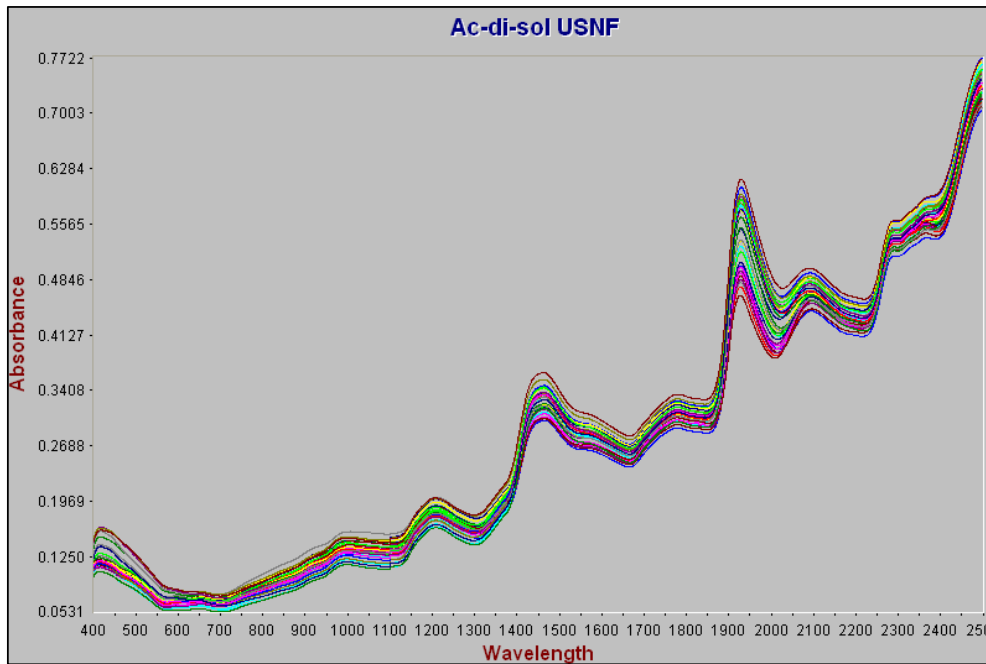
3.4 NIR METHOD DEVELOPMENT

3.4.1 Visual inspection and mathematical pre-treatment of spectra

Figures 3.4 (a) and (b) to Figure 3.9 (a) and (b) represent the raw spectrum and the second derivative respectively of the raw materials for inclusion in the spectral library. The spectral library represents the acceptable variation from batch to batch. The second derivative is useful in reducing noise and accommodating for the baseline shifts. For the application of the second derivative to the spectrum a segment size of 10 nm and a gap size of zero was used (this is recommended by the supplier). The segment size is the group size of the information used in the calculation and the gap is the distance between the groups. The software uses the absorbance values of the spectra in the segments to calculate the selected mathematical pre-treatment causing the generation of a new spectral pattern.

The spectra of the raw materials were visually examined for any potential anomalies. Povidone K25 showed some variation from batch to batch. This acceptable variation was included in the library as these samples fell within the specified acceptable standards used by the facility. Thereafter the sample selection option on the Vision® software was applied to statistically identify any potential outliers.

a)



b)

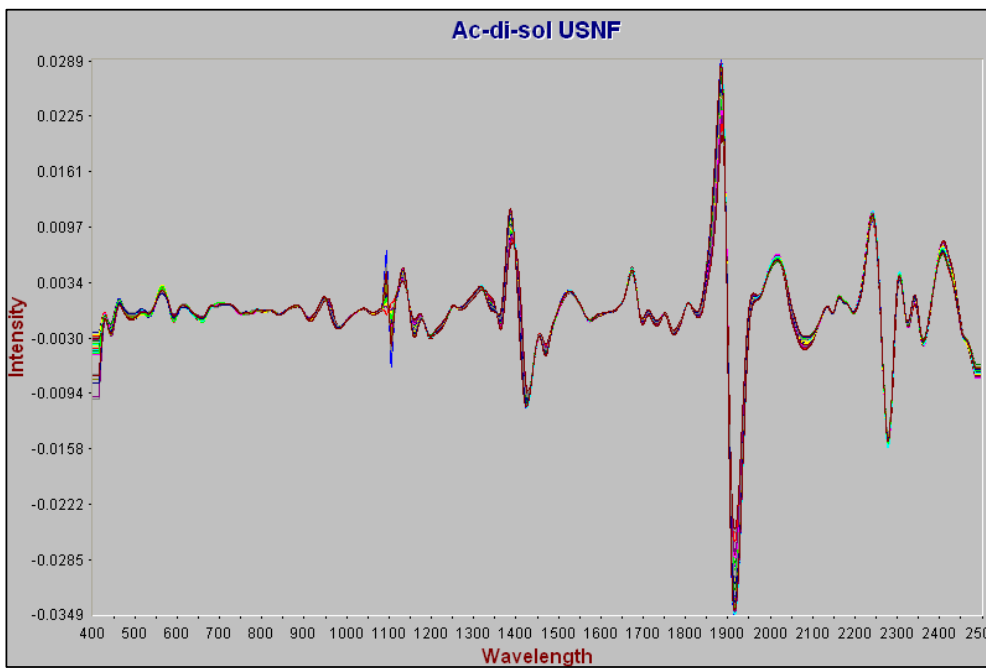
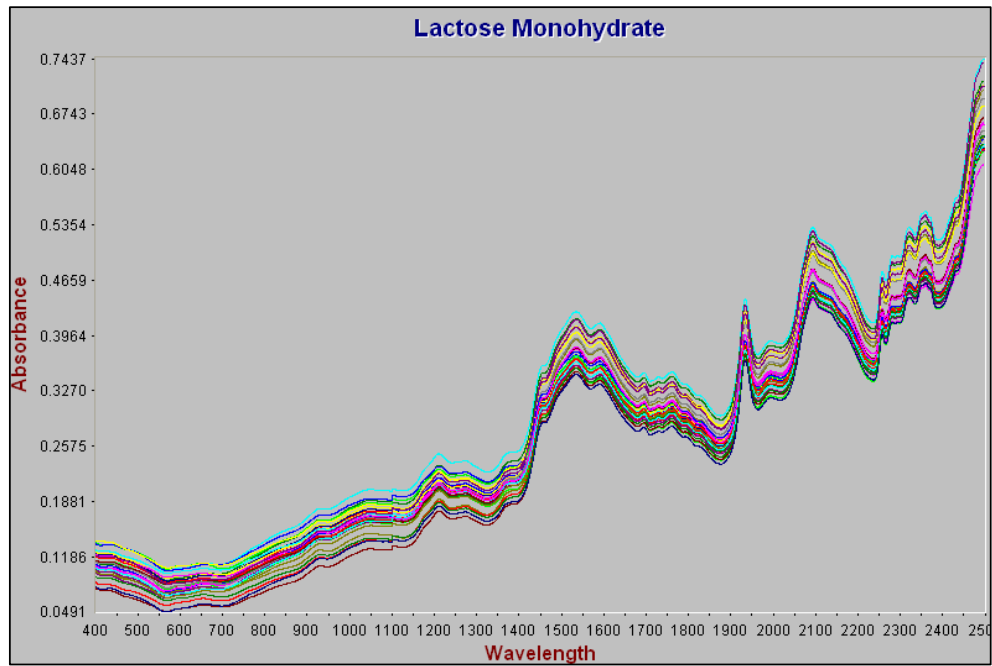


Figure 3.4 (a) Untreated spectra of 31 batches of ac-di-sol USNF
(b) Second derivative of 31 batches of ac-di-sol USNF

a)



b)

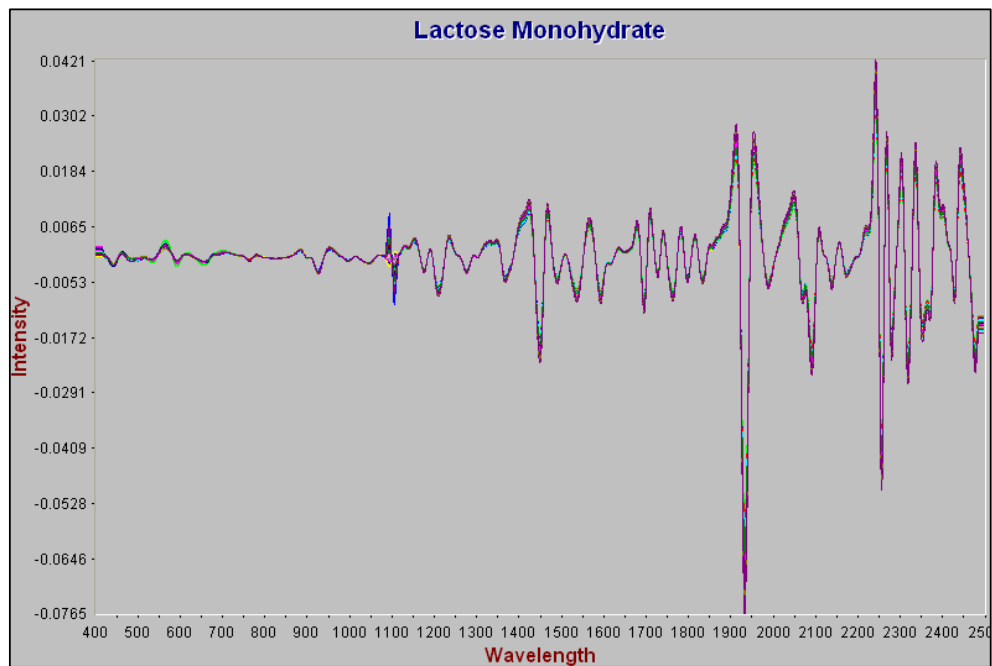
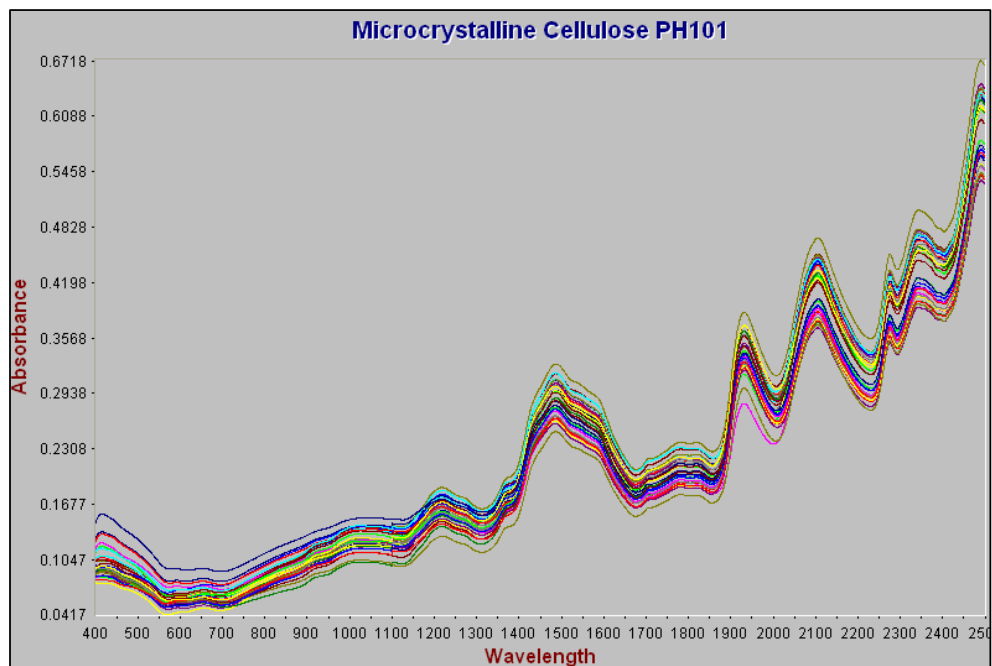


Figure 3.5 (a) Untreated spectra of 30 batches of lactose monohydrate
(b) Second derivative of 30 batches of lactose monohydrate

a)



b)

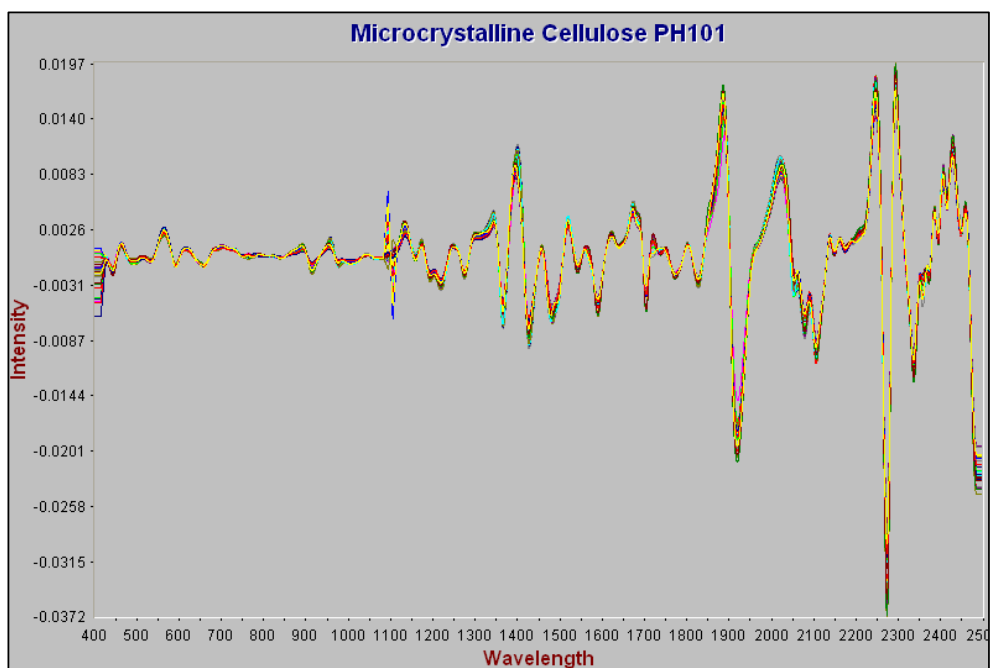
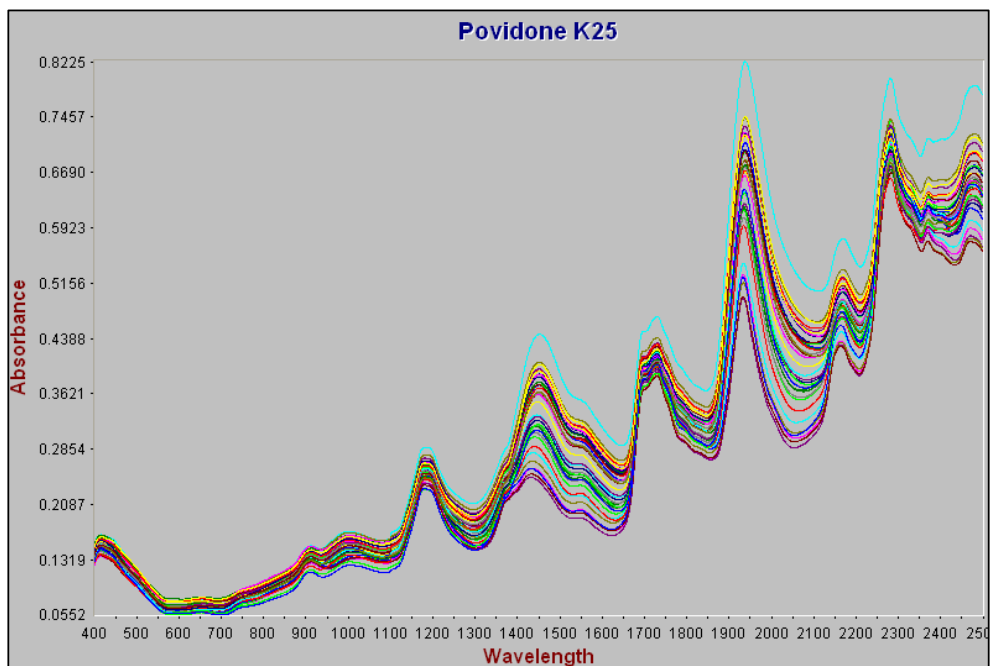


Figure 3.6 (a) Untreated spectra of 34 batches of microcrystalline cellulose
(b) Second derivative of 34 batches of microcrystalline cellulose

a)



b)

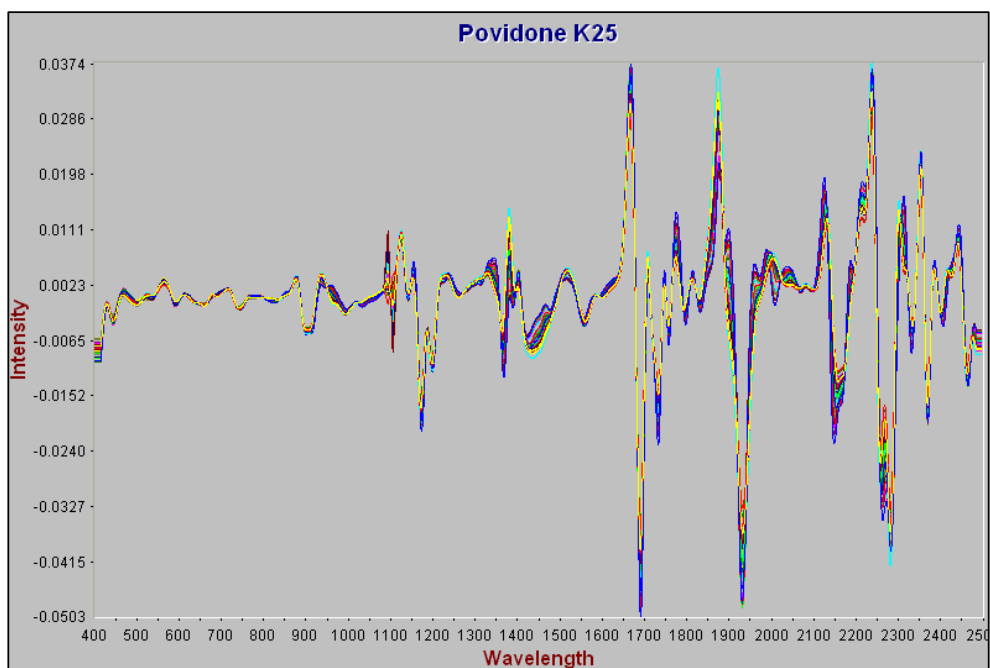
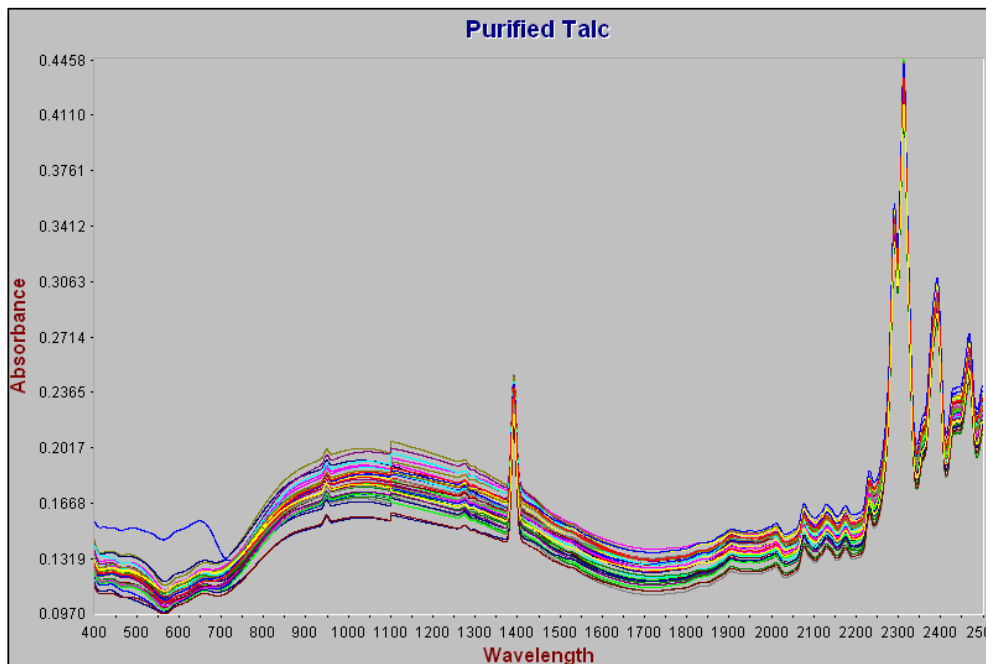


Figure 3.7 (a) Untreated spectra of 37 batches of povidone K25

(b) Second derivative of 37 batches of povidone K25

a)



b)

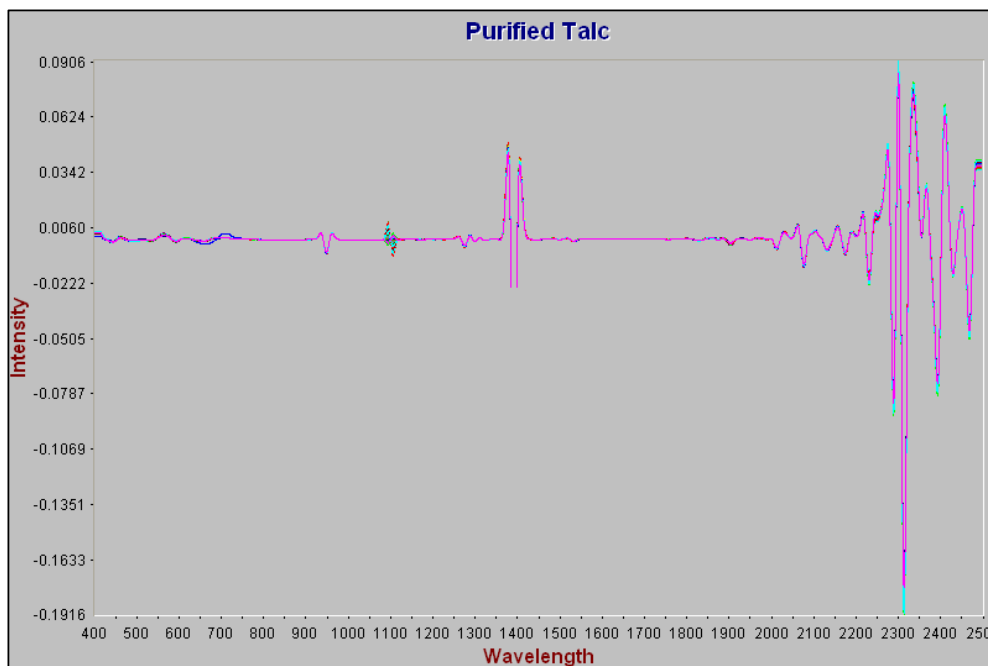
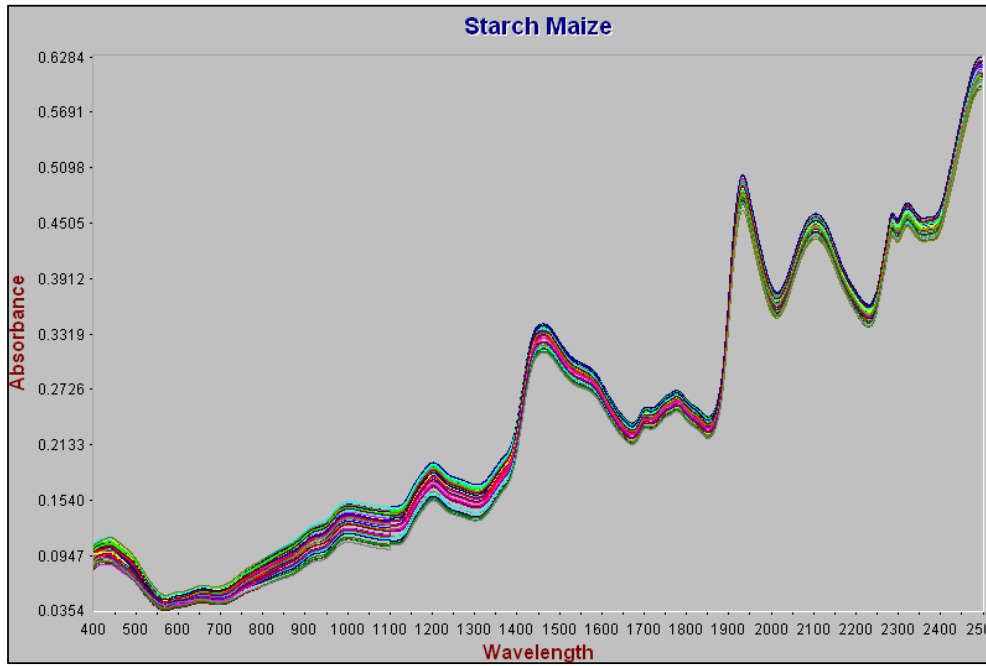


Figure 3.8 (a) Untreated spectra of 34 batches of purified talc
(b) Second derivative of 34 batches of purified talc

a)



b)

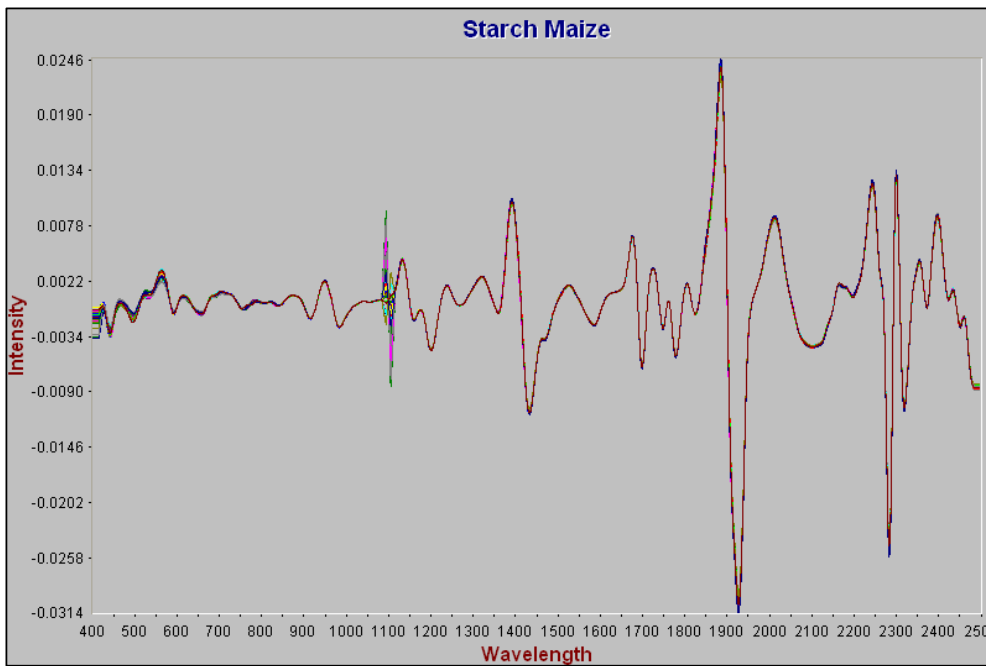


Figure 3.9 (a) Untreated spectra of 42 batches of starch maize
(b) Second derivative of 42 batches of starch maize

3.4.2 Library calibration

Authentic samples were used to construct the spectral library, that is, the batches have undergone chemical testing in the quality control laboratory and satisfied the quality control specifications. The spectra were then processed through the sample selection route available on the Vision® software. The purpose of sample selection is to identify spectral outliers or redundant samples. The sample selection route results in three sets of samples, namely, a training set or calibration set, an acceptance set and a rejection set. Spectra that fall into the rejection set are defined as outliers and are statistically different to the rest of the samples in the set. If sample spectra are identified as outliers then a decision must be made to either include or exclude these spectra from the library based on the authenticity of the sample, which can be confirmed by chemical analysis. Based on the fact that all samples chosen for the building of the library were authentic, the mathematics used was customized so that all samples fell in the training set. Table 3.2 tabulates the default sample selection option on the Vision® software.

Table 3.2 Recommended sample selection options

Mahalanobis Distance in Principal Component Space	
2nd derivative Segment = 10.0 nm Gap = 0.0 nm	
Components: Cumulative Variance	
Wavelength Region	
Minimum	Maximum
416 nm	1090 nm
1114 nm	2484 nm
Outlier threshold = 0.95	Threshold Type: Probability Level
Outlier threshold = 3	Threshold Type: Match Value

This sample selection option was applied to the spectra of the raw materials. The outlier threshold type used was either a probability level of 0.95 % or a match value of 3. With the probability level, a level of confidence is generated that the sample belongs to the set. With a match value, a chemometric value is generated for the spectrum and if this value is equal to or below the threshold then the spectrum belongs to the sample set.

The rationale of choosing the wavelength region 416 nm to 1090 nm and 1114 nm to 2484 nm was to remove the “noise” that resulted from the transition from the visible part of the spectrum to the near infrared part of the spectrum at 1100 nm.

The sample selection option produces four types of figures that visually display the results obtained namely:

- An intensity versus (vs.) wavelength figure that shows all the spectra in the sample set. In the event that any of the samples were outliers, these would be visible in red. The purpose of this figure is to view how different the outlier spectrum is to the rest of the spectra.
- A percentage vs. principle component (PC) figure that shows the explained variance in the spectrum. Each principle component explains a percentage of the variance that exists in the samples. The fewer principle components present the lower is the variation in the sample set.
- A three-dimensional (3-D) cluster plot figure that visually displays the principle components in 3-D space. It is possible to view how far from the mean the outliers are located from the 3-D cluster plot.
- In the case where the threshold type is probability, a frequency vs. probability figure shows the probability that the sample belongs to the set and the frequency at which it occurs. The value one shows the probability that the sample does not belong to the set and the value zero shows the probability that the sample belongs to the set (a perfect fit).
- In the case where the threshold type is match value, a frequency vs. distance figures shows the actual number representing distance or residual variance. The smaller the distance, the greater the chance that the sample belongs to the set.

The following subsections represent the data obtained from the calibration of the spectral library.

a) Ac-di-sol USNF22 Supp

The recommended sample selection option was used for ac-di-sol USNF, with the threshold type being probability set at a value of 0.95 %. No samples were identified as rejects (outliers) and all samples fell into the training set as can be seen in Figure 3.10.

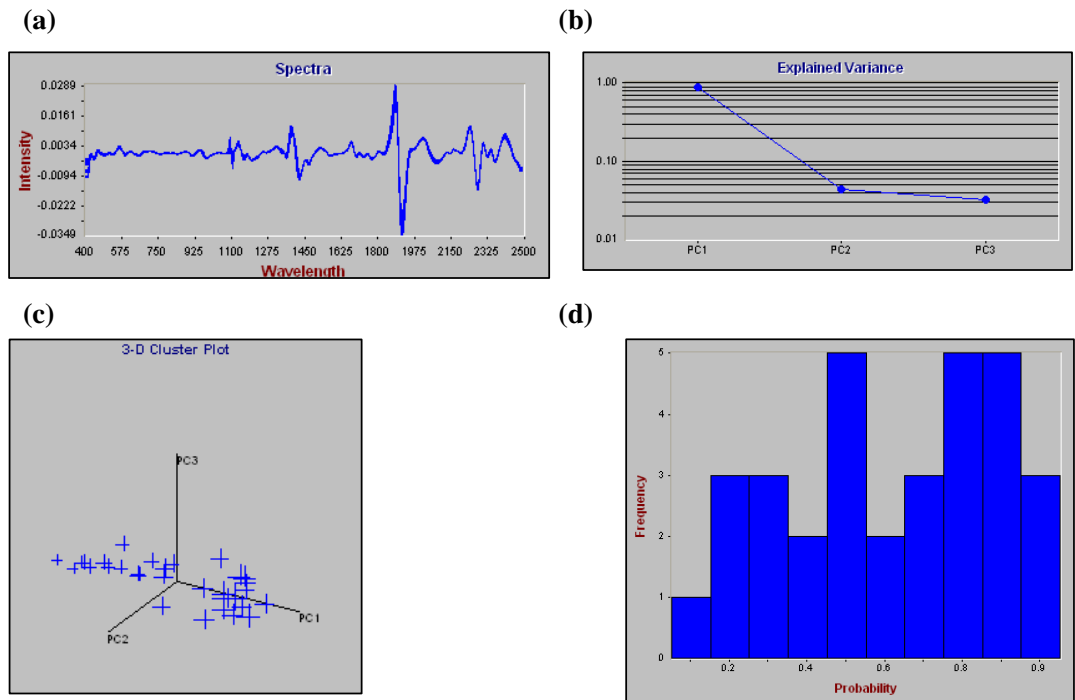


Figure 3.10 (a) Spectra of samples of ac-di-sol USNF
(b) Explained variance within the samples of ac-di-sol USNF
(c) 3-D cluster plot of ac-di-sol USNF
(d) Frequency vs. probability of the samples of ac-di-sol USNF

Figure 3.10 (a) shows that no samples were identified as rejects or outliers. The variance in the samples can be explained in three principal components (seen in Figure 3.10 (b) and (c)), therefore there is no great variation in the samples. PC 1 can explain approximately 90 % of the variance in the samples therefore; there is no great variation in the samples.

b) Lactose monohydrate EP 2002

The recommended sample selection option was used for lactose monohydrate, with the threshold type being probability set at a value of 0.95 %. Two samples were identified as outliers as can be seen in Figure 3.11 (in red).

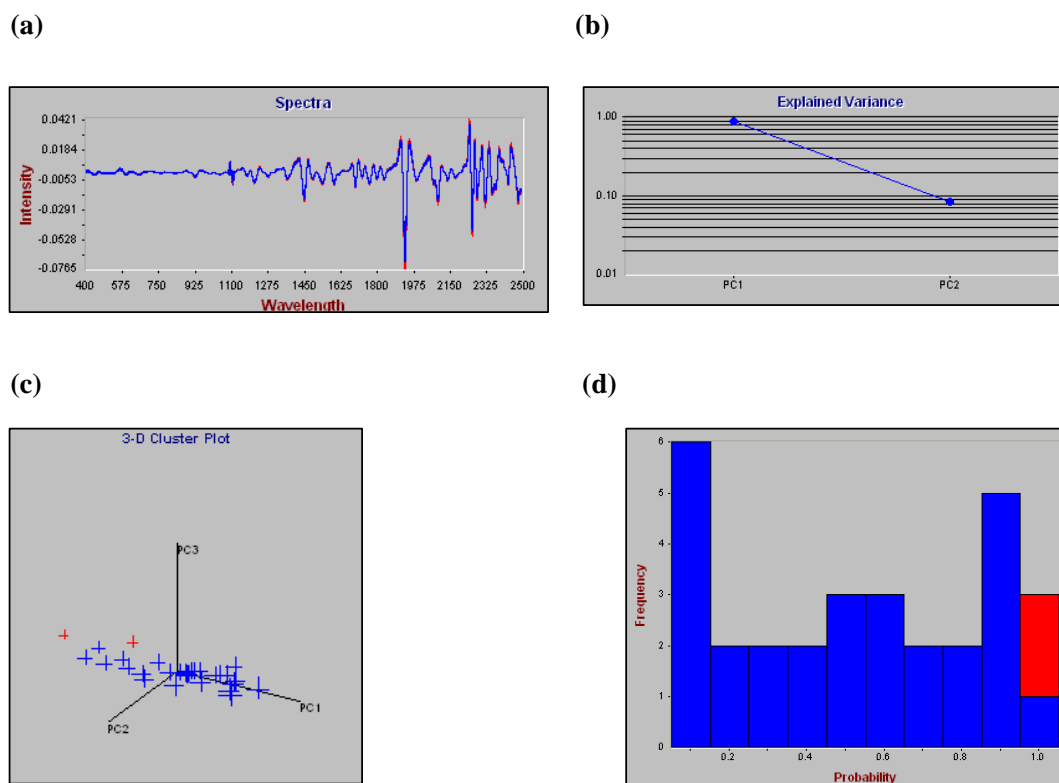
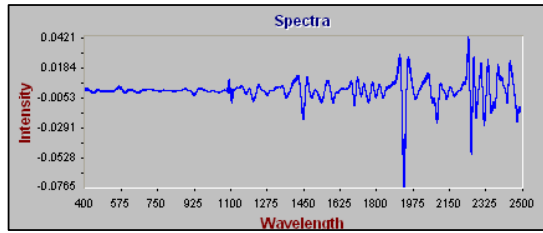


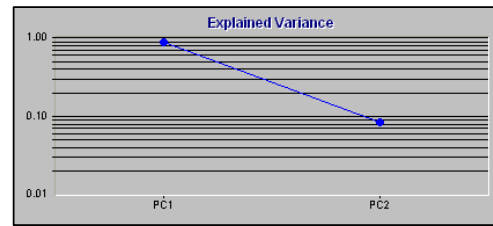
Figure 3.11 (a) Spectra of samples of lactose monohydrate
(b) Explained variance within the samples of lactose monohydrate
(c) 3-D cluster plot of lactose monohydrate
(d) Frequency vs. probability of the samples of lactose monohydrate

According to the certificate of analysis for the two batches namely, X052276 and X037695, these batches are authentic samples. It is evident that these samples are statistically different to the other samples. However, these samples need to be represented in the library to incorporate this accepted variation. Another mathematical approach was taken to allow these samples to be included in the training set. Instead of using the probability threshold, the match value threshold with a match value of 3 was used. This resulted in all the samples being classified in the acceptance set as seen in Figure 3.12.

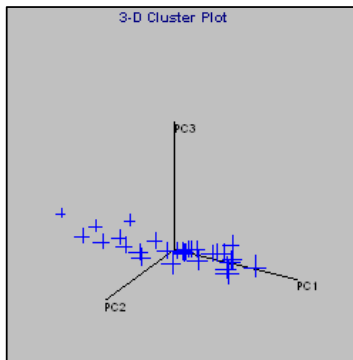
(a)



(b)



(c)



(d)

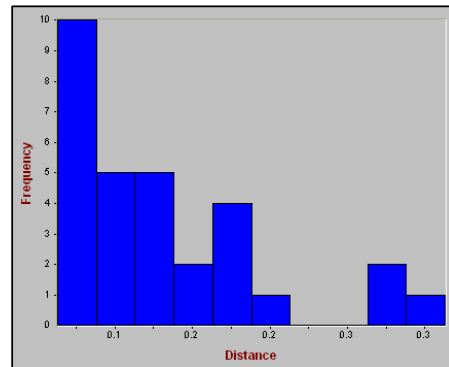


Figure 3.12 (a) Spectra of samples of lactose monohydrate
(b) Explained variance within the samples of lactose monohydrate
(c) 3-D cluster plot of lactose monohydrate
(d) Frequency vs. distance of the samples of lactose monohydrate

Figure 3.12 (a) shows that no samples were identified as rejects or outliers. The variance in the samples can be explained in two principal components (seen in Figure 3.12 (b) and (c)), therefore there is no great variation in the samples. PC 1 can explain approximately 95 % of the variance in the samples therefore; there is no great variation in the samples.

c) Microcrystalline cellulose

The recommended sample selection option was used for microcrystalline cellulose with the outlier threshold type being a match value of 3, no samples were identified as rejects (outliers) and all samples fell into the training set as seen in Figure 3.13.

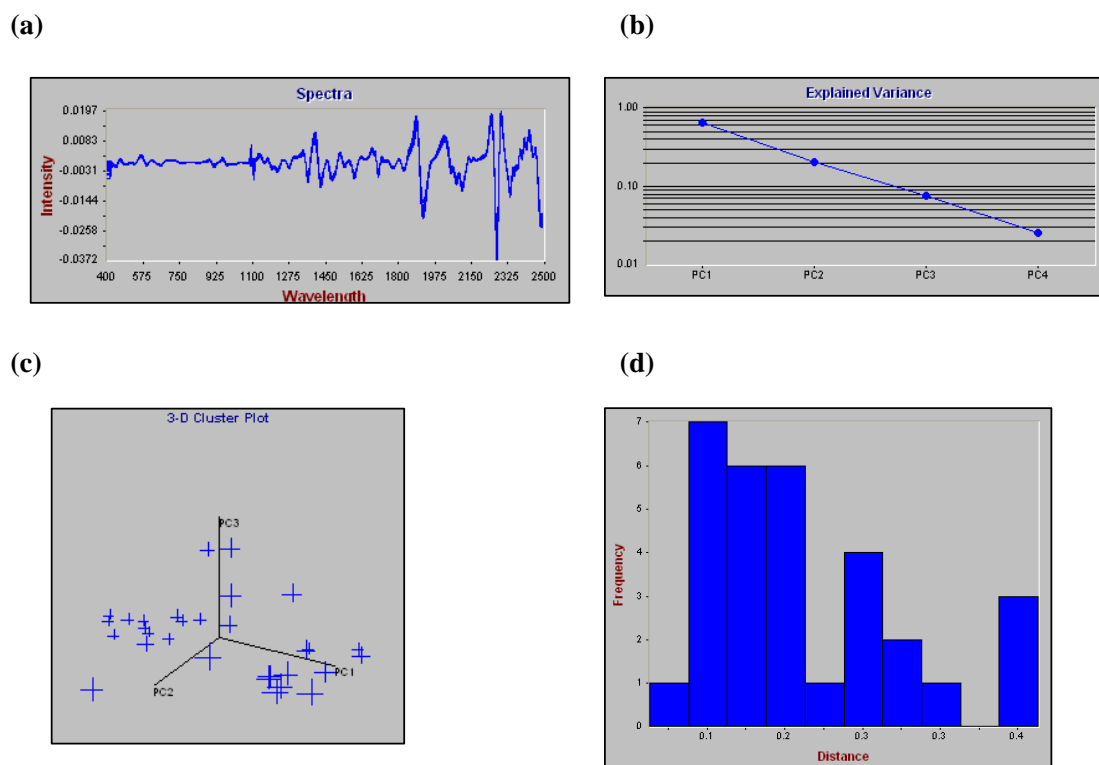


Figure 3.13 (a) Spectra of samples of microcrystalline cellulose
(b) Explained variance within the samples of microcrystalline cellulose
(c) 3-D cluster plot of microcrystalline cellulose
(d) Frequency vs. distance of the samples of microcrystalline cellulose

Figure 3.13 (a) shows that no samples were identified as rejects or outliers. The variance in the samples can be explained in four principal components (seen in Figure 3.13 (b) and (c)), therefore there is a slightly greater variation in the samples. PC 1 can explain approximately 80 % of the variance in the samples while PC 4 can explain approximately 10 % by of the variance in the samples.

d) Povidone K25 EP 1997

The recommended sample selection option was used for povidone K25 with the outlier threshold type being a match value of 3, no samples were identified as rejects (outliers) and all samples fell into the training set as seen in Figure 3.14.

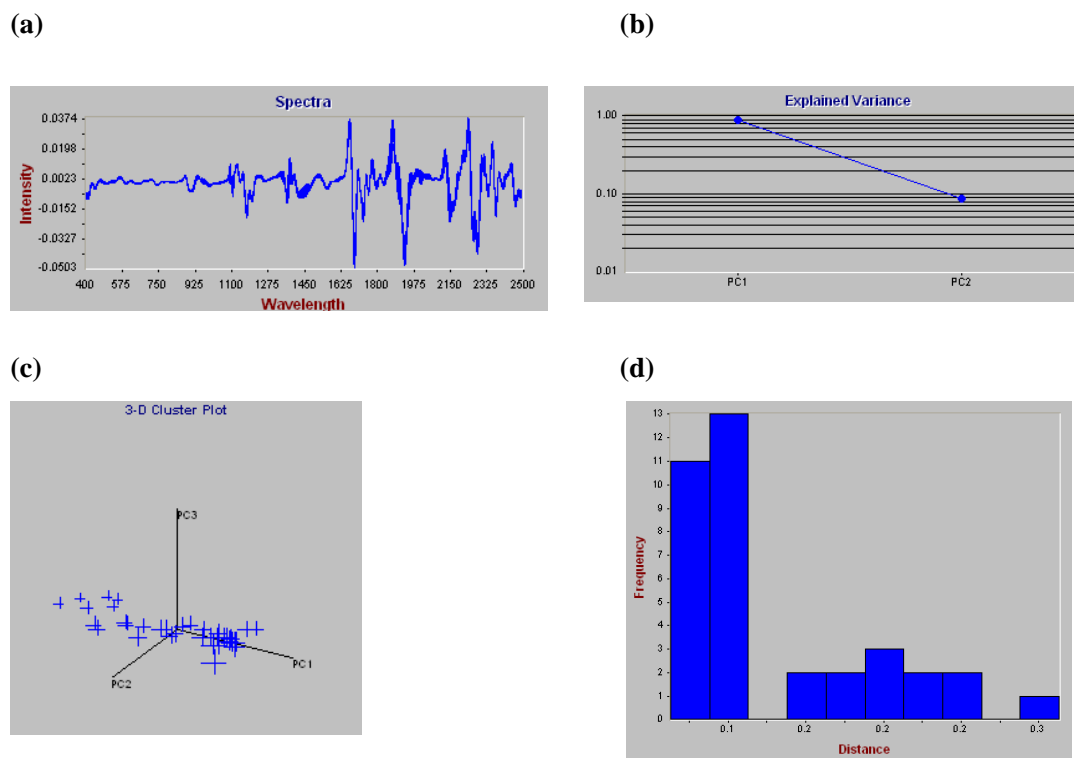


Figure 3.14 (a) Spectra of samples of povidone K25
(b) Explained variance within the samples of povidone K25
(c) 3-D cluster plot of povidone K25
(d) Frequency vs. distance of the samples of povidone K25

Figure 3.14 (a) shows that no samples were identified as rejects or outliers. The variance in the samples can be explained in two principal components (seen in Figure 3.14 (b) and (c), therefore the samples do not differ to a significant level. PC 1 can explain approximately 95 % of the variance in the samples.

e) Purified talc EP 5.01

The recommended sample selection option was used for purified talc with the outlier threshold type being probability of 0.95 %, no samples were identified as rejects (outliers) and all samples fell into the training set as seen in Figure 3.15.

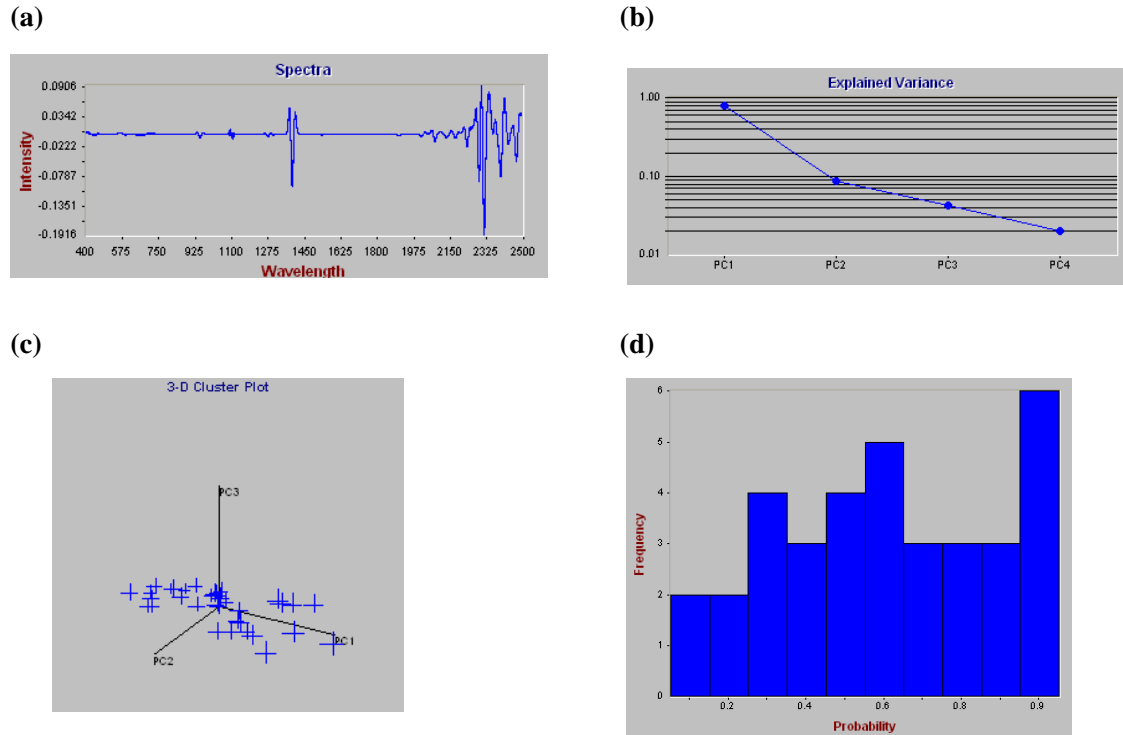


Figure 3.15 (a) Spectra of samples of purified talc
(b) Explained variance within the samples of purified talc
(c) 3-D cluster plot of purified talc
(d) Frequency vs. probability of the samples of purified talc

Figure 3.15 (a) shows that no samples were identified as rejects or outliers. The variance in the samples can be explained in four principal components (seen in Figure 3.15 (b) and (c)), therefore there is no great variation in the samples. PC 1 can explain approximately 90 % of the variance in the samples.

f) Starch maize EP 2002

The recommended sample selection option was used for starch maize with the outlier threshold type being a match value of 3, no samples were identified as rejects (outliers) and all samples fell into the training set as seen in Figure 3.16.

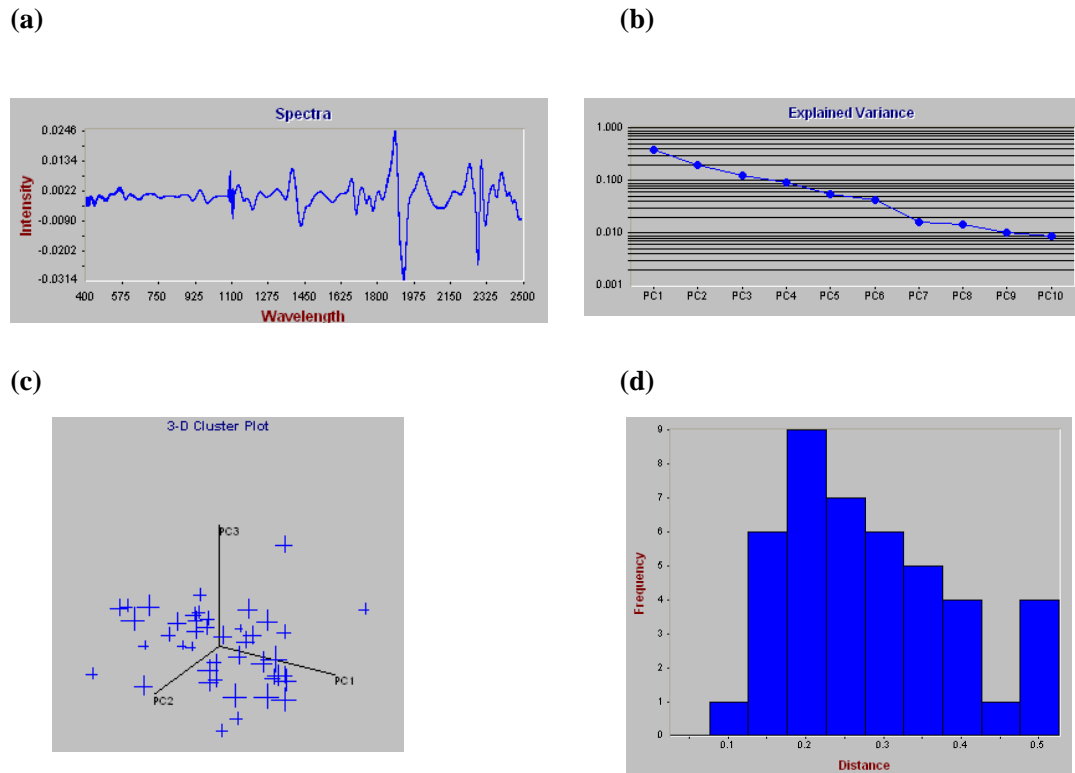


Figure 3.16 (a) Spectra of samples of starch maize
(b) Explained variance within the samples of starch maize
(c) 3-D cluster plot of starch maize
(d) Frequency vs. distance of the samples of starch maize

Figure 3.16 (a) shows that no samples were identified as rejects or outliers. The variance in the samples can be explained in ten principal components (seen in Figure 3.16 (b) and (c), therefore there is a significant variation in the samples. This variation is acceptable as defined by the internal quality control of the facility as all the samples are approved samples. This variation in starch maize may be due to it being a naturally occurring material.

3.4.3 Qualification of products

For a pharmaceutical company it is imperative that the raw materials always meet pre-defined quality criteria. Product qualification on the Vision® software allows for the creation of more stringent limit on the particular material. The products in the library were qualified to ensure that the quality of tested material always meet the pre-defined limits. It is possible that a test material could be identified but not qualified, as the quality is not equivalent to batches accepted in the past.

The qualification method used was correlation in wavelength space with the threshold type being a match value of 0.9. The mathematical pre-treatment was the second derivative as seen in Table 3.3.

Table 3.3 Qualification method used for the raw materials in the library

Correlation in wavelength space	
2nd derivative	
Segment = 10.0 nm Gap = 0.0 nm	
Wavelength Region	
Minimum	Maximum
416 nm	1090 nm
1114 nm	2484 nm
Threshold = 0.9	Threshold Type: Match Value

3.4.4 Identification method

The identification method is a global mathematical method that is used by the software to distinguish between individual materials in the spectral library during the internal validation. Upon application of this method, all materials in the spectral library must be correctly identified and there must be no mismatches. There are different chemometric algorithms available on the software, these were applied in turn until the algorithm used can differentiate between the different materials. Table 3.4 shows the method that was used.

Table 3.4 Identification method used for the raw materials in the library

Residual variance in principal component space	
2nd derivative	
Segment = 10.0 nm Gap = 0.0 nm	
Cumulative variance: 95 %	
Wavelength Region	
Minimum	Maximum
416 nm	1090 nm
1114 nm	2484 nm
Threshold Type: Match Value	Threshold = 0.3

3.4.5 Internal validation

Following the development of the identification method, an internal library validation was conducted on the software to evaluate the performance of the library. The purpose of an internal validation is to demonstrate that the samples can be discriminated from each other. The results show that the chemometrics applied is sufficient to discriminate between the different samples in the library. (Refer to Appendix A.1 for the spectral library validation report). Table 3.5 shows a summary of the internal validation results; all of the raw materials in the library were correctly identified. The chemometrics used is sufficient to discriminate between all the products in the spectral library.

Table 3.5 Summary of internal library validation

Product	Pass	Fail
Starch Maize EP 2002 Supp	42	0
Purified Talc EP 5.01	34	0
Povidone K25 EP 1997	37	0
Microcrystalline cellulose	34	0
Lactose Monohydrate EP	30	0
Ac-di-sol USNF 22 Supp	31	0

3.4.6 Positive challenge

The purpose of the positive challenge is to verify that the spectral library can recognize authentic samples during a routine analysis. Authentic samples of starch maize and lactose monohydrate were presented to the spectrometer and a routine analysis run. The spectral library correctly identified the samples used for the positive challenge which indicated that the algorithms and threshold values that were set in the database were sufficient for positive identification of authentic samples. (Refer to Appendix A.2 and A.3 for results of positive challenge of starch maize and lactose monohydrate)

3.4.7 Negative challenge

The algorithms and threshold values used to create the spectral library need to be efficient enough to pass an authentic sample but at the same time stringent enough to fail a sample that is not authentic although the sample may be similar to the materials in the spectral library. These materials are not represented in the library but can be logically confused with materials that are in the library.

a) Starch maize

Starch maize is obtained from the mature grain of corn, *Zea mays*. Starch maize is widely used in oral solid formulations where it is utilized as a glidant, diluent, disintegrant or binder. (Farhadieh 1994)

Pregelatinized starch, on the other hand, is a starch that has been chemically and mechanically processed to rupture the starch granules. In comparison with starch maize, pregelatinized starch may be produced with enhanced flow and compression characteristics. Pregelatinized starch is utilized as a binder, diluent or disintegrant. (Lordi 1994)

Starch maize and pregelatinized starch have the same chemical structure. It is possible that there could be a potential for misidentification when using the compendial methods for identification. It is therefore necessary for the NIR model created to be able to distinguish between the two.

Figure 3.17 shows the overlay of the spectra of starch maize and pregelatinized starch in the second derivative. Spectral differences are especially noted in the 400 - 500 nm range that corresponds to the visible part of the electromagnetic spectrum. This could be as a result of the difference in particle size distribution between starch maize (2 – 45 μm) and pregelatinized starch (30 – 150 μm) (Farhadieh 1994).

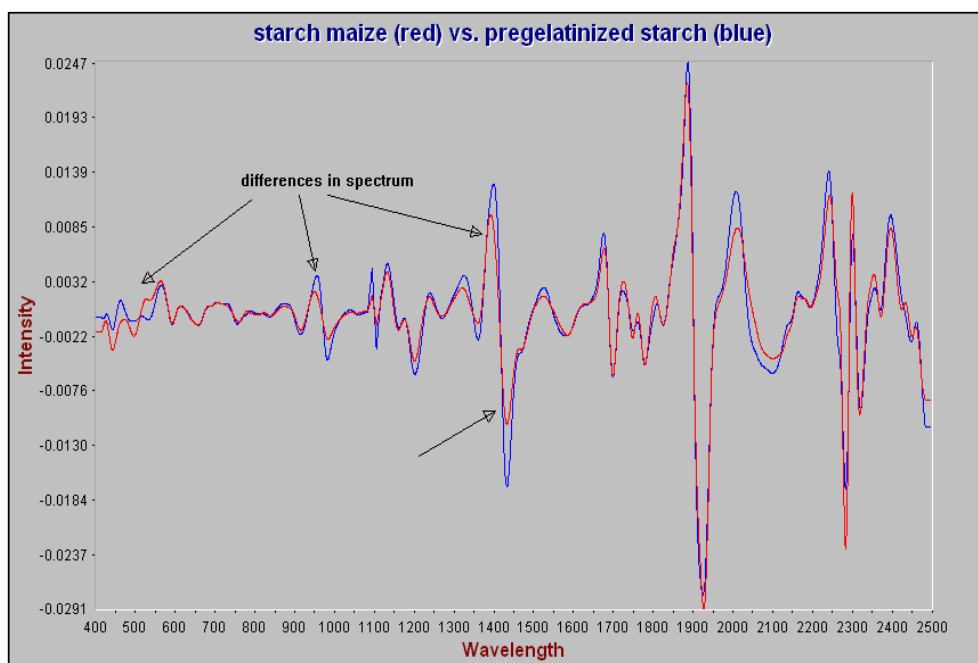


Figure 3.17 Overlay of starch maize and pregelatinized starch in the second derivative

The spectral library created was able to distinguish between starch maize and pregelatinized starch as the pregelatinized starch was not misidentified as starch maize and resulted in a “fail” status. (Refer to Appendix A.4 for the results report of the negative challenge with pregelatinized starch)

b) Lactose monohydrate

Lactose monohydrate is widely used as a diluent in oral solid preparations. Lactose monohydrate is available in many grades and one being a direct compression grade, tablettose. Tablettose is more fluid and compressible than crystalline or powdered lactose. Tablettose is often used to carry small quantities of drug and this permits tablets to be made without a need to granulate. (Goodhart 1994)

Lactose monohydrate and tablettose have the same chemical structure. It is possible that there could be a potential for misidentification when conventional methods are used. It is therefore necessary for the NIR model created to be able to distinguish between the two.

Figure 3.18 shows a magnified portion of the overlay of the spectra for lactose monohydrate and tablettose in the second derivative. Of note is that both spectra follow the same pattern of peaks and troughs, except that the tablettose spectrum has a higher intensity.

Samples of tablettose were run using the spectral library. The spectral library created was able to distinguish between lactose monohydrate and tablettose as the tablettose was not misidentified as lactose monohydrate and resulted in a “fail” status. (Refer to Appendix A.5 for results report of the negative challenge with tablettose)

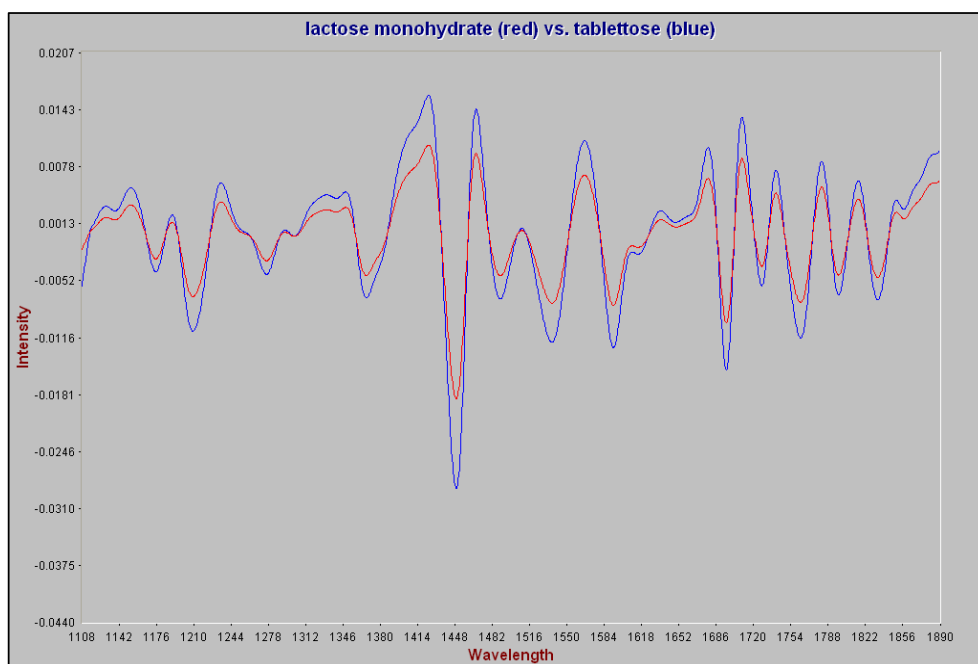


Figure 3.18 Overlay of lactose monohydrate and tablettose in the second derivative (part of spectrum magnified to show spectral differences)

Table 3.6 shows some of the positive and negative challenges to the library. The “ID result” represents chemometric values that are generated due to the algorithms used to

create the model. For the global identification method, the threshold value was set at 0.3, and as can be seen from the table that the positive challenges pass with values below 0.3 and the negative challenges fail with values above 0.3.

Table 3.6 Positive and negative challenges to the library

Challenge material	Type of challenge	ID result	Result
Starch maize	Positive	0.156	Match with library starch maize
Lactose monohydrate	Positive	0.130	Match with library lactose monohydrate
Pregelatinized Starch	Negative	7.107	No match in library
Tablettose	Negative	0.350	No match in library

3.4.8 Robustness

The robustness of the spectral library tests the effect of minor changes to the normal operating conditions on the analysis (PASG 2001). The robustness of the spectral library will have to be monitored over a longer period than was used for the experimentation. This can be achieved by varying the manner in which the samples are scanned, changing the operator and scanning on different days.

For routine use, procedures were implemented at the facility to address the case of “NIR non-conformance” against the spectral library. These include that the test sample should be verified using appropriate alternative tests, prior to its acceptance and incorporation into the spectral library.

3.5 DISCUSSION

The MCC (2003) define validation as a process to provide documented evidence that an item of equipment, process, system or method is in a state of control (i.e. that all assignable causes of variation have been eliminated) and is able to consistently deliver specified results. The term validation, in the regulatory context of a NIR method, refers to the establishment of appropriate data and documentation to certify that the method performs as intended, thus proving that a NIR method is providing results that correlate with reference methods (Ciurczak & Drennen III 2002b). There are three types of validation that need to be satisfied; namely, validation of the software, hardware and the NIR spectroscopic method.

The validation team of the facility conducted the validation of the software and hardware, which complies with all the specifications. The algorithms used to create the NIR method are capable of distinguishing between the different raw materials in the library. In addition, the NIR method satisfies the positive and negative challenges.

The negative challenge for starch maize was successfully achieved, as the spectral library did not misidentify pregelatinized starch as starch maize. One particular instance where a misidentification of the materials could have adverse effects on the production of product is in the use of starch maize and pregelatinized starch as binders. At this pharmaceutical company, when pregelatinized starch is used as a binder, the paste is prepared by dispersing the pregelatinized starch in cold water. The use of starch maize as a binder would entail that it is first dispersed in cold water before the addition of boiling water to form a paste. It is evident that the method of preparation of the binding solution is specific to the material that is used.

Identification tests should be able to discriminate between compounds with closely related structures (ICH 1994). The spectral library was also able to discriminate between lactose and tablettose. In a pharmaceutical environment, it is critical to be able to distinguish between different grades of material as the physical properties associated with different grades may have a profound effect on the manufacture of the final product. In this particular instance, the use of the incorrect grade of lactose could result in a failure to manufacture the product.

3.6 SUMMARY

For the validation of the NIR method to be accepted, evidence of specificity and robustness must exist (PASG 2001). The spectral library conforms to these standards thus the spectral library is validated for the identification and qualification of starch maize and lactose monohydrate.

As demonstrated by the specificity tests conducted, NIR has the ability to differentiate between chemically similar materials. This provides a great advantage to the pharmaceutical environment, and the fact that the NIR analysis can take as little as 30 seconds with no need for sample preparation makes the method advantageous over traditionally used chemical methods.

The general procedure that is followed when the company receives a consignment of raw material is that the material is held in quarantine until it is tested. It may take as long as one week for a batch of raw material to be tested and approved for production. With the application of NIR analysis to raw material identification and material qualification, time, cost and resource saving can be achieved. It also becomes possible to ensure 100 % identification in a batch with several containers instead of reduced testing that may sometimes be employed to certain raw materials.

The robustness of the spectral library was only monitored for the period of the experimentation however; this will have to be monitored over a greater period during daily operation to ensure reliability and repeatability.

The current protocol for the testing of starch maize and lactose monohydrate cannot be changed without prior approval from the MCC. It would be advisable to use the NIR method in parallel with the compendial testing methods for a period of 3 months. This would verify that the samples in the library are representative of the current raw materials received and that the library can identify samples correctly. The data collected over the set period can be used to demonstrate confidence in the NIR method and thereafter be submitted to the regulatory authorities for approval.

In addition to the positive and negative challenges, it would be beneficial to assess the levels of contamination or adulteration that can be picked up by the NIR method.

This would entail “spiking” the authentic sample with different levels of contaminate and running a routine analysis using NIR. It would be of interest to observe at what percentage of contaminate the sample is not qualified and at what level of contaminate the sample is not identified. This would also facilitate understanding, if any, of the limitations of the NIR method.

CHAPTER 4

BLEND UNIFORMITY ANALYSIS

4.1 INTRODUCTION

The blending of solids is a critical step in the production of many pharmaceutical products. Homogeneity of blends is essential for obtaining high quality products of uniform content. The overall intent of blending is to obtain a uniform mixture of all ingredients including actives and excipients. Lack of content uniformity can lead to serious therapeutic implications on patients. (El-Hagrasy *et al.* 2001) In addition, poor mixing after the addition of lubricants to a blend can lead to compression problems as outlined in section 2.3.2.3.

At present, blend quality is measured by looking at the concentration and distribution of the active pharmaceutical ingredient. This is generally conducted at the end of the manufacturing process by taking samples across three layers from the blend i.e. top, middle and bottom using a sample thief. The concern with this method is that the sampling techniques could influence the results and that only one component of the blend is analyzed. It is important to note as discussed by Ciurczak and Drennen III (2002a) that the actual materials blended and the efficiency of the blender contributes to the optimal blending time determination. Factors such as particle size, shape and density add to the complexity of end-point determination.

Most pharmaceutical active ingredients and excipients absorb radiation in the NIR region, therefore the NIR method provides advantages over traditional methods of assay for blend homogeneity or it can complement the traditional methods by providing homogeneity information on all components in the blend (Ciurczak & Drennen III 2002a). Lubricants are added to granule and blended to form a film of low shear strength around the granule thereby reducing the friction at the die wall during tablet compression (Marshall 1986). The prediction of blend homogeneity of lubricants in granule using NIR was assessed to identify and prevent problems associated with poor lubrication.

4.2 EQUIPMENT

The SP15 NIR Laboratory Blender manufactured by Buck Systems was used for this study. The technology works by using a combination of a Zeiss Corona NIR measuring head, a Corona data analyser and radio frequency transmitters and receivers. There are proximity switches in the blending head that activate the measuring head at the right time to trigger the data acquisition. The system is integrated and has a permanent power supply to the Corona head. The spectrometer and radio frequency communication system is fully enclosed within the body of the blender. (Buck Systems 2005)

The SP15 NIR Laboratory Blender used for the experimentation can be seen in Figure 4.1. The fibre optic bundles pick up the reflected light from the test material in the intermediate bulk container (IBC), via the sapphire window, and this is sent into the data analyzer. Data is transferred by radio frequency from the Laboratory Blender to a local computer. The blender is supplied with a combination of Winaspect® and ProcessXplorer® software, version 1.1 (Carl Zeiss Jena GmbH), to allow the data to be analysed and displayed. The software provides analytical techniques, such as fingerprint methodology for each ingredient, and rate of change of the blend.

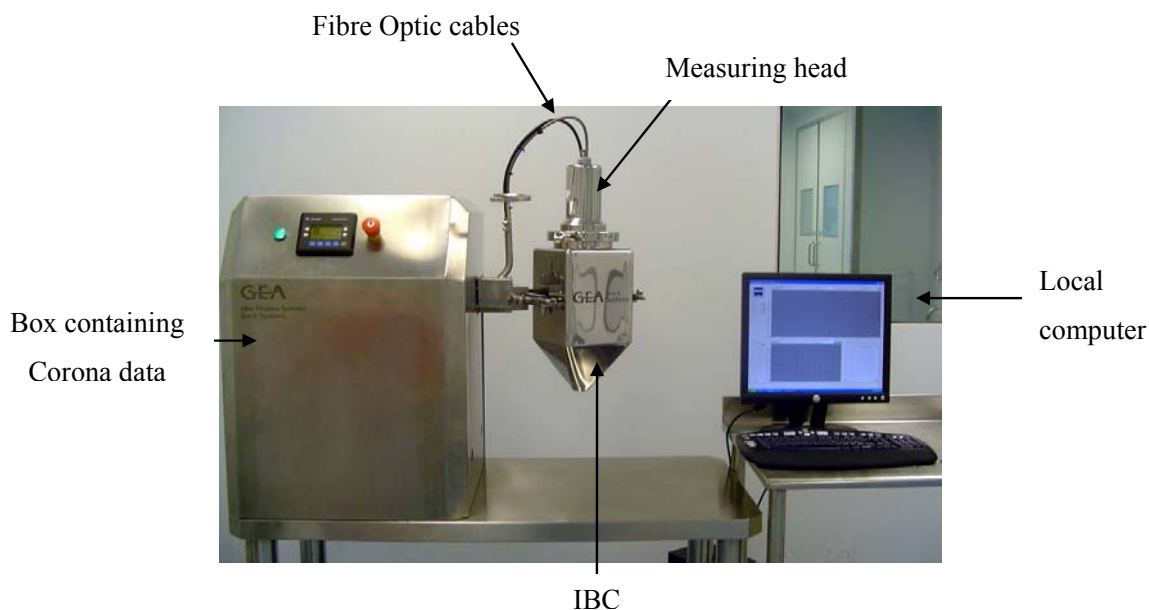


Figure 4.1 SP15 NIR Laboratory Blender

There are two gravity switches that are housed in the spectrometer and are triggered for acquisition of spectra when the IBC is in a vertical state. Figure 4.2 depicts a schematic of the IBC and the trigger switches. The IBC is shown in an inverted state and the switches are triggered for data acquisition.

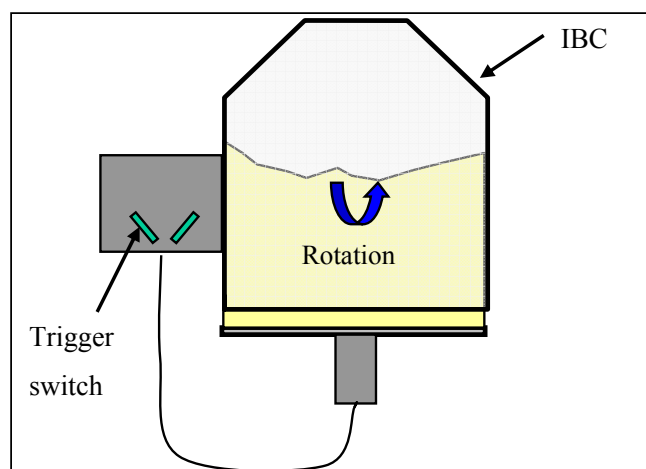


Figure 4.2 Schematic of IBC and gravity trigger switches (Hammond 2005)

The IBC blending bins are designed to mix through the conical lower section, but the flat top means that the blend “falls” on the lid during the part of the revolution when the IBC is inverted. At this point the sample is static in relation to the lid. The blend is stationary from approximately 45 degrees prior through to 45 degrees post the bottom dead centre position. At a blend rotation of 10 rpm – 15 rpm the blend is static for 1-1.5 seconds per revolution, which makes NIR data analysis ideal, as the NIR spectrometer is capable of generating an average spectrum in less than one second. (Warman 2004)

4.3 METHODOLOGY

Two types of blend monitoring experiments were conducted, namely a powder blend and a granule blend. Both types of blends were designed to monitor the homogeneity of the lubricant (i.e. magnesium stearate) in the blend.

4.3.1 Materials used

The materials that were used for the powder blend monitoring were lactose monohydrate and magnesium stearate. The lactose monohydrate and magnesium stearate were obtained from the drug dispensary of the facility in powder form.

The materials that were used for the granule blend monitoring were Ridaq® granule and magnesium stearate. The magnesium stearate was obtained from the drug dispensary of the facility in powder form. The granulation department of the facility supplied one batch of 100 kg of Ridaq® granule, which is an in-house proprietary granule. This was manufactured according to the production directive. The excipients that were used to manufacture the Ridaq® granule were dye Len Lake yellow, starch maize, microcrystalline cellulose, hydrochlorothiazide (active ingredient) and lactose. The material was granulated in a high shear mixer using purified water, starch maize and polysorbate as the granulating medium. No lubricants were added to the granule prior to the addition of magnesium stearate during the blend experiments.

4.3.2 Software method development for blend monitoring

For the powder blend the pure spectra of the lactose monohydrate and magnesium stearate were measured individually to obtain the fingerprint spectrum of the each material. This was achieved by placing approximately 50 g of each material on the Corona head and measuring the NIR spectrum. The NIR spectra of four random samples of the lactose monohydrate and magnesium stearate were measured to ensure that the natural variability within the materials was captured. The mean spectrum was obtained for the lactose monohydrate and the magnesium stearate using the software and these were over-layed. A second derivative was applied to the spectra to reduce the baseline shifts (Bokobza 1998). The spectra were then analysed for distinct markers that could be used as an indicator of the change occurring in the blend.

For the granule blend, the pure spectra of six random samples of the Ridaq® granule were measured and the mean was calculated to obtain a fingerprint spectrum. The fingerprint spectrum of the magnesium stearate (already obtained from the powder blends) and the Ridaq® granule were over-layed.

The significant wavelengths for blend monitoring for the materials were obtained by examining the spectra in the second derivative. The software was used to highlight the peaks on the spectra and preliminary blends were conducted using the wavelengths obtained from the software. The criteria used to choose the most suitable wavelengths was that the standard deviation of the absorbance at the wavelength

representing the magnesium stearate and the other material in the blend should increase when the magnesium stearate was added to the blend and level off after a period of time. A single wavelength was chosen for each material.

Following the determination of the significant wavelengths for each type of blend monitoring, a method was created on the processXplorer® software (version 1.1- by Carl Zeiss Jena GmbH) for the powder blend and another for the granule blend to interpret the spectral data. The second derivative was used for spectral pre-processing and the results were evaluated at the wavelengths of significance. The processXplorer® software (version 1.1- by Carl Zeiss Jena GmbH) was set to evaluate the standard deviation of the absorbance at the wavelengths of significance in a “moving block of eight” as outlined below.

Figure 4.3 shows a schematic of the variance calculation. Spectra are added to the block until eight spectra are obtained (seen in block 1). Then for every spectrum that moves out of the block, one spectrum is added to the block (seen in block 2 and block 3). As the spectral difference decreases so too does the moving block difference. The standard deviation is calculated over the block and plotted as a function of time to monitor the rate of change in the blend. When a process is complete, the spectra will not change, therefore the standard deviation will be small. (Hammond 2005)

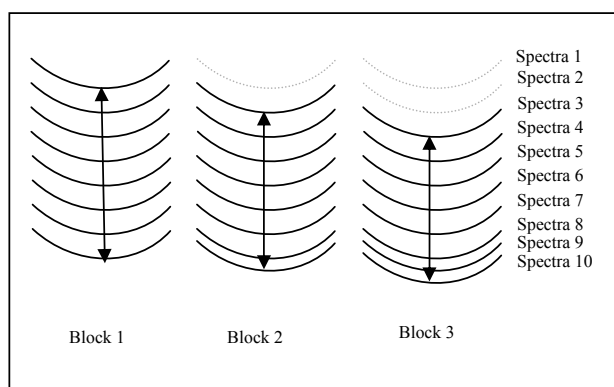


Figure 4.3 Moving variance calculation – Block 1 representing the first 8 spectra and block 2 and 3 representing the spectra as the blend progresses (Hammond 2005).

4.3.3 Spectral data from blends

During blending, spectral data was collected by the NIR probe during every rotation of the IBC. The IBC was set to rotate at 10 rotations per minute (rpm). The data was

mathematically treated with the algorithms available on the procXplorer® software (version 1.1- by Carl Zeiss Jena GmbH) created during the method development. The blend was monitored by the standard deviation versus time plot that was generated. When the standard deviation of the absorbance at the wavelengths of significance showed no more change in relation to time (i.e. reached a plateau level), it was assumed that the blend had reached an end-point as no more change in absorbance occurred at the wavelengths of significance.

4.3.4 Methods of sampling and analysis

End-point is used to show a state that has reached completion. When applied to blend monitoring, end-point refers to a state when the blend is homogeneous. To confirm the prediction of end-point using NIR, the blends were sampled using a sample thief when the NIR spectrum showed no more change in absorbance with respect to time at the wavelengths of significance (when a plateau level was reached) and at selected time intervals.

In order to determine the time intervals at which to sample, preliminary investigations were performed for each type of blend. A series of blends were run for approximately 20 minutes each. The standard deviation versus time plots were examined to identify three time intervals in the blend to predict three states namely before end-point, end-point and after end-point. The first time interval chosen was when the standard deviation had not levelled out and was high (depicting before end-point). The second time interval chosen was when the standard deviation was lower than the first time interval (depicting end-point) and the third time interval chosen was when the standard deviation maintained a low value for a longer period of time (depicting after end-point). Following these preliminary experiments, the times for sampling as stated below were obtained.

The interval of sampling for the powder blend was 1 minute and 40 seconds (before end-point), 8 minutes (end-point) and 16 minutes (after end-point). The intervals for sampling of the granule blend were 1 minute and 30 seconds (before end-point), 6 minutes (at end-point) and 17 minutes (after end-point). A five point sample plan was used to sample from the blender and one sample per point was taken, due to the decreased capacity of the blender (as shown in Figure 4.4). The samples were

analysed using an atomic absorption (AA) spectroscopic method for magnesium stearate to ascertain the distribution of the magnesium stearate in the blend.

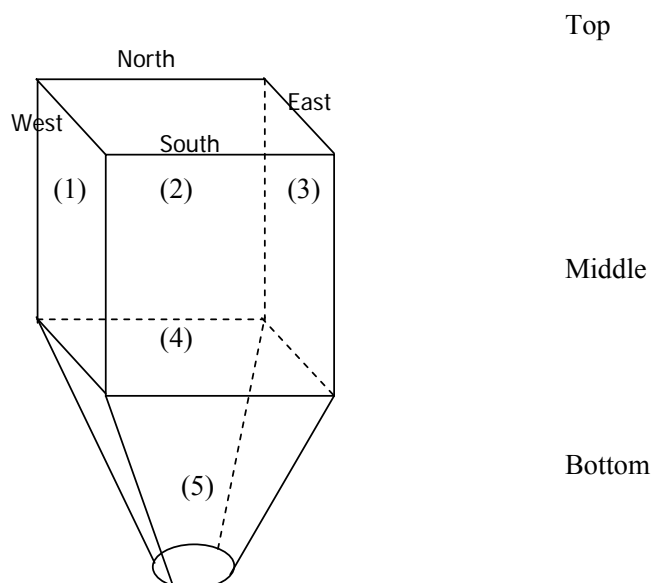


Figure 4.4 Areas of sample removal in the pilot scale blender (Technical Support 2005)

4.3.5 Analytical methods

An AA method for the detection of the magnesium stearate in the powder matrix and granule matrix was developed. The method was used to analyze the blend samples obtained during the blends.

4.3.5.1 Apparatus and operating conditions

An AA spectrometer with a magnesium lamp was used. The lamp current was set to 75 % with a delay time of 3 seconds. The measurement time was set to 10 seconds with 3 replicates. The wavelength used was 213.9 nm with a slit width of 0.5 nm. An air/acetylene flame was used with dilute acetic acid (30 %) as the solvent for the preparation of all samples.

4.3.5.2 Preparation of standard solution

The magnesium stearate (15 mg) was weighed out into a 1000 ml volumetric flask. 300 ml of solvent was added. This was sonicated for 15 minutes and allowed to cool to room temperature. The solution was made up to volume with solvent and

thereafter filtered through a Watman® number 41 filter paper. This concentration of magnesium stearate represented 200 % in relation to the quantity of magnesium stearate present in a unit dose (unit dose: 0.75 mg of magnesium stearate in 102.2 mg Ridaq® granule, as per formulation).

The 50 % standard was prepared by pipetting 25 ml of the 200 % solution into a 100 ml volumetric flask and diluting to volume with solvent. The 100 % standard was prepared by pipetting 50 ml of the 200 % solution into a 100 ml volumetric flask and diluting to volume with solvent. The 150 % standard was prepared by pipetting 75 ml of the 200 % solution into a 100 ml volumetric flask and diluting to volume with solvent.

Three standards were also prepared with the Ridaq® granule that contained no added magnesium stearate. 102.2 mg of Ridaq® granule was weighed into a 100 ml volumetric flask. 50 ml of solvent was added. This was sonicated for 15 minutes and allowed to cool to room temperature. The solution was made up to volume with solvent and was thereafter filtered through a Watman® number 41 filter paper. This was done to establish the response of Ridaq® granule with no added magnesium stearate and to assess the influence of other materials in the granule matrix that contributed to magnesium absorption. This approach was not used with lactose monohydrate as it is a single component ingredient.

Comment [k1]: Please review this comment.

4.3.5.3 Preparation of sample solution

The samples were powdered using a mortar and pestle. 102.2 mg of powdered sample was weighed into a 100 ml volumetric flask and 50 ml of solvent was added. This was sonicated for 15 minutes and then allowed to cool to room temperature. The solution was made up to volume with solvent and filtered through a Watman® number 41 filter paper. The solvent was used as the blank.

4.3.5.4 Procedure

The AA spectrometer was optimised as per manufacturer's recommended procedure, using the blank (solvent) to zero the instrument. The standard and the sample preparations were read on the AA spectrometer under the specified conditions. For the granule matrix, the average of the three standard samples of the Ridaq® granule

(with no added magnesium stearate) was subtracted from the result of the samples from the blend.

4.3.6 Statistical analysis

The lactose monohydrate/magnesium stearate and the Ridaq® granule/magnesium stearate blends were run in triplicate at each of the sampling intervals namely before the end-point, at end-point and at an interval after end-point. These samples were chemically analyzed using the AA method developed. The percentage relative standard deviation (RSD) of the replicates of magnesium stearate containing samples was determined at the sampling intervals.

The degree of variation of the blends at the specific wavelengths was analyzed using the mean of the standard deviation of the absorbance of the 3 blends plus/minus the standard deviation.

In addition, six Ridaq® granule and magnesium stearate blends were run to a potential end-point as predicted by NIR. The RSD of the magnesium stearate present in the samples as determined by using AA was calculated. The purpose was to show if a relationship existed between the results from the conventional analytical techniques (i.e. AA) and the end-point as predicted by the NIR results.

4.3.7 Experimental

4.3.7.1 Lactose monohydrate and magnesium stearate blends

The initial stage of the experimentation was to determine if blend uniformity of magnesium stearate in a powder matrix could be predicted using the Carl Zeiss NIR system. Powder blends containing 3 kg of lactose and 22.18 g magnesium stearate were prepared. The concentration of magnesium stearate (0.7 %) used per blend experiment was in keeping with the concentration that is generally used in current formulations at the pharmaceutical company.

The lactose was loaded into the IBC and the IBC was rotated for 8 rotations. Thereafter the blender was stopped and 22.18 g of magnesium stearate was added to the lactose. Care was taken to ensure that the magnesium stearate was evenly spread

over the top of the lactose. The IBC was then closed and blended for the predetermined time intervals. The blend was then sampled using a sample thief according to the stated sampling plan.

Three blend experiments per time interval were conducted for a blend duration of 1 minute and 40 seconds (before end-point), 8 minutes (at end-point) and 16 minutes (after end-point) using the above procedure.

4.3.7.2 Ridaq® granule and magnesium stearate blends

The desired use of the NIR blender at this pharmaceutical company is in the prediction of blend uniformity end-point after the addition of the lubricant to a granule matrix. The second phase of the experimentation was to investigate the application of NIR monitoring of the lubricant in a granule matrix.

Granule blends containing 3 kg of Ridaq® and 22.18 g magnesium stearate were prepared. The Ridaq® granule was loaded into the IBC and the IBC was rotated for 8 rotations. Thereafter the blender was stopped and 22.18 g of magnesium stearate was added to the granule. Care was taken to ensure that the magnesium stearate was evenly spread over the top of the granule. The IBC was then closed and blended for the predetermined time intervals. The blend was then sampled using a sample thief according to the stated sampling plan.

Three blend experiments per time interval were conducted for a blend duration of 1 minute and 30 seconds (before end-point), 6 minutes (at end-point) and 17 minutes (after end-point) using the above procedure. A further six blends were run and stopped at the time interval when the standard deviation at the selected wavelengths showed no more change (real end-point determined by NIR per individual blend run). The standard deviation that predicted a homogeneous blend was obtained from the data of the blends run to the time intervals stated above.

4.3.7.3 Atomic Absorption

The samples from both types of blends were analyzed using the AA method for magnesium stearate. A unit dose of 102.2 mg was weighed, of which 0.75 mg consists of magnesium stearate. The United States Pharmacopoeia limits for

uniformity of content was used which states that the content uniformity of the active should lie within the 85.0 % to 115.0 % of the label claim and the RSD should be less than or equal to 6.0 % (Pharmacopeial Forum 2006). This limit was applied to the magnesium stearate as the amount of magnesium stearate present per dosage unit should be in keeping with the content uniformity of the dosage unit.

4.4 RESULTS AND DISCUSSION

4.4.1 Lactose monohydrate and magnesium stearate blends

4.4.1.1 Software method

A software method to monitor the change in absorbance at the wavelengths of significance was developed. Figure 4.5 shows the second derivative of the four scans of the lactose monohydrate and Figure 4.6 shows the second derivative of the four scans of magnesium stearate. The second derivative was used to remove the baseline shifts or “noise” (Bokobza 1998). No significant variation existed in the scanned samples.

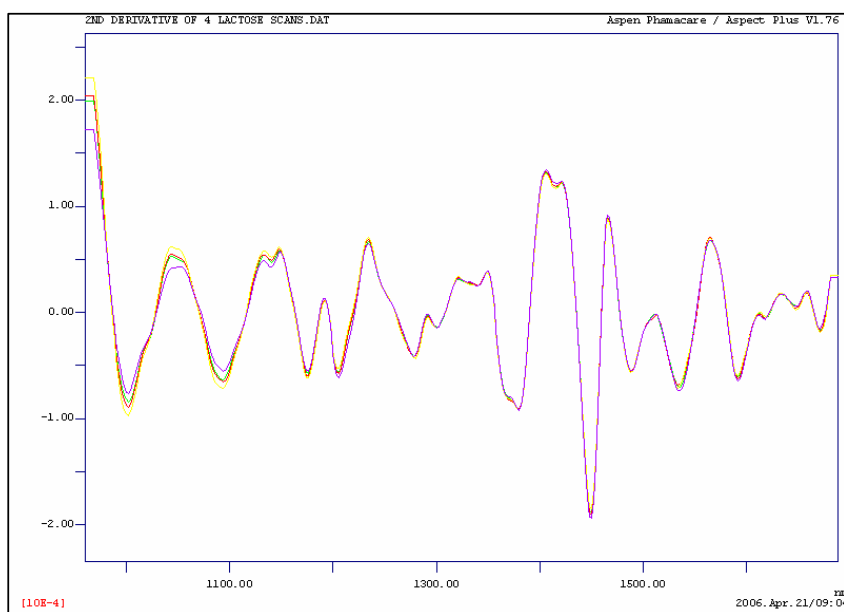


Figure 4.5 Second derivative of 4 scans of lactose monohydrate

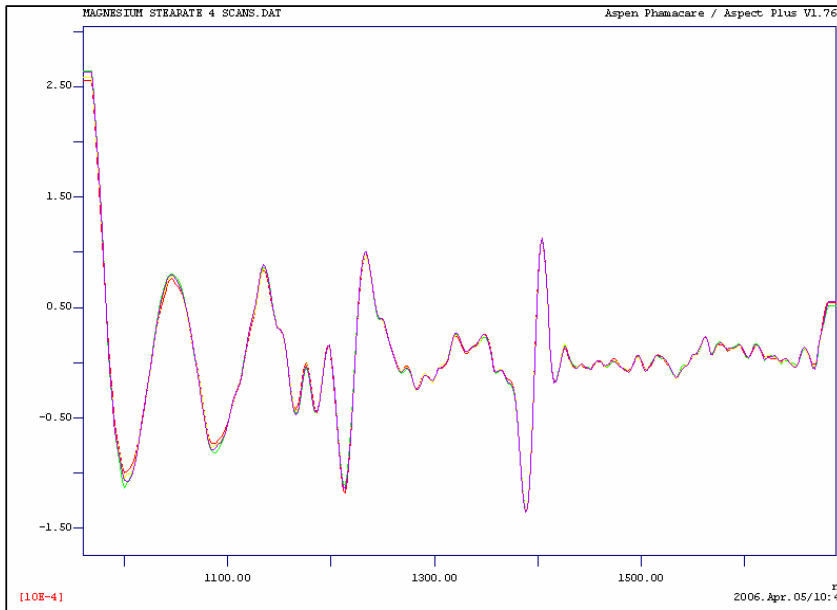
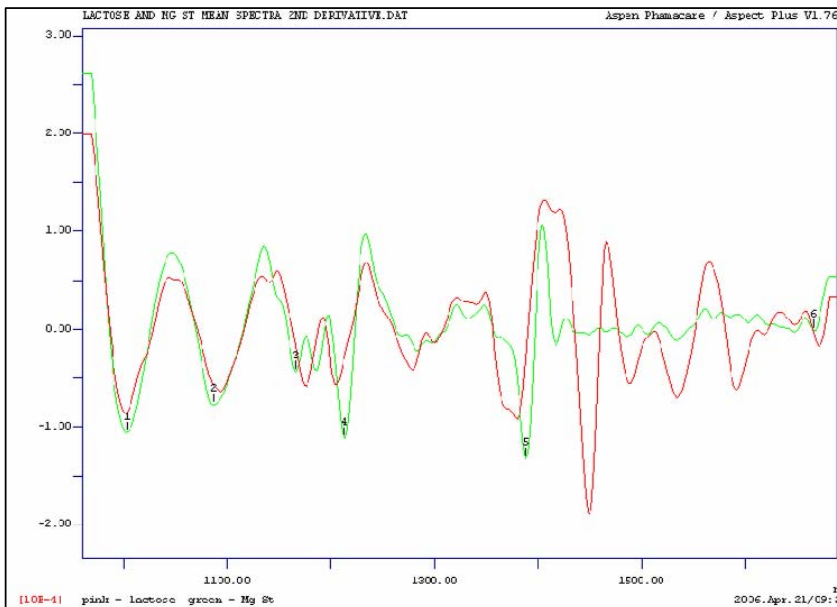


Figure 4.6 Second derivative of 4 scans of magnesium stearate

Figure 4.7 a) shows the overlay of the mean spectra of the lactose monohydrate and magnesium stearate in the second derivative with all the minimum peaks for magnesium stearate (green) and Figure 4.7 b) shows the overlay of lactose monohydrate and magnesium stearate showing the minimum peaks for lactose monohydrate (red).

a)



b)

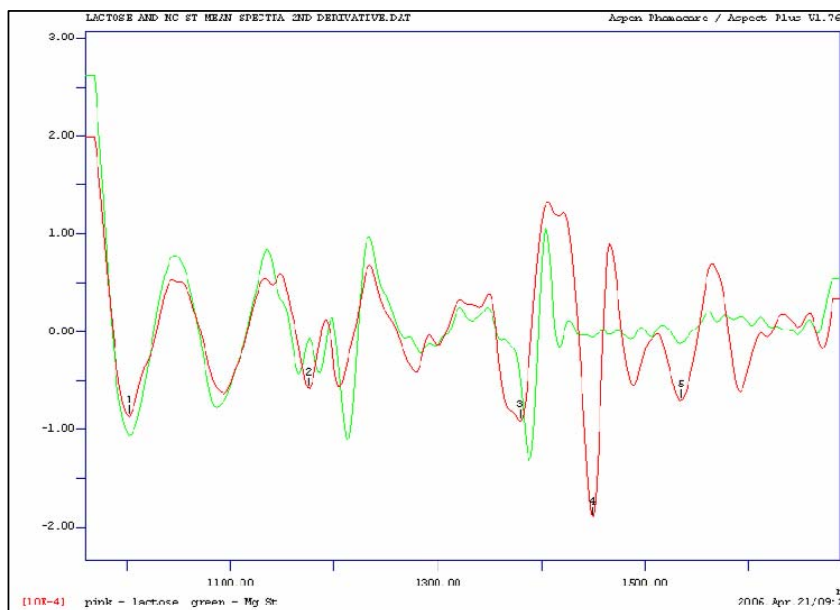


Figure 4.7 a) Overlay of lactose monohydrate and magnesium stearate showing the minimum peaks for magnesium stearate (green). b) Overlay of lactose monohydrate and magnesium stearate showing the minimum peaks for lactose monohydrate (red).

Table 4.1 and Table 4.2 list the wavelengths identified for magnesium stearate and lactose monohydrate respectively.

Table 4.1 NIR absorption peaks identified for magnesium stearate

Peak number	Wavelength
1	1002 nm
2	1086 nm
3	1166 nm
4	1213 nm
5	1388 nm
6	1666 nm

Table 4.2 NIR absorption peaks identified for lactose monohydrate

Peak number	Wavelength
1	1001 nm
2	1175 nm
3	1379 nm
4	1448 nm
5	1534 nm

From the preliminary blends that were run with the lactose monohydrate and magnesium stearate, using some of the wavelengths identified in Table 4.1 and 4.2, the potential wavelengths that were isolated for blend monitoring were 1213 nm (magnesium stearate) and 1448 nm (lactose monohydrate). On visual examination of the spectra, it could be seen that the peaks at these wavelengths are unique to each material. These wavelengths showed a sharp increase in absorbance when magnesium stearate was added to the blend and a levelling off after a period of time.

The software method that was developed monitored the standard deviation of the absorbance at 1213 nm and 1448 nm in the second derivative in a “moving block of eight”. This parameter method was applied to all the lactose monohydrate and magnesium stearate blends. The standard deviation at 1213 nm showed the change in absorbance that occurred at the wavelength that monitored the magnesium stearate while the standard deviation at 1448 nm showed the change in absorbance that occurred at the wavelength that monitored the lactose monohydrate.

4.4.1.2 Lactose monohydrate and magnesium stearate blends conducted

A: Blend for 1 minute 40 seconds

Figures 4.8 and 4.9 represent the standard deviation of the absorbance at 1213 nm and 1448 nm plotted against the number of rotations for the three blends that were run for 1 minute and 40 seconds. At the end of the blend duration it was observed that the standard deviation at 1213 nm for all three blends was above 3×10^{-6} .

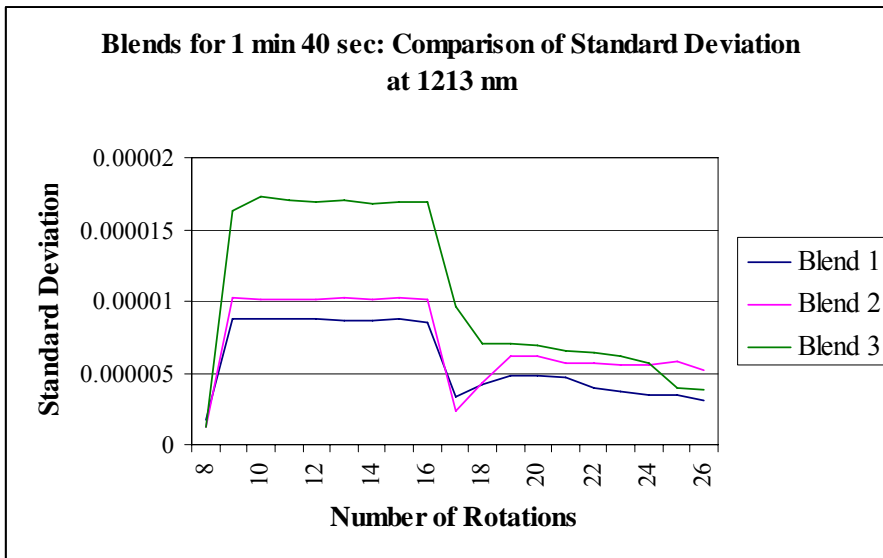


Figure 4.8 Standard deviation across the three blends at 1213 nm

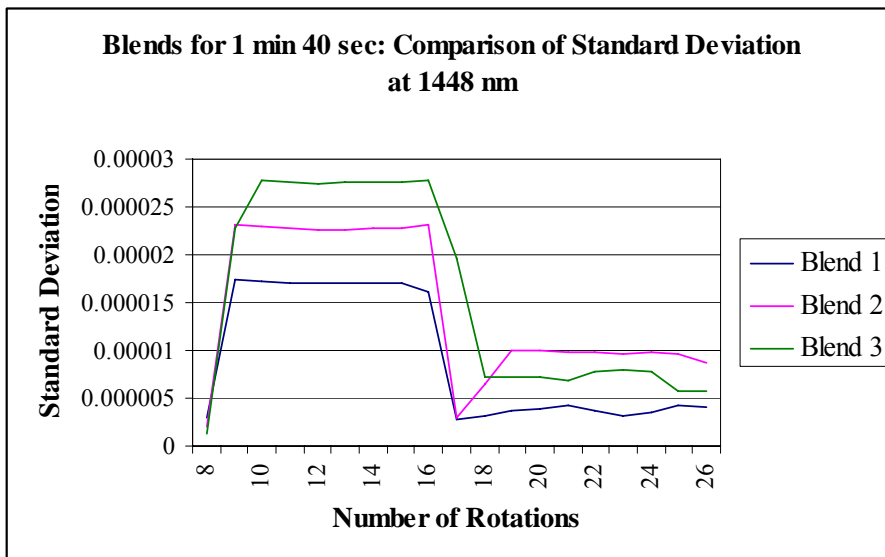


Figure 4.9 Standard deviation across the three blends at 1448 nm

Table 4.3 represents the AA results for magnesium stearate per 102.2 mg of sample sampled according to the sample plan. The results show that the blends were not homogeneous after a blend period of 1 minute and 40 seconds as the amount of magnesium stearate did not fall within the 15 % limit (0.6375 mg – 0.8625 mg) and the RSD is above 6 %.

Table 4.3 AA results for magnesium stearate per 102.2 mg sample mass for blends run for 1 minute and 40 seconds

1 minute 40 seconds	Blend 1	Blend 2	Blend 3
Point 1	0.8820 mg	0.5182 mg	0.5035 mg
Point 2	0.8604 mg	0.6260 mg	0.4759 mg
Point 3	0.5820 mg	0.8341 mg	0.8820 mg
Point 4	0.8281 mg	0.4725 mg	0.6390 mg
Point 5	0.7480 mg	0.5084 mg	0.5801 mg
Mean	0.7801 mg	0.5918 mg	0.6161 mg
RSD	15.62 %	24.84 %	26.28 %

During blending it was noticed that the wavelengths showed a sharp increase in absorbance when the magnesium stearate was added after 8 rotations. This demonstrated that NIR was able to detect the magnesium stearate that was added. The magnesium stearate also contributed to an increase in absorbance at the 1448 nm wavelength (wavelength for lactose monohydrate).

B: Blend for 8 minutes (at end-point)

Figures 4.10 and 4.11 represent the standard deviation of the absorbance at 1213 nm and 1448 nm plotted against the number of rotations for the three blends that were run for 8 minutes. At the 27th rotation the standard deviation of both wavelengths were below 5×10^{-6} . Thereafter a levelling out or an equilibrium state of both the wavelengths is noted. At the end of the 8 minutes it was observed that the standard deviation at 1213 nm for all three blends was below 2×10^{-6} .

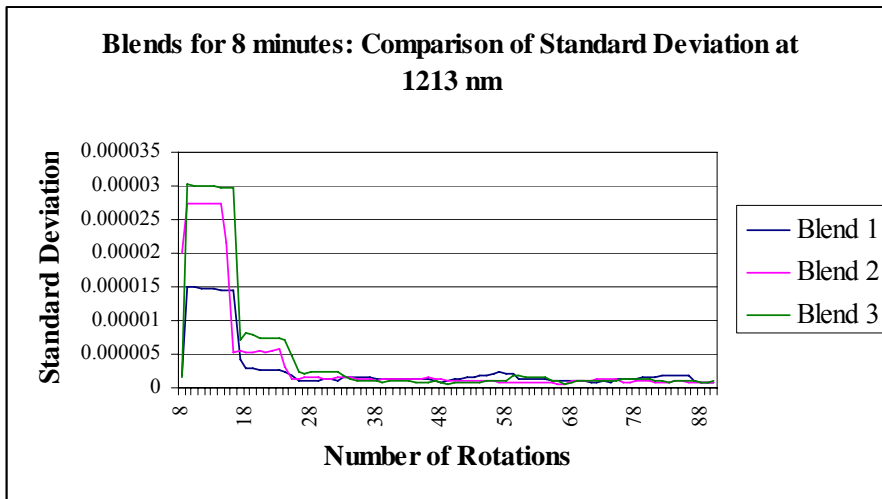


Figure 4.10 Standard deviation across the three blends at 1213 nm

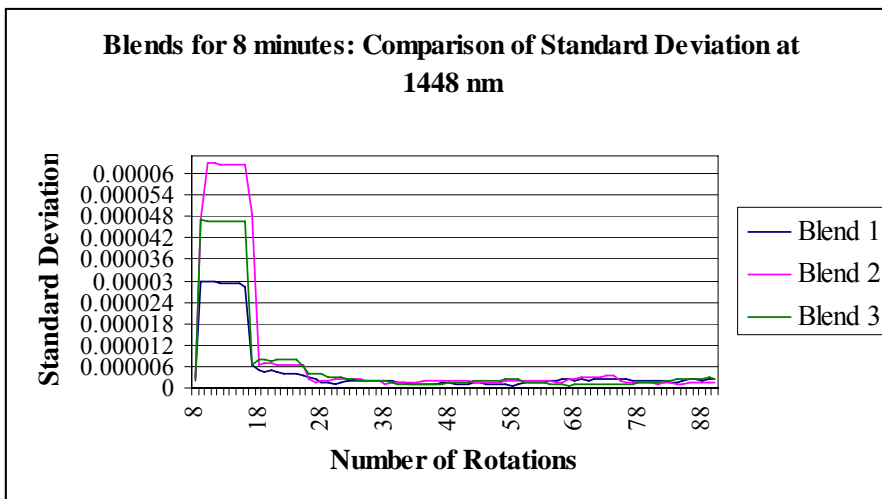


Figure 4.11 Standard deviation across the three blends at 1448 nm

Table 4.4 represents the AA results for magnesium stearate per 102.2 mg of sample sampled according to the sample plan. The results show that the blends were homogeneous after a blend period of 8 minutes as the amount of magnesium stearate is within the 15 % limit (0.6375 mg – 0.8625 mg) and the RSD is below 6 %.

Table 4.4 AA results for magnesium stearate per 102.2 mg sample mass for blends run for 8 minutes

8 minutes	Blend 1	Blend 2	Blend 3
Point 1	0.8201 mg	0.7961 mg	0.7595 mg
Point 2	0.7863 mg	0.8006 mg	0.7226 mg
Point 3	0.7858 mg	0.7886 mg	0.7098 mg
Point 4	0.7949 mg	0.7753 mg	0.7244 mg
Point 5	0.7795 mg	0.7855 mg	0.7620 mg
Mean	0.7928 mg	0.7892 mg	0.7356 mg
RSD	2.05 %	1.24 %	3.20 %

Although 8 minutes was used in these experiments as a possible end-point for the powder blends, it is evident from Figure 4.10 that the standard deviation for 1213 nm reaches a constant value after the 48th rotation, which is after approximately 4 minutes blend duration. Thus the blend time could be decreased by a further 50 % and still result in a homogeneous blend. With NIR monitoring it becomes possible to blend for the exact time duration that is necessary to assure a homogeneous blend.

C: Blend for 16 minutes (after end-point):

Figures 4.12 and 4.13 represent the standard deviation of the absorbance at 1213 nm and 1448 nm respectively plotted against the number of rotations for the three blends conducted for 16 minutes. At the 26th rotation the standard deviation of both wavelengths were below 5×10^{-6} . Thereafter a levelling out or an equilibrium state of both the wavelengths is noted. At the end of the 16 minutes it was observed that the standard deviation at 1213 nm for all three blends was below 2×10^{-6} .

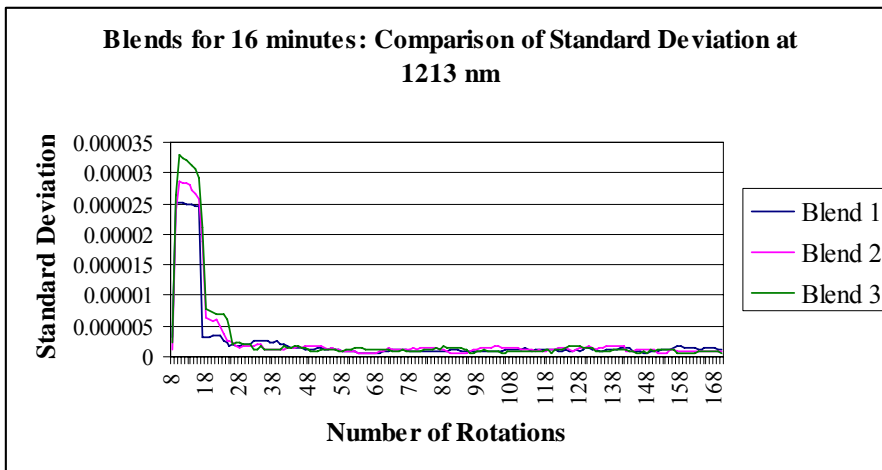


Figure 4.12 Standard deviation across the three blends at 1213 nm

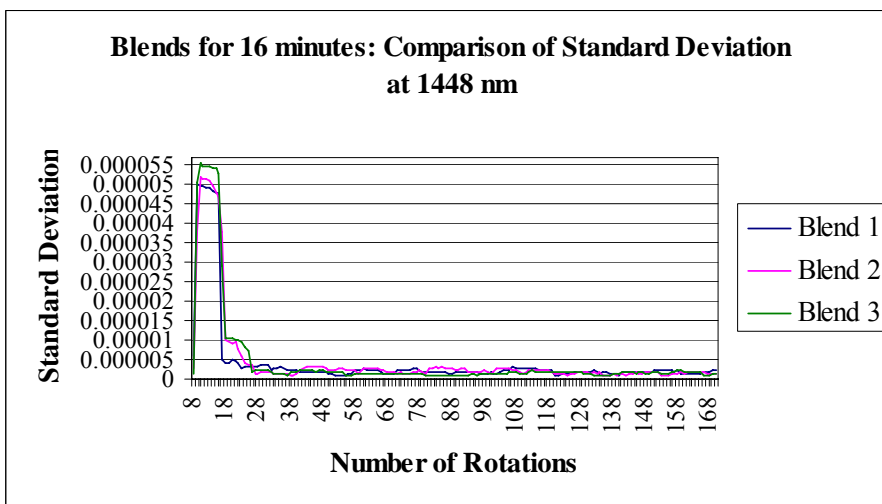


Figure 4.13 Standard deviation across the three blends at 1448 nm

The standard deviation values show a difference from each other in terms of the maximum peaks reached for the three blends and time taken to reach the lowest standard deviation value but level out comparably at the end of the 16 minutes. This can be seen in Figure 4.14, which represents the mean standard deviation of the absorbance at 1213 nm plus/minus the standard deviation for the three blends (graph only plotted until 150 rotations as no significant change was observed after this). This demonstrated that although the blends were conducted in an identical manner, each blend had a unique behaviour, which could have an influence on the duration for homogeneity to be reached. There is also the possibility that over-mixing could occur if blended for a longer period than is required.

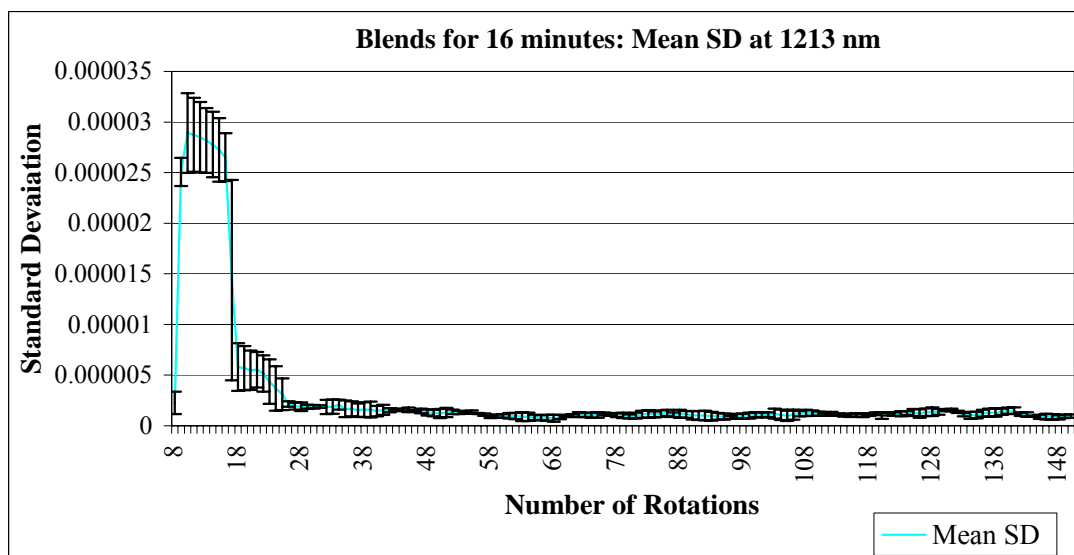


Figure 4.14 Mean standard deviation of absorbance at 1213 nm \pm SD for the three blends (error bars indicate standard deviation of the mean standard deviation of absorbance calculated for the 3 blends)

Table 4.5 represents the AA results for magnesium stearate per 102.2 mg of sample sampled according to the sample plan. The results show that the blends were homogeneous after a blend period of 16 minutes as the amount of magnesium stearate is within the 15 % limit (0.6375 mg – 0.8625 mg) and the RSD is below 6 %. It is observed that a low standard deviation value for the wavelengths resulted in a homogeneous mix.

Table 4.5 AA results for magnesium stearate per 102.2 mg sample mass for blends run for 16 minutes

16 minutes	Blend 1	Blend 2	Blend 3
Point 1	0.7984 mg	0.8470 mg	0.7697 mg
Point 2	0.7721 mg	0.8536 mg	0.7718 mg
Point 3	0.7239 mg	0.8333 mg	0.7757 mg
Point 4	0.8255 mg	0.8079 mg	0.7428 mg
Point 5	0.7676 mg	0.8247 mg	0.7577 mg
Mean	0.7775 mg	0.8333 mg	0.7635 mg
RSD	4.87 %	2.18 %	1.76 %

The standard deviation for the blends that were found to be homogeneous (blends for 16 minutes and 8 minutes) were lower when compared to the blends that were not homogeneous (blend for 1 minute and 40 seconds). The distribution of magnesium stearate in the blends for 16 minutes and 8 minutes are comparable with each other in that both sets of blends are homogeneous and the standard deviation was below 2×10^{-6} . The blends for 1 minutes and 40 seconds had a higher standard deviation (greater than 3×10^{-6}) and were found to have an uneven distribution of magnesium stearate.

4.4.2 Ridaq® granule and magnesium stearate blends

4.4.2.1 Software method

A software method to monitor the change in absorbance that occurred at the wavelengths of significance was developed. Figure 4.15 shows the second derivative of the six scans of the Ridaq® granule and Figure 4.16 shows the second derivative scans of the four samples of magnesium stearate. The second derivative was used to remove the baseline shifts or “noise” (Bokobza 1998).

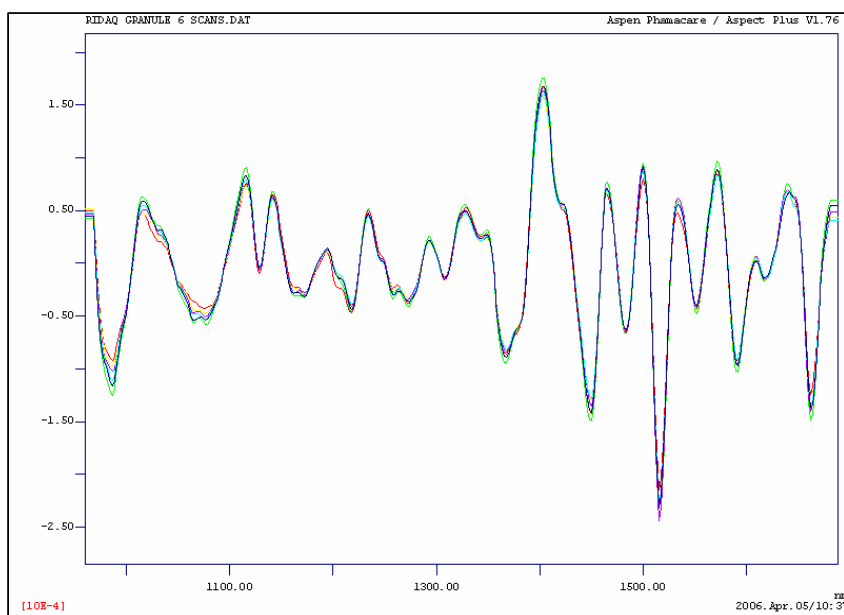


Figure 4.15 Second derivative of the 6 scans of Ridaq® granule

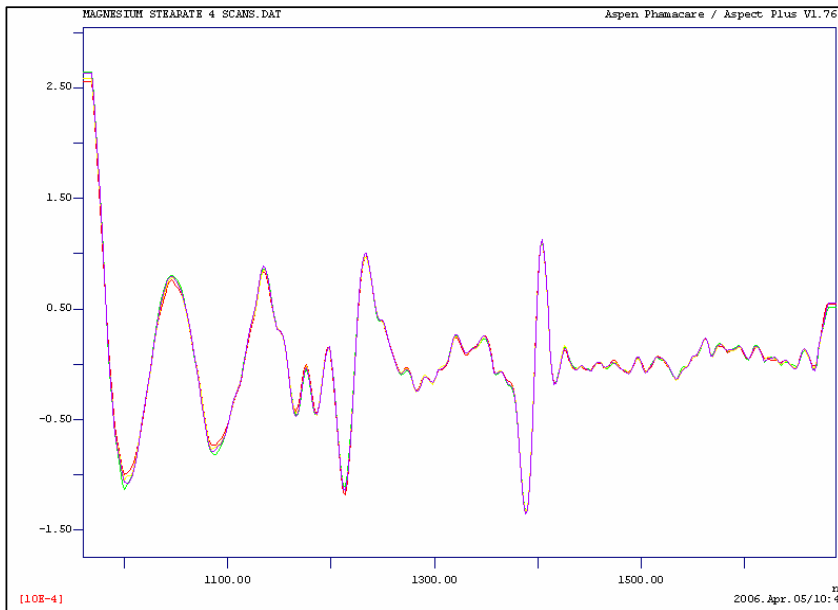
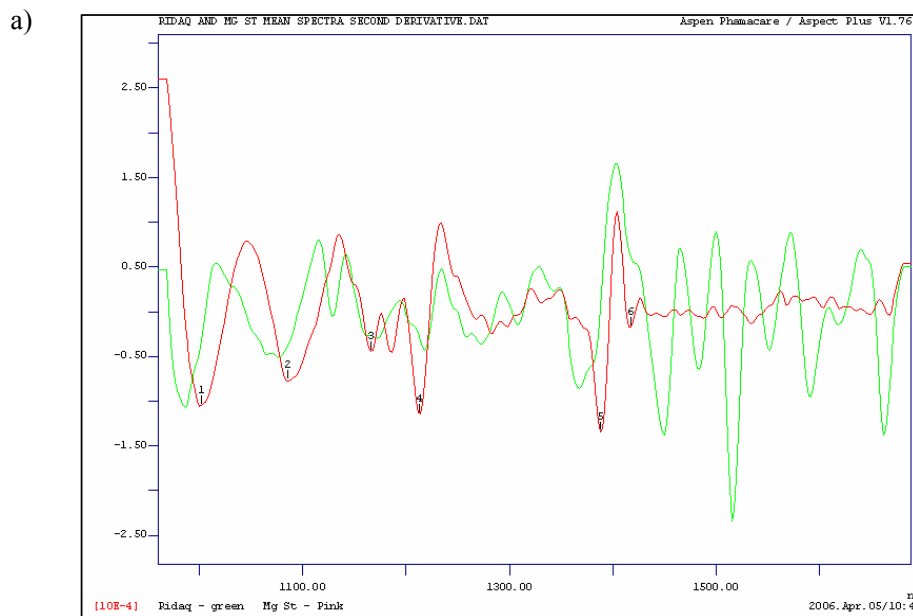


Figure 4.16 Second derivative of 4 scans of magnesium stearate

Figure 4.17 a) shows the overlay of the Ridaq® granule and magnesium stearate spectra in the second derivative with all the minimum peaks for magnesium stearate (red) and Figure 4.17 b) shows the overlay of the Ridaq® granule and magnesium stearate spectra in the second derivative with all the minimum peaks for Ridaq® granule (green).



b)

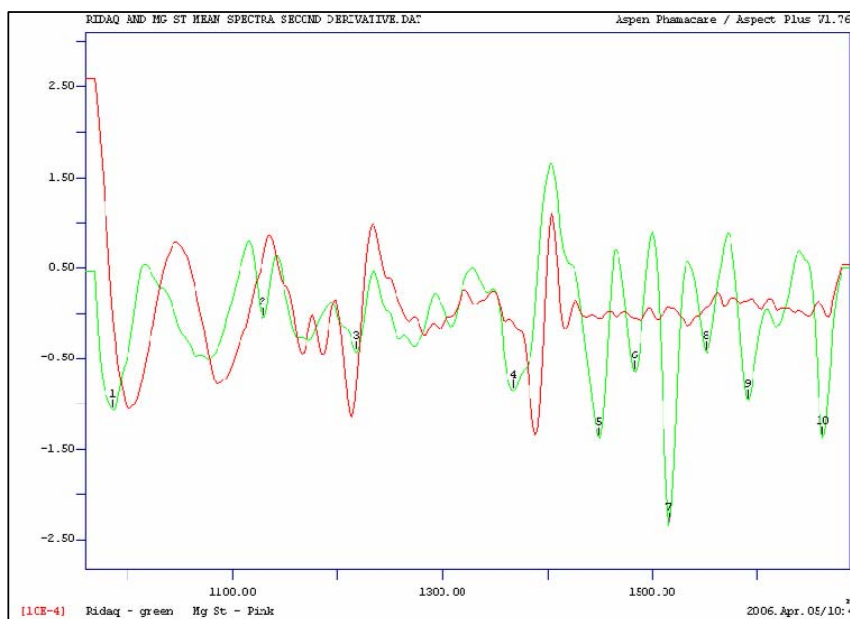


Figure 4.17 a) Overlay of Ridaq® granule and magnesium stearate showing the minimum peaks for magnesium stearate (red). b) Overlay of Ridaq® granule and magnesium stearate showing the minimum peaks for Ridaq® granule (green).

Table 4.6 and 4.7 list the significant wavelengths for magnesium stearate and Ridaq® granule respectively.

Table 4.6 NIR absorption peaks identified for magnesium stearate

Peak number	Wavelength
1	1002 nm
2	1086 nm
3	1166 nm
4	1213 nm
5	1388 nm
6	1417 nm

Table 4.7 NIR absorption peaks identified for Ridaq® granule

Peak number	Wavelength
1	985 nm
2	1128 nm
3	1218 nm
4	1367 nm
5	1448 nm
6	1483 nm
7	1516 nm
8	1551 nm
9	1591 nm
10	1662 nm

From the preliminary blends that were run with the Ridaq® granule and magnesium stearate, using selected wavelengths identified in Table 4.6 and 4.7, the potential wavelengths that were isolated for blend monitoring were 1213 nm (magnesium stearate) and 1591 nm (Ridaq® granule). On visual examination of the spectra, it can be seen that the peaks at these wavelengths are unique to each material. These wavelengths showed a sharp increase in absorbance when the magnesium stearate was added to the blend and a levelling off after a period of time.

The software method that was developed monitored the standard deviation of the absorbance at 1213 nm and 1591 nm in the second derivative in a “moving block of eight”. This parameter method was applied to all the Ridaq® granule and magnesium stearate blends. The standard deviation at 1213 nm showed the change in absorbance that occurred at the wavelength that monitored the magnesium stearate. The standard deviation at 1591 nm showed the change in absorbance that occurred at the wavelength that monitored the Ridaq® granule.

4.4.2.2 Ridaq® granule and magnesium stearate blends conducted

A: Blend for 1.5 minutes (before end-point)

Figures 4.18 and 4.19 represent the standard deviation of the absorbance at 1213 nm and 1591 nm plotted against the number of rotations.

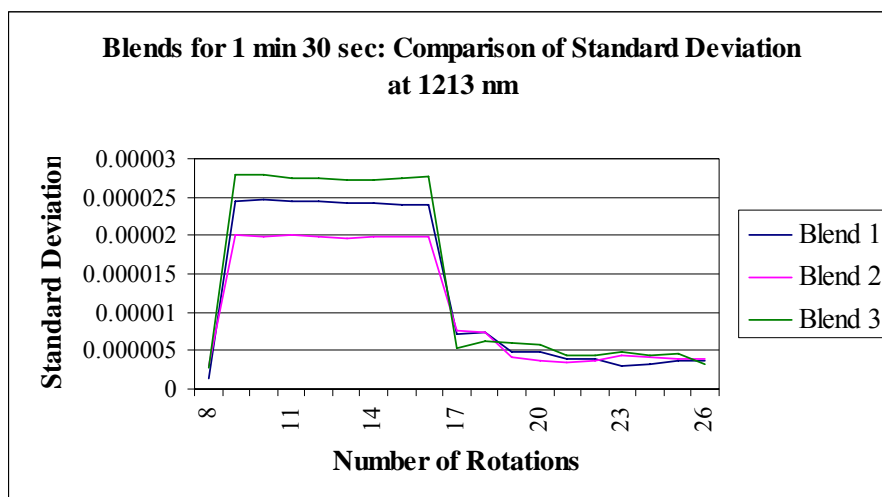


Figure 4.18 Standard deviation across the three blends at 1213 nm

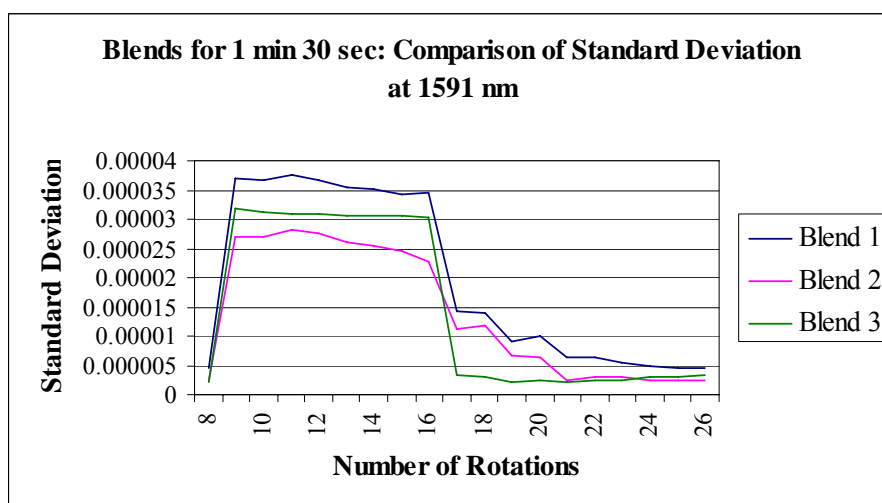


Figure 4.19 Standard deviation across the three blends at 1591 nm

The blend was stopped before the standard deviation had levelled out. At the end of the 1.5 minutes, it was observed that the standard deviation at 1213 nm (magnesium stearate) for all three blends was above 3×10^{-6} . It was noted that, as with the powder

blends, the blends showed a sharp increase in absorbance when the magnesium stearate was added after 8 rotations. The magnesium stearate also contributed to an increase in absorbance at 1591 nm.

Table 4.8 represents the AA results for magnesium stearate per 102.2 mg of sample sampled according to the sample plan. The results show that the blends were not homogeneous after a blend period of 1.5 minutes as the amount of magnesium stearate did not fall within the 15 % limit (0.6375 mg – 0.8625 mg) and the RSD is above 6 %.

Table 4.8 AA results for magnesium stearate per 102.2 mg sample mass for blends run for 1.5 minutes

1.5 minutes	Blend 1	Blend 2	Blend 3
Point 1	0.5508 mg	0.3890 mg	0.6375 mg
Point 2	0.7756 mg	0.4875 mg	0.6327 mg
Point 3	0.6916 mg	0.4737 mg	0.3155 mg
Point 4	0.7813 mg	0.4480 mg	0.3079 mg
Point 5	0.7178 mg	0.4122 mg	0.1108 mg
Mean	0.7034 mg	0.4421 mg	0.4009 mg
RSD	13.28 %	9.33 %	57.13 %

B: Blend for 6 minutes (end-point)

Figures 4.20 and 4.21 represent the standard deviation of the absorbance at 1213 nm and 1591 nm plotted against the number of rotations.

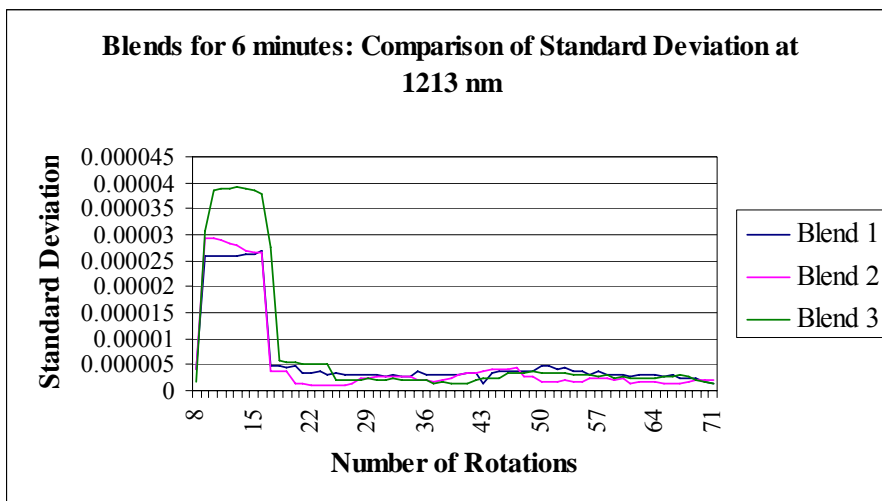


Figure 4.20 Standard deviation across the three blends at 1213 nm

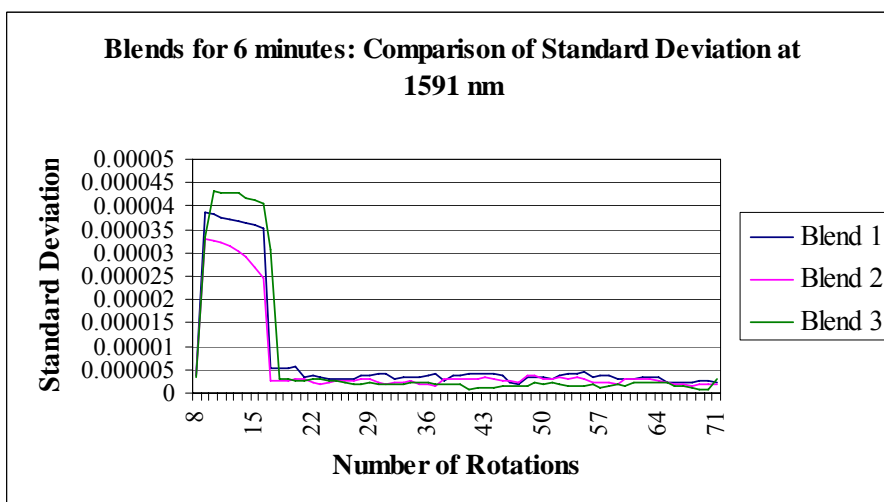


Figure 4.21 Standard deviation across the three blends at 1591 nm

A levelling out or an equilibrium state of both the wavelengths is noted after the 28th rotation. At the end of the 6 minutes, it was observed that the standard deviation at 1213 nm for all three blends was below 2×10^{-6} . Table 4.9 represents the AA results for magnesium stearate per 102.2 mg of sample sampled according to the sample plan.

Table 4.9 AA results for magnesium stearate per 102.2 mg sample mass for blends run for 6 minutes.

6 minutes (end-point)	Blend 1	Blend 2	Blend 3
Point 1	0.7894 mg	0.6861 mg	0.8147 mg
Point 2	0.7262 mg	0.6739 mg	0.7767 mg
Point 3	0.6821 mg	0.6445 mg	0.7407 mg
Point 4	0.7234 mg	0.6505 mg	0.7532 mg
Point 5	0.6989 mg	0.6466 mg	0.8336 mg
Mean	0.7240 mg	0.6603 mg	0.7838 mg
RSD	5.64 %	2.8 %	5.055 %

The results show that the blends were homogeneous after a blend period of 6 minutes as the amount of magnesium stearate is within the 15 % limit (0.6375 mg – 0.8625 mg) and the RSD is below 6 %.

C: Blend for 17 minutes (after end-point):

Figures 4.22 and 4.23 represent the standard deviation of the absorbance at 1213 nm and 1591 nm plotted against the number of rotations for the three blends conducted for 17 minutes.

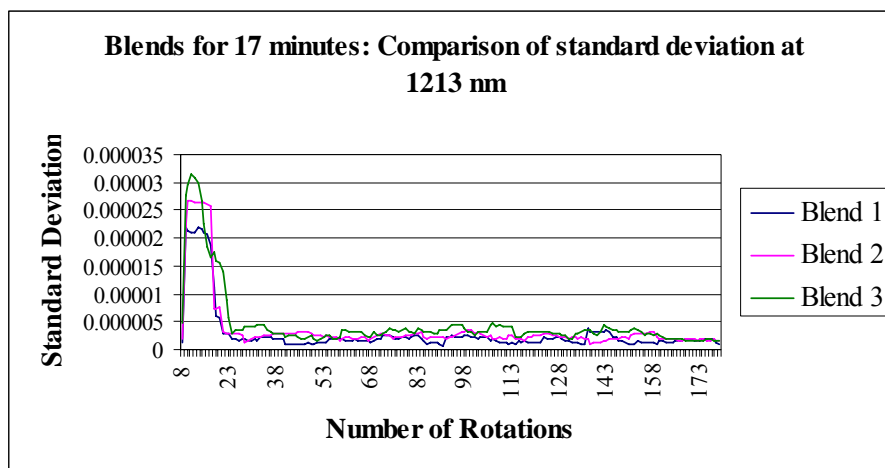


Figure 4.22 Standard deviation across the three blends at 1213 nm

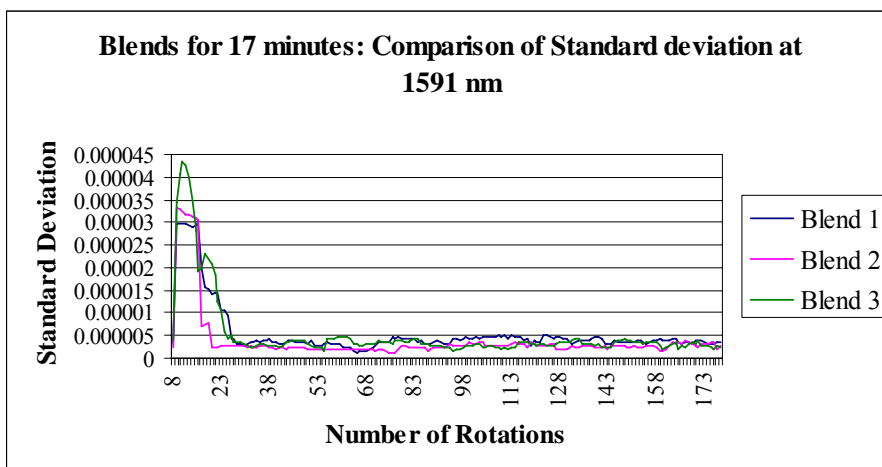


Figure 4.23 Standard deviation across the three blends at 1591 nm

At the 28th rotation, the standard deviation value at 1213 nm and 1591 nm were below 5×10^{-6} . Thereafter a levelling out or an equilibrium state of both the wavelengths is noted. At the end of the 17 minutes, it was observed that the standard deviation at 1213 nm for all three blends was below 2×10^{-6} . Table 4.10 represents the AA results for magnesium stearate per 102.2 mg of sample sampled according to the sample plan.

Table 4.10 AA results for magnesium stearate per 102.2 mg sample mass for blends run for 17 minutes.

17 minutes (after end-point)	Blend 1	Blend 2	Blend 3
Point 1	0.7806 mg	0.655 mg	0.7164 mg
Point 2	0.8290 mg	0.7157 mg	0.7128 mg
Point 3	0.8158 mg	0.6444 mg	0.7286 mg
Point 4	0.8171 mg	0.7085 mg	0.6792 mg
Point 5	0.7853 mg	0.6628 mg	0.7305 mg
Mean	0.8055 mg	0.6772 mg	0.7135 mg
RSD	2.65 %	4.81 %	2.89 %

The results show that the blends were homogeneous after a blend period of 17 minutes as the amount of magnesium stearate is within the 15 % limit (0.6375 mg – 0.8625 mg) and the RSD is below 6 %; however it is noted that the RSD does differ

from batch to batch. The RSD is generally lower when compared to the RSD at 6 minutes. Although the blends behaved differently in terms of the NIR absorbance values, the degree of homogeneity of magnesium stearate is comparable with the different blends.

The wavelength of particular interest is 1213 nm as this wavelength represents magnesium stearate. A levelling out of this wavelength will be indicative of no further change in the absorbance at that point, indicating that the magnesium stearate is evenly distributed in the blend when the standard deviation at 1213 nm reaches a steady value. The maximum absorbance values reached for the individual blends differ significantly as can be seen in Figure 4.24 where the mean of the standard deviation of the absorbance at 1213 nm plus/minus the standard deviation for the three blends is plotted.

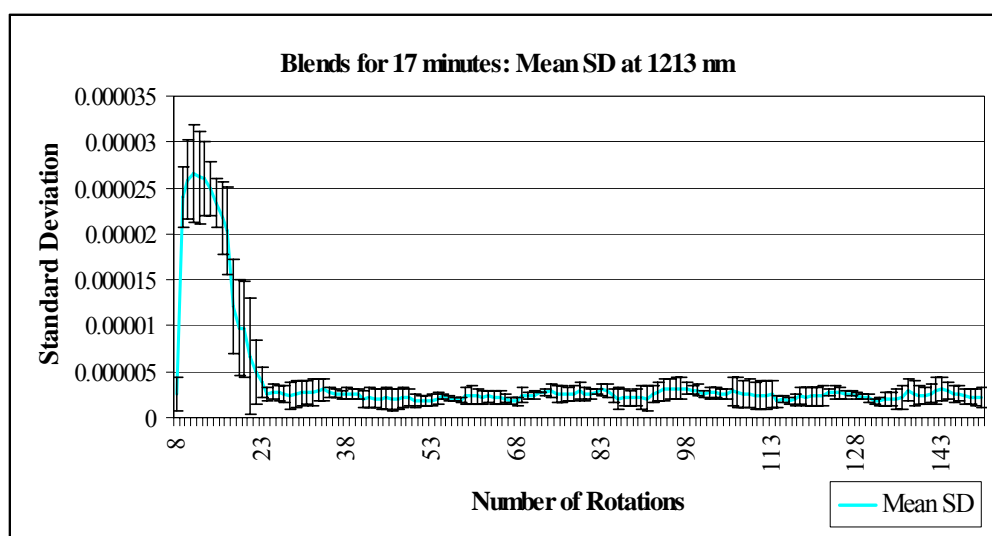


Figure 4.24 Mean of standard deviation of absorbance at 1213 nm (error bars indicate standard deviation of the mean standard deviation of absorbance calculated for the 3 blends)

However, the absorbance values are more similar as the blend progresses and at the end of the blend duration, the degree of difference in the absorbance is negligible (graph plotted only to 150 rotations, as there was no significant change after this).

This illustrates that although the blends were identical in terms of preparation and blend duration and the fact that only one batch of granule was used, each blend behaved differently. It therefore becomes important to recognise that blends are not identical although the external factors are kept constant. Another concern is inter-batch variation, where the conventional approach of blending for a pre-determined time may not be sufficient to assure the quality of the mix of the blend.

Of significance is that a decrease in blend time of 11 minutes (from 17 minutes to 6 minutes) still gave a homogeneous blend. Blending for longer durations than is necessary could lead to de-mixing which is the segregation of particles due to variations in particle size, shape and density (Travers 1988). One of the limitations of this study is that the time at which de-mixing occurs was not investigated due to time restrictions. It is possible that at some time point, de-mixing does occur, however it is important to note that the time taken for de-mixing could differ from blend to blend, as each blend behaves uniquely as can be seen in the difference in absorbance in the identical blends carried out in triplicate. Using NIR monitoring, de-mixing could possibly be observed when the standard deviation at the selected wavelengths starts to increase again and the difference between the wavelengths becomes larger and it is therefore recommended that this aspect be researched further.

In addition to de-mixing, blending for longer periods than is necessary could lead to the physical destruction of the granule. Coupled with this, due to the hydrophobic nature of magnesium stearate, over-blending may lead to a decrease in dissolution rates and also a decrease in tablet hardness. (Kanfer *et al.* 2005) With this in mind, real-time analysis becomes very significant as it avoids the danger of de-mixing and destruction of the properties of the granule.

The standard deviation for the blends that were found to be homogeneous (blends for 17 minutes and 6 minutes) were lower when compared to the blends that were non-homogeneous (blend for 1.5 minutes). The distribution of the magnesium stearate in the blends for 17 minutes and 6 minutes relate with each other in that both sets of blends are homogeneous and the standard deviation was below 2×10^{-6} . The blends for 1.5 minutes had a higher standard deviation (greater than 3×10^{-6}) and were found to have an uneven distribution of magnesium stearate.

D: Blend to end-point:

Based on the previous blends it was decided that a standard deviation value below 3×10^{-6} for 1213 nm (wavelength for magnesium stearate monitoring) at four consecutive data points would be used as a possible indicator for a complete blend process.

Figure 4.25 represents the standard deviation at 1213 nm for the 6 blends that were run to a possible end-point as predicted by NIR.

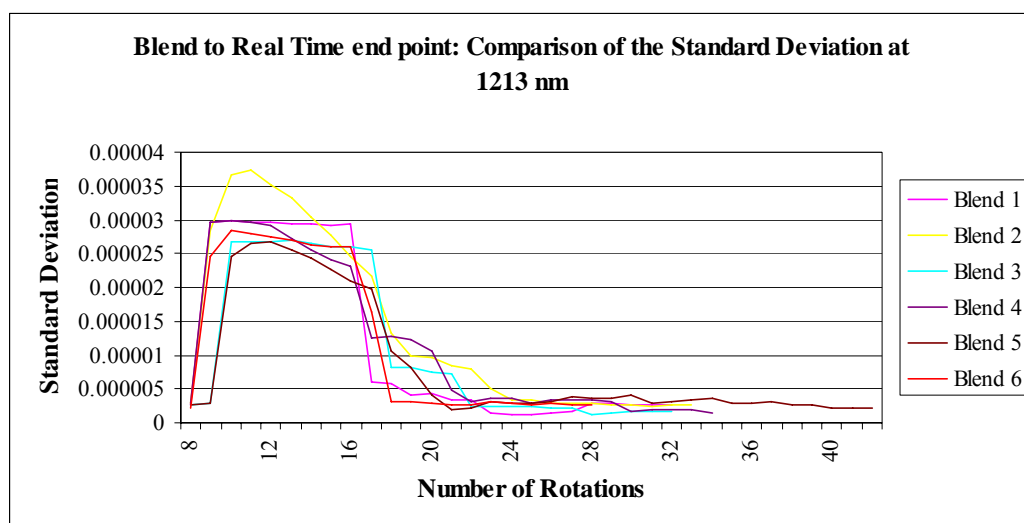


Figure 4.25 Standard deviation across the six blends at 1213 nm

As is evident from the graph, all blends exhibit a unique behaviour in terms of the absorbance in the NIR spectrum. The blend time for each is different although as seen in Table 4.11 the AA results show that the blends are homogeneous with the exception of blend 6, where the amount of magnesium stearate is marginally out of specification.

Table 4.11 AA results for magnesium stearate per 102.2 mg sample mass
(Out of specification results highlighted in red)

End-point	Blend 1	Blend 2	Blend 3	Blend 4	Blend 5	Blend 6
Actual Blend Time	3 min 18 sec	2 min 23 sec	2 min 10 sec	2 min 27 sec	3 min 9 sec	1 min 52 sec
Point 1	0.6780 mg	0.7807 mg	0.6857 mg	0.6551 mg	0.6968 mg	0.6295 mg
Point 2	0.7025 mg	0.6792 mg	0.7063 mg	0.7258 mg	0.6746 mg	0.6546 mg
Point 3	0.6837 mg	0.7433 mg	0.7063 mg	0.7437 mg	0.7178 mg	0.6494 mg
Point 4	0.7173 mg	0.7439 mg	0.6971 mg	0.6817 mg	0.7101 mg	0.6271 mg
Point 5	0.6935 mg	0.7147 mg	0.7357 mg	0.7060 mg	0.7005 mg	0.6868 mg
Mean	0.6950 mg	0.7324 mg	0.7062 mg	0.7025 mg	0.7000 mg	0.6495 mg
RSD	2.24 %	5.17 %	2.62 %	5.00 %	2.34 %	3.71 %

Blend 6 represents the shortest blend duration. Upon closer examination of the results for blend 6, it can be seen that at the end of the blend, the standard deviation at 1591 nm is highest of all the blends conducted to end-point as can be seen in Figure 4.26 where the standard deviation at 1591 nm is compared.

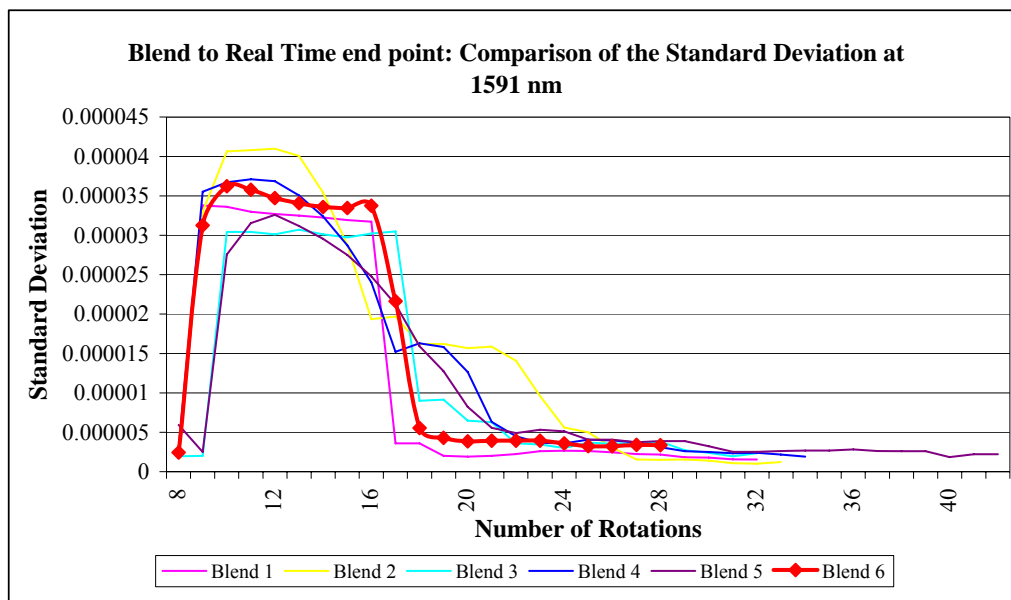


Figure 4.26 Standard deviation across the six blends at 1591 nm

The last four data points at 1591 nm for blends that were run to real-time end-points as predicted by NIR can be seen in Table 4.12.

Table 4.12 Last four data points at 1591 nm for blends that were run to real-time end-points

Blend 1	Blend 2	Blend 3	Blend 4	Blend 5	Blend 6
1.8×10^{-6}	1.4×10^{-6}	2.7×10^{-6}	2.4×10^{-6}	2.6×10^{-6}	3.2×10^{-6}
1.8×10^{-6}	1.1×10^{-6}	2.4×10^{-6}	2.4×10^{-6}	1.8×10^{-6}	3.2×10^{-6}
1.6×10^{-6}	1.0×10^{-6}	2.0×10^{-6}	2.2×10^{-6}	2.2×10^{-6}	3.4×10^{-6}
1.5×10^{-6}	1.2×10^{-6}	2.3×10^{-6}	1.9×10^{-6}	2.2×10^{-6}	3.4×10^{-6}

Due to the time restrictions of the study, only the standard deviation at 1213 nm was considered. As can be seen from Figure 4.26 and the AA results of blend 6, there is perhaps a degree of contribution from 1591 nm, which needs to be explored further.

Also of note is that the value for the standard deviation of 1213 nm below 3×10^{-6} for four data points being used as an indicator of end-point could only be confirmed by the experiments conducted. This standard deviation still needs to be optimized as it could be any value between 2×10^{-6} and 3×10^{-6} as determined from the blends carried out to points after end-point, to end-point and before end-point.

At present, Ridaq® granule is blended for a period of 10 minutes in the facility. This blend duration is significantly higher when compared to the times predicted by NIR which range from 3 minutes and 18 seconds to 1 minute 52 seconds. The production batch size is approximately 180 kg as opposed to the 3 kg used for the experiments; however, the shape, motion and speed of the blenders used for the experiments and at a production level are congruent. The experiments simulate the blending conducted at a production level therefore the principle be applied to the production level. Process optimization needs to be conducted on production size batches to establish optimum blend time.

4.5 SUMMARY

The results show that there is a relationship between the degree of homogeneity and the standard deviation of the absorbance at the wavelength chosen. Blends were shown to be homogeneous when the standard deviation value of the absorbance was low and non-homogeneous when the standard deviation value of the absorbance was high. Although the significant wavelength for magnesium stearate was used for the predictions, it is evident that information could also be obtained from the 1591 nm wavelength to aid an accurate prediction of end-point using NIR.

With a process driven end-point approach, it becomes possible to have blend durations that are particular for each type of blend, without the possibility of de-mixing or denaturing the granule. This approach will benefit the pharmaceutical industry as there will be significant time saving and an improvement in the quality of the final product.

CHAPTER 5

MOISTURE DETERMINATION IN THE FLUID BED DRYER

5.1 INTRODUCTION

The product temperature in a FBD can be used as a tool for the determination of granule moisture during drying (Van Scoik *et al.* 1989). An alternate technique would be to use a NIR probe to monitor the entire drying process and determine the moisture content of the granule in real-time (Stowell, Peck, Luy, Battig & Olivero 2002).

Fluidization is an efficient technique for the drying of granular solids as each particle is completely surrounded by the drying air. The intense mixing between the solids and the drying air results in uniform conditions of temperature, composition and particle size distribution throughout the bed. (Van Scoik *et al.* 1989)

At this pharmaceutical company, the optimum product temperature for the correct prediction of moisture content is determined by a series of experimental batches. As the product is dried in the FBD, granule moisture analysis is conducted on a series of temperatures using a LOD analyzer. The drying is stopped when the optimum moisture is reached and the temperature is noted. This end-point temperature is then validated to ensure repeatability and reliability.

The purpose of this chapter is to assess the current technique of moisture determination in the FBD. The suitability and feasibility of the introduction of PAT using a NIR probe to monitor moisture in the FBD will be assessed.

5.2 PRODUCT TEMPERATURE AS A MONITORING TOOL

Figure 5.1 shows a schematic of a FBD, similar to the one that is utilized at this pharmaceutical company. A fan mounted in the upper part of the apparatus induces the fluidizing air stream. The air is heated to the required temperature in an air heater and flows upward through the wet material, which is contained in a drying chamber fitted with a wire mesh support at the bottom. The airflow rate is adjusted by means of a damper. (Van Scoik *et al.* 1989)

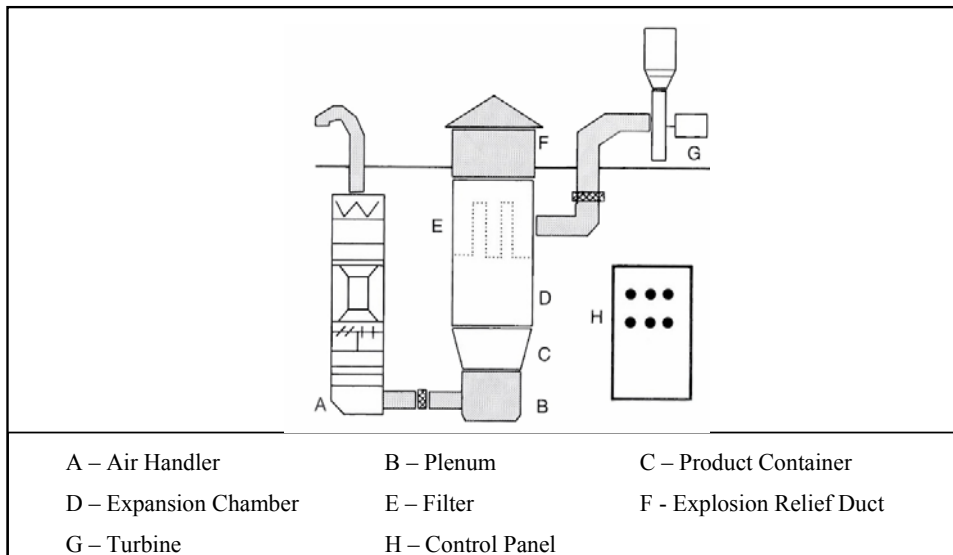


Figure 5.1 Schematic of a FBD (Van Scoik *et al.* 1989).

The temperature probe for the product is situated in the product bowl (c) and in addition there is a probe for the inlet air temperature and the exhaust temperature. This facilitates monitoring of the inlet, product and exhaust temperatures.

The fluid bed system allows material to be dried with a temperature profile. Moisture evaporating from the granule will cool the drying air. The energy consumed by evaporating moisture will be reflected in the constant temperature difference between the incoming warm, dry air and the cooler more humid exhaust air. As drying proceeds the increase in temperature of the exhaust air can be detected and the temperature of the drying air can be reduced to prevent overheating and over-drying. The monitoring of the granule temperature is usually used to determine the set point for specific moisture values. (Van Scoik *et al.* 1989)

Drying is controlled for individual products by means of a validated recipe programmed into the FBD. The recipe is made up of a series of phases that start from the granulation of a product to the drying and finally the discharge of the granule into IBC's (refer to Appendix B.3 for an example of a recipe used for drying in the FBD). The actual parameter that must be followed during the manufacture of a product is contained in the recipe. In addition, the recipe can be set with a trip where a limit is set and when this is reached, the process will move to the next phase. For the purpose

of this project, the phases relating to drying will be considered. The initial phase of the FBD is preheating which ensures that the FBD reaches the predetermined temperature, thus preventing the sticking of wet granule to the walls of the FBD. The next phase is charging, where the granule is charged from the vertical granulator into the FBD and this is followed by drying of the granule. There are generally four heating phases that differ from each other in terms of the inlet air temperature and airflow. These parameters are product specific.

Figure 5.2 shows the plot of temperature versus time of the inlet, product and exhaust temperature in the FBD during the drying of granule for a selected product. The first phase indicated by (a) is the preheating phase. The inlet air is set to a specific temperature, in this case 60 °C, and the FBD is allowed to heat up. At this point the product and exhaust air temperature differ slightly as the FBD is being heated.

As soon as the FBD reaches the specified temperature, the trip switch is activated and the process moves to the next phase, which is charging, indicated by (b). During the charging phase, the granule enters into the FBD. As the granule enters the FBD, there is a sharp drop in the product and exhaust temperature as a result of the moisture that is being evaporated from the granule. This drop in temperature is very significant as it can be used to detect any problems in the discharge from the granulator into the FBD. For example, an increase in product temperature could be an indication of a blockage in the down-pipe between the granulator and the FBD. An increase in the exhaust temperature could be as a result of bed channeling, which is due to uneven granule size resulting in air flow through selected portions of the bed (Van Scoik *et al.* 1989). Thus, it can be seen that the temperature probes provide a significant amount of information regarding the state of the granule in the FBD.

The next phase that begins is the heating phase where the inlet air temperature increases as illustrated by (c). During these heating phases the product and exhaust temperature reach a state of equilibrium. After a period the product temperature increases and separates from the exhaust temperature. The product temperature reaches the maximum set temperature thereby activating the trip and causing the inlet air temperature to decrease, thereby starting the cooling phases, illustrated by (d).

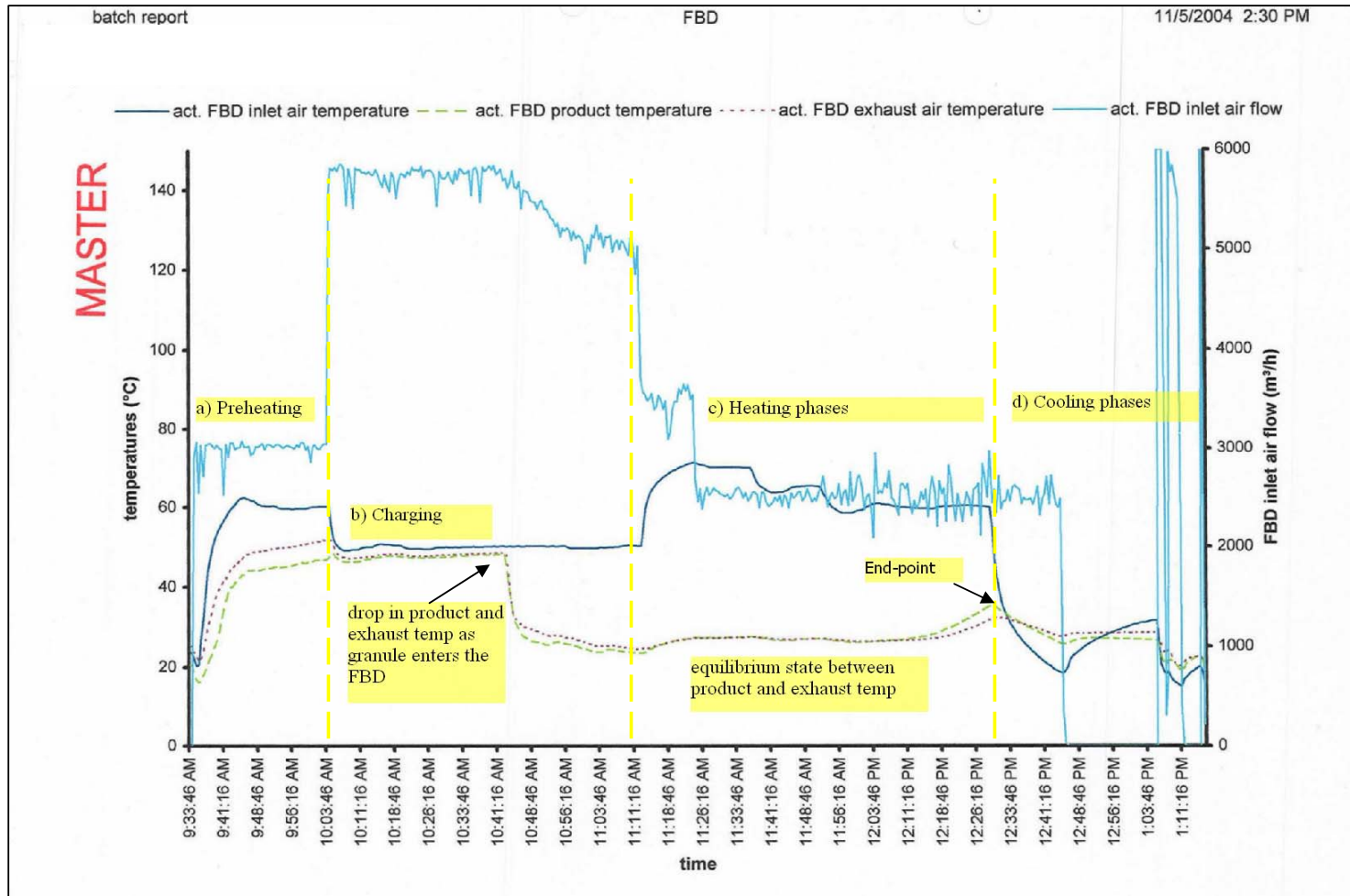


Figure 5.2 Temperature vs. time in the FBD during drying

When the product temperature is reached, a sample is taken from the sample port and the moisture of the granule is determined using a LOD analyser.

In addition, the airflow in the FBD can be seen which is the highest during the phase when granule enters the FBD and the lowest when the granule has reached the end-point product temperature. This is so as the initial granule is heavier than the dried granule and the airflow is decreased to prevent damage of the granule or blocking of the filters.

These methods are usually imprecise as they can be influenced by ambient temperature changes. Fouling of the product temperature is also a point for consideration as this can result in inaccurate temperature readings. (Van Scoik *et al.* 1989)

5.3 NEAR INFRARED AS A MONITORING TOOL

NIR spectroscopy in combination with either an in-line diffuse reflectance measurement or a non-contact measurement through a viewing port could provide a means of continuously monitoring the drying process (Bruker Optics 2005).

NIR spectra result from combination and overtone bands of C-H, N-H, O-H vibrations, and the fact that most reaction mixtures and solvents contain some organic compounds with these bonds, NIR analysis becomes a good option for analysis (Bokobza 1998).

FBD bowls often have a window through which a non-contact NIR diffuse reflection measurement can be made. When using non-contact devices, it is important that the material does not build up on the measuring window. The material should be continuously exchanged on the viewing window so that the NIR spectra are representative of the changing moisture in the bulk material. (Stowell *et al.* 2002)

The advantages of real-time monitoring include process optimization, equipment capacity increases, cycle time reductions and also elimination of the need to sample, which can lead to improved efficiencies. However, significant engineering trials and development may be necessary to ensure that the spectra can be reliably collected in a

dryer. The spectroscopic measurement will not be affected by operating conditions, or require all other drying process parameters to be controlled within a range, to ensure a reliable result, as opposed to the conventional approach of using secondary measurements such as exhaust air temperature or product temperature. (Shering 2005)

The greatest challenge with a NIR spectroscopic method is the collection of spectra. The spectra need to be representative of the rest of the batch within the dryer. Common problems associated with the collection of spectra include fouling of the probe or window (the sampler sees the same sample every time); contamination of the window (the spectrum collected is affected by the previous sample); positioning of the window; engineering aspects such as the ease of cleaning the sampler, removal and maintenance. (Shering 2005)

The CORONA Dryer is an example of an instrument that is commercially available to monitor the moisture continuously and non-invasively in the FBD using NIR technology. This apparatus is illustrated in Figure 5.3. The CORONA uses the unique OMK measuring head that produces a beam of light with a diameter of 25 mm that is passed through a window with a maximum thickness of 30 mm. The diffuse reflectance is collected by a ring of 15 fibres that is directed to the NIR sensor. In general, 50 scans per second are averaged to produce high-quality spectra. The spectra produced are processed to give an end-point output to stop further drying. The end-point can be programmed by a pre-selected moisture value following calibration or trending the rate of change as it reaches a steady state. Full spectrum analysis between 950 – 1700 nm is used, thereby allowing pre-processing functions such as second derivative. (Carl Zeiss 2005)



Figure 5.3 FBD fitted with CORONA NIR device (Carl Zeiss 2006)

5.4 STATISTICAL EVALUATION OF MOISTURE VALUES

Moisture values were collected retrospectively from 35 production batches using convenience sampling for two products that are manufactured in the facility. Product A has a set point temperature of 35 °C and a moisture range of 1.5 -2.5 % and Product B has a set point temperature of 40 °C and a moisture range of 2.0 – 4.0 %.

A process capability study was conducted. The process capability is the ability of a process to meet the specification limits. A measure of the process capability called the capability index is symbolized by C_p . A minimum value of 1.33 is recommended for C_p . It is also necessary to determine if the process is centered on the nominal value, which is symbolized as C_{pk} and is a measure of centering. A minimum value of 1.00 is recommended for C_{pk} . (Besterfield 1994)

The Capability Sixpack (Normal) option available on the statistical program MINITAB® Release 14 was used to conduct the process capability study. The Capability Sixpack (Normal) combines a capability histogram and a normal probability plot, which can be used to verify if the data is normally distributed and a capability plot, which displays the process variability compared to the specifications.

The plots can be used to verify if the process is in control and if the data follow the chosen distribution. The Capability Sixpack (Normal) calculates both the short term and long term variation. The capability statistics associated with short term variation are Cp and Cpk, and with long term variation, Pp and Ppk. The normal probability plot generates Anderson-Darling (AD) statistics and a p-value. The AD statistics is a measure of how far the plot points fall from the fitted line in a probability plot. A smaller AD statistic indicates that the distribution fits the data better. (Besterfield 1994)

5.4.1 Statistical evaluation of Product A

The upper control limit (UCL) and the lower control limit (LCL) are established at plus/minus 3 standard deviations from the mean. The UCL and LCL are 2.4975 and 1.6527 respectively. From the definition of a normal curve, the number of items that fall between $+3\sigma$ and -3σ is equal to 99.73 % therefore it is expected that 997 times out of 1000, the moisture values will fall between the UCL and LCL thus indicating that the process is in control as the UCL and the LCL are within the specifications of the product that is, within the upper specification limit (USL) and lower specification limit (LSL) (1.5 – 2.5 %).

On the Capability histogram (Figure 5.4), it can be seen that the data approximately follow a normal distribution.

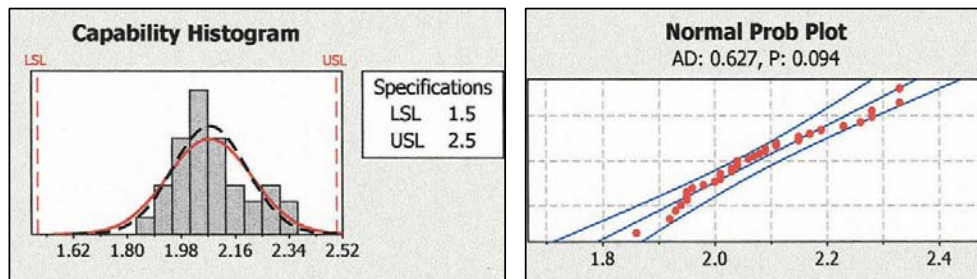


Figure 5.4 Capability histogram and Normal probability plot for product A

From the capability histogram it can also be seen that the moisture values fall more to the upper specification limit (positively skewed) but all values fall within the process tolerance limits.

On the normal probability plot the points approximately follow a straight line. The AD statistics (0.627) and p-value (0.094) suggests that the data are normally distributed.

The capability plot (Figure 5.5) shows a Cp value (1.18) greater than 1 which is a desirable state but below the industrial norm of 1.33.

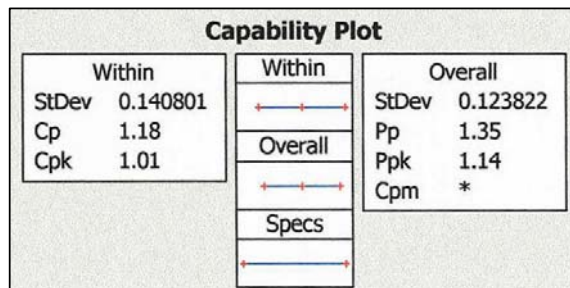


Figure 5.5 Capability plot of Product A (* no value calculated)

This illustrates that the process is in a desirable state although there is some room for improvement. The Cpk (1.01) is greater than 1.00, indicating that the values for moisture are centred around a target value.

5.4.2 Statistical evaluation of Product B

The UCL and LCL for Product B are 3.461 and 2.159 respectively. As discussed for Product A, the number of items that fall between $+3\sigma$ and -3σ is equal to 99.73 % therefore it is expected that 997 times out of 1000 the moisture values will fall between the UCL and LCL. This indicates that the process is in control as the UCL and the LCL are within the specifications of the product (i.e. 2.0 – 4.0 %).

On the Capability histogram (Figure 5.6) it can be seen that the data approximately follow a normal distribution.

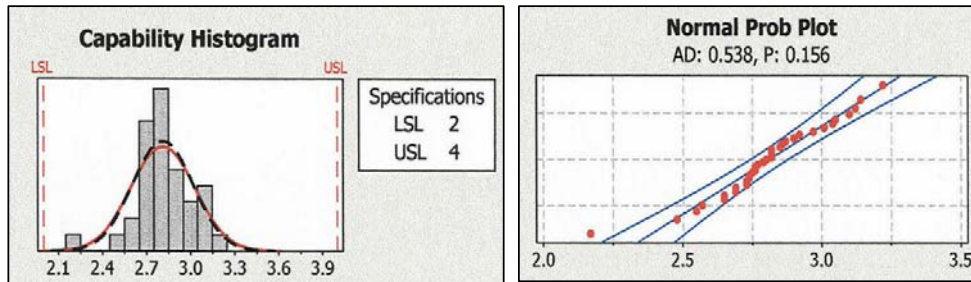


Figure 5.6 Capability histogram and Normal probability plot for Product B

On the normal probability plot the points approximately follow a straight line which indicates that the data are normally distributed. The AD statistics (0.538) and p-value (0.156) suggests that the data are normally distributed.

The Capability plot (Figure 5.7) shows that the Cp value (1.54) satisfies the industrial norm standards (minimum of 1.33). In addition, the greater the Cp value, the greater is the process capability (Besterfield 1994).

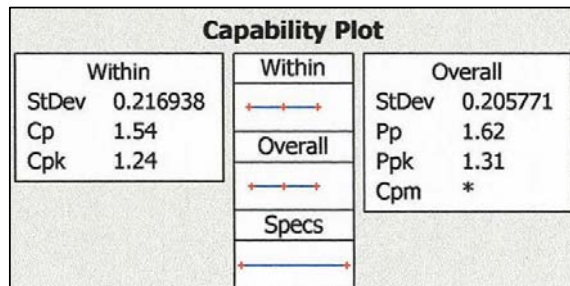


Figure 5.7 Capability Plot of Product B (* no value calculated)

The process is in a very desirable state. The Cpk (1.24) is greater than 1.00, indicating that the values for moisture are centred around a target value. It can be seen that is process is stable and in control.

5.5 SUMMARY

As can be seen from the statistical evaluation of the moisture values for Product A and Product B, the use of the product temperature to monitor the moisture gives consistent results. The current process is stable and capable of producing repeatable results.

NIR provides a means for continuously monitoring the product moisture and allows one to take action to prevent over-drying or under-drying. With the current method of product temperature monitoring to obtain the moisture the actual moisture value is only determined when the FBD is in the cooling phase. At this point, if the product moisture is not within the specification, corrective action will be a challenge.

The US FDA guidelines for the introduction of PAT recommend that processes that are relatively stable will not benefit significantly from the introduction of a PAT tool to the process. PAT is not recommended if the product efficiency is high, or if there is a low percentage of failed batches as PAT will add little to the understanding and the control of the process. Further PAT is not recommended if traditional validation techniques have established that the process design is adequate. (US FDA *et al* 2004)

From the process capability study of the two products it can be seen that Product A is stable but can still be optimized while Product B is at a desirable state. Traditional validation and optimization techniques can be used to optimize Product A. The application of NIR monitoring should therefore be considered on a product specific basis.

The cost of a NIR device for monitoring the product moisture is approximately 200,000 Euro. In addition, the system has to be calibrated which is time consuming. It appears that the cost justification for the introduction of a NIR probe to monitor the moisture in the FBD is questionable in this case.

CHAPTER 6

CONCLUSION AND RECOMMENDATIONS

6.1 RAW MATERIAL IDENTIFICATION AND QUALIFICATION

One of the objectives of the study was to investigate the application of NIR analysis to incoming raw material identification. This was successfully achieved by the development of the NIR method using the FOSS XDS instrument and the PASG guidelines.

The introduction of NIR analysis to raw material identification and material qualification shows great promise. The algorithms used to create the NIR method are capable of distinguishing between the different raw materials in the spectral library. As demonstrated by the specificity tests conducted, NIR has the ability to differentiate between chemically similar material, which is an important factor to the pharmaceutical environment as misidentifications of material can have serious consequences. This provides a great advantage to the pharmaceutical environment, and the fact that the NIR analysis can take as little as 30 seconds, with no need for sample preparation, makes the method advantageous over traditionally used chemical methods.

At present the spectral library is validated according to the PASG guidelines for NIR method development for two raw materials namely, starch maize and lactose monohydrate. The current protocol for the testing of starch maize and lactose monohydrate cannot be changed without prior approval from the MCC. It is recommended that the NIR method be used parallel with compendial testing methods for a period of 3 months. This would confirm that the samples in the library are representative of the current raw materials received and that the library can identify samples correctly. The data collected over the set time period can be used to demonstrate confidence in the NIR method. This data can then be submitted to the regulatory authorities for approval.

6.2 BLEND UNIFORMITY ANALYSIS

The objective of the study with regards to blend uniformity was to predict blend uniformity using NIR technology and to evaluate the feasibility of a blender fitted with a NIR device for blend monitoring.

From the experiments conducted it can be concluded that a relationship exists between the degree of homogeneity and the standard deviation of the absorbance at the chosen wavelengths. Blends sampled at the predetermined time intervals demonstrated a homogeneous state when the standard deviation of the absorbance was low and a non-homogeneous state when the standard deviation of the absorbance was high, thus the NIR prediction on the state of the blend was confirmed by the atomic absorption method.

During the blend experiments, it was evident that each blend had a unique behaviour although the experiments were conducted in an identical manner. This observation draws ones attention to the statement by the US FDA that no two processes are identical and therefore there is a growing need to move to a process determined end-point as opposed to the conventional time determined end-points (US FDA *et al.* 2004).

The cost of a laboratory scale blender is approximately 70,000 Great British Pounds (GBP). The feasibility of the blender with the NIR monitoring device needs to be considered in terms of product quality. With a process driven end-point approach, it becomes possible to have blend durations that are particular for each type of blend, without the possibility of de-mixing or denaturing the granule. Under mixing or over mixing after the addition of lubricants to granule could result in poor compression and/or dissolution profiles. There is therefore a need to move from the conventional time-determined end-points to process-determined end-points. A process-determined end-point will benefit the pharmaceutical industry as there will be significant time saving and will also improve the quality of the final product. Time and cost saving will be achieved as a result of improved granule quality thus minimising or eliminating compression problems or poor dissolution profiles.

The PAT focus is process understanding and the use of the NIR blender could facilitate this understanding. Due to time restrictions, the number of blend experiments was limited and it would therefore be advisable to conduct blend monitoring at other significant wavelengths instead of the current study that utilized only two wavelengths. The standard deviation used to predict a uniform blend needs to be optimized with further experimentation. It would also be of interest to investigate the possible standard deviations of the absorbance at which de-mixing occurs.

Due to the process understanding that is still to be achieved with the NIR blender, it is recommended that the blender be used at a research level or in a pilot plant prior to implementation at a production level.

6.3 MOISTURE DETERMINATION IN THE FBD

The objective of the study with regards to moisture determination in the FBD was to retrospectively determine the accuracy of the current method for moisture content determination in the FBD, using statistical analysis of past production batches and to evaluate the feasibility of installing a NIR device to continuously monitor the drying process in a FBD.

The process capability study conducted on two pharmaceutical products showed that the use of product temperature to monitor granule moisture content yielded consistent results. In addition, the monitoring of the inlet, exhaust and product temperature in the FBD could provide information on the state of the granule in the FBD, such as bed channeling or blockage in the discharge of the granule from the vertical granulator into the FBD.

One of the greatest advantages that NIR moisture monitoring offers over the traditional method of temperature monitoring is that the results are obtained in real-time and corrective action can be taken if needed. On the other hand, the US FDA guidelines for the introduction of PAT recommend that processes that are relatively stable will not benefit significantly from the introduction of a PAT tool to the process.

The cost of a NIR device for monitoring the product moisture is approximately 200,000 Euro. In addition, the system has to be calibrated, which is time consuming. The cost justification for the introduction of a NIR probe to monitor the moisture in the FBD is questionable in this case.

6.4 PAT IMPLEMENTATION – THE WAY FORWARD

PAT implementation can assure acceptable end-product quality, reduce or eliminate end-product testing, reduce manufacturing cost through increased efficiency, reduce production cycle times and reduce rejects and re-processing. The initiative also has the potential of reducing raw material cost by precise formulation, increasing automation to improve operator safety and reducing human errors, improving efficiency and managing variability. (The PAT team & The Manufacturing Science Working Group 2005)

Currently, quality assurance is based on whether the analysis result of a sample is within the specification limits. PAT provides a means of continuously monitoring a process to assure quality, thus it builds quality into a product as opposed to testing the quality at the end of the process. (The PAT team & The Manufacturing Science Working Group 2005)

From this study, it can be seen that it will be beneficial for this pharmaceutical company to utilise the NIR method for raw material identification and qualification. With regards to blend uniformity predictions using NIR, it is recommended that more experimentation be conducted at a laboratory scale level to gain process understanding prior to implementation in production. The current approach of product temperature monitoring in the FBD to monitor granule moisture seems to be an adequate tool at present and it appears that no added benefit will be gained from the implementation of an NIR device to monitor the moisture. It is recommended that the PAT guidelines be followed in terms of areas of priority for PAT implementation in order for the implementation to be successful (US FDA *et al.* 2004).

This project has investigated the three possible areas for PAT implementation, however, the first step to successful implementation of PAT requires the formation of a PAT team consisting of technical, operational, manufacturing, quality assurance,

managerial and financial team members. It is also necessary to provide ongoing post-implementation PAT support. The PAT team will then be responsible for screening processes to identify those that would benefit from PAT. The critical quality attributes need to be identified and the critical control points must be recognised. Thereafter potential PAT opportunities need to be explored and a PAT plan should be created. (Davis & Wasynczuk 2005)

The second step requires the development of statistical models and the design of experiments for the reduction of variance. Experimental studies will need to be conducted and thereafter the analytical technology will need to be researched, bearing in mind that the analytical technology should be sufficiently developed and robust enough for a production line. (Davis & Wasynczuk 2005)

The third step to PAT implementation is to demonstrate the efficiency of the analytical instrumentation, the information technology system and the statistical reporting. While there is no guidance for a definitive number of batches that should be used to demonstrate the success of the consolidated PAT system, sufficient data should be gathered to demonstrate reliable hardware or software functionality. Statistical correlations should be substantiated and variability between batches should be reduced. After sufficient information is gathered and the manufacturer has confidence that the system is operating as desired, then a dossier should be compiled for submission to the regulatory authorities. (Davis & Wasynczuk 2005)

The final step to PAT implementation is the introduction of PAT concepts through training and the implementation of procedural changes. The robustness and process performance of the PAT related equipment and the process must be continually reviewed, analyzed, approved and where necessary improved. (Davis & Wasynczuk 2005)

From the investigations conducted, it can be seen that there is definitely a niche for PAT at this pharmaceutical company. To ensure success of the implementation, it is recommended that the guidelines stated above be followed. PAT implementation is a gradual process of change, which will take time, probably several years (Heinze & Hansen 2005). Davis and Wasynczuk (2005) also add that while the time, resources

and financial commitments required for PAT implementation may be great, the rewards in terms of reduced processing time and improved product quality are greater, particularly if these steps are added to the earliest stages of the product's development life cycle.

REFERENCE LIST

- Afnan, A. M. 2004. PAT: What's in a Name? *The Journal of Process Analytical Technology*, vol. 1, no. 1 pp. 8-9.
- Bakeev, K. A. 2003. Near-infrared spectroscopy as a process analytical tool. *Pharmaceutical Technology – Europe* [online]. Available: www.ptemag.com/pharmtecheurope [Accessed: 20 August 2005].
- Besterfield, D. H. 1994. “Ch. 4: Control charts for variables” in *Quality Control*, 4th edn., D. H. Besterfield, ed., Prentice Hall International, United States of America, pp. 103-167.
- Bokobza, L. 1998. Near infrared spectroscopy. *Journal of Near Infrared Spectroscopy*, vol. 6, pp. 3-17.
- Boysworth, M. C. and Booksh, K. S. 2001. “Ch. 9: Aspects of Multivariate Calibration Applied to Near Infrared Spectroscopy”, in *Handbook of Near-infrared Analysis*, 2nd edition, vol. 27, D. A. Burns and E. W. Ciurczak, eds., Marcel Dekker Inc, New York, pp. 209-240.
- Brereton, R. G. 2005. Chemometrics and PAT. *The Journal of Process Analytical Technology*, vol. 2, no. 3, pp. 8-11.
- Bruker Optics 2005. *Near infrared analysis of powder moisture in a fluid bed dryer* [online]. Available: www.brukeroptics.com [Accessed: 20 January 2006]
- Buck Systems 2005. Lab-scale blender boasts NIR analysis. *In-Pharma Technologist* [online]. Available: www.in-pharmtechnologist.com [Accessed: 25 July 2005]
- Carl Zeiss 2005. *Online Drying, Blending and Cleaning Verification Products from Carl Zeiss* [online]. Available: www.touchbriefings.com/pdf/15/pg031_t_carlzei.pdf [Accessed: 12 January 2006]

Cinier, R. and Guilmant, J. 1998. Qualification of solid raw materials using near infrared spectroscopy. *Journal of Near Infrared Spectroscopy*, vol. 6, pp. A231-A237.

Ciurczak, E. W. 2001. "Ch. 1: Principle of near infrared spectroscopy", in *Handbook of Near-infrared analysis*, vol. 27, D. A. Burns and E. W. Ciurczak, eds., Marcel Dekker Inc, New York, pp. 7-18.

Ciurczak, E. W. 2006. Near infrared spectroscopy: Why is it still the number one technique in PAT? *The Journal of Process Analytical Technology*, vol. 3, no. 1, pp. 19-22.

Ciurczak, E. W. and Drennen III, J. K. 2002a. "Ch. 3: Blend uniformity Analysis", in *Pharmaceutical and medical applications of near infrared spectroscopy*, vol. 31, E. W. Ciurczak and J. K. Drennen III, eds., Marcel Dekker Inc, New York, pp. 33-54.

Ciurczak, E. W. and Drennen III, J. K. 2002b. "Ch. 2: Instrumentation", in *Pharmaceutical and medical applications of near infrared spectroscopy*, vol. 31, E. W. Ciurczak and J. K. Drennen III, eds., Marcel Dekker Inc, New York, pp. 15-31.

Davis, J. R. and Wasynczuk, J. 2005. The four steps of PAT implementation. *Pharmaceutical Engineering*, vol. 25, no. 1, pp. 1-8.

Drennen III, J. K. and Lodder, R. A. 1993. "Pharmaceutical applications of near-infrared spectroscopy", in *Advances in near-infrared measurements*, vol. 1, G. Patonay ed., Jai press Ltd, United Kingdom, pp. 93-112.

El-Hagrasy, A. S., Morris, H. R., Damico, F., Lodder, R. A. and Drennen III, J. K. 2001. Near-infrared spectroscopy and imaging for the monitoring of powder blend homogeneity. *Journal of Pharmaceutical Sciences*, vol. 90, no. 9, pp. 1298-1307.

Ellis, S. and Davies, B. 2005. Process analytical technology: The route of process understanding and control. *Pharmaceutical Technology Europe*, Europe, pp. 17-23.

Erni, F. 2005. Quality by Design in Pharmaceutical Development. *The Journal of Process Analytical Technology*, vol. 2, no. 2, pp. 23-26.

Farhadieh, B. 1994. "Starch", in *Handbook of pharmaceutical excipients*, 2nd edn., A. Wade and P. J. Weller, eds., American Pharmaceutical Association and Pharmaceutical Press London, Great Britain, pp. 483-488.

FOSS NIRSystems 2005. *XDS Rapid content analyzer installation and user manual*, version 1.03, United States of America.

Geoffroy, J. M. 2004. Impact of Process analytical technology implementation on product and process specifications. *American Pharmaceutical Review*, vol. 7, no. 3, pp. 35-38, 69.

Gilbert, S. B. and Anderson, N. R. 1986. "Tablets", in *The theory and practice of industrial pharmacy*, 3rd edn., L. Lachman, H. A. Liberman and H. L. Kanig, eds., Lea and Febiger, Philadelphia.

Goodhart, F. W. 1994. "Lactose" in *Handbook of pharmaceutical excipients*, 2nd edn., A. Wade and P. J. Weller, eds., American Pharmaceutical Association and Pharmaceutical Press London, Great Britain, pp. 252-261.

Hammond, S. 2005. *PAT strategies for identifying, measuring and controlling process risk: Process to measurement interface issues- Set up and remote triggering* [online]. Available: www.fda.com [Accessed: 20 September 2005].

Heinze, C. L. and Hansen, J. R. 2005. Implementing PAT. *Pharmaceutical Engineering*, vol. 25, no. 3, pp. 8-16.

International Conference on Harmonization (ICH) 1994. *Text on Validation of Analytical procedures-Q2A* [online]. Available: www.ich.org [Accessed: 23 August 2005].

International Conference on Harmonization (ICH) 2004. *Note for the guidance on pharmaceutical development- ICH Q8* [online]. Available: www.ich.org [Accessed: 23 August 2005].

Kanfer, I., Walker, R. B. and Persicaner, P. 2005. "Experimental formulation development", in *Generic drug product development: Solid oral dosage forms*, L. Shargel and I. Kanfer, eds., Marcel Dekker, New York, pp. 53-75.

Kemper, M. S. and Luchetta, L. M. 2003. A guide to raw material analysis using near infrared spectroscopy. *Journal of Near Infrared Spectroscopy*, vol. 11, pp. 155-174.

Kourti, T. 2004. Process Analytical Technology and Multivariate Statistical Process Control. *The Journal of Process Analytical Technology*, vol. 1, no. 1, pp. 13-19.

Lantz, R. J. and Schwartz, J. B. 1989. "Mixing" in *Pharmaceutical Dosage forms: Tablets*, 2nd edn., H. A. Liberman and J. B. Schwartz, eds., Marcel Dekker Inc, New York, pp. 1-71.

Lordi, N. G. 1994. "Pregelatinized Starch" in *Handbook of pharmaceutical excipients*, 2nd edn., A. Wade and P. J. Weller, eds., American Pharmaceutical Association and Pharmaceutical Press London, Great Britain, pp. 491-493.

Marshall, K. 1986. "Compression and consolidation of powdered solids", in *The theory and practice of industrial pharmacy*, 3rd edn., L. Lachman, H. A. Liberman and H. L. Kanig, eds., Lea & Febiger, Philadelphia, pp. 66-99.

Masterton, W. and Hurley, C. 1993. "Ch. 6: Electronic structure and the periodic table", in *Chemistry: Principles and Reactions*, 2nd edn., W. Masterton and C. Hurley, eds., Saunders College, Orlando, pp. 130-162.

Mattes, R. A., Schroeder, R., Dhopeswarker, V., Kowal, R. and Randolph, W. 2005. Monitoring granulation drying using near-infrared spectroscopy. *Pharmaceutical Technology Europe* [online]. Available: www.pharmtech.com [Accessed: 28 March 2006].

Medicines Control Council 2003. *Post-Registration Amendments*. Pretoria, South Africa.

Muzzio, F. J., Alexander, A., Goodridge, C., Shen, E., and Shinbrot, T. 2003. "Solids mixing", in *Handbook of industrial mixing: Science and practice*, E. L. Paul, V. Atiemo-Obeng and S. M. Kresta, eds., Wiley & Sons Inc., New York, pp. 906-907.

Palermo, J. P. 2001. "Ch. 6: Solid Dosage-form Analysis", in *Handbook of Modern Pharmaceutical Analysis*, vol. 3, S. Ahuja and S. Scypinski, eds., Academic Press, London, pp. 235-267.

Pharmaceutical Analytical Science Group (PASG) 2001. *Development and validation of near infrared spectroscopic methods* [online]. Available: www.fda.com [Accessed: 20 September 2005].

Pharmacopeial Forum 2006. "Uniformity of dosage units" in *USP29-NF24*, USPC, Inc. Official.

Pharmacopoeial Forum 1997. "Near infrared spectrophotometry", in *European Pharmacopoeia*, version 5.0, Europe, pp. 59-63.

Rankell, A. S., Liberman, H. A. and Schiffmann, R. F. 1986. "Drying", in *The Theory and Practice of Industrial Pharmacy*, 3rd edn., L. Lachman, H. A. Liberman and H. L. Kanig, eds., Lea and Febiger, Philadelphia, pp. 47-65.

Rudd, D. 2004. The use of acoustic monitoring for the control and scale-up of a tablet granulation process. *The Journal of Process Analytical Technology*, vol. 1, no. 2, pp. 8-11.

Shering, P. 2005. Engineering a system to enable spectroscopy in a filter dryer. *Spectroscopy Europe*, vol. 17, no. 6, pp. 30-31.

Stowell, J. G., Peck, G. E., Luy, B., Battig, M. and Olivero, F. 2002. End-point of drying determination by near infrared monitoring. *Consortium for the advancement of manufacturing pharmaceuticals Report*, Prude University.

Technical Support 2005. Process Validation Protocol [unpublished work]. Port Elizabeth, South Africa.

The PAT team and The Manufacturing Science Working Group 2005. *Innovation and continuous improvement in pharmaceutical manufacturing- Pharmaceutical CGMPs for the 21st century* [online]. Available: www.fda.com [Accessed: 12 October 2005].

Travers, D. N. 1988. "Mixing", in *Pharmaceutics: The science of dosage form design*, M. E. Aulton, ed., Churchill Livingstone, Edinburgh, pp. 550-563.

United States Food and Drug Administration (US FDA), United States Department of Health and Human services (US DHHS), Centre for Drug Evaluation and Research (CDER), Centre for Veterinary Medicine (CVM), and Office of Regulatory Affairs (ORA) 2004. *Guidance for Industry PAT: A Framework for the Innovative Pharmaceutical Development, Manufacturing, and Quality Assurance: Guidance for industry* [online]. Available: www.fda.com [Accessed: 10 July 2005].

United States Department of Health and Human services (US DHHS) and United States Food and Drug Administration (US FDA) 2004. *Pharmaceutical cGMPs for the 21st Century- A risk-based approach Final report - Fall* [online]. Available: www.fda.com [Accessed: 10 July 2005].

Van Scoik, K. G., Zoglio, M. A. and Carstensen, J. T. 1989. "Drying" in *Pharmaceutical Dosage forms: Tablets*, 2nd edn., Marcel Dekker Inc, New York, pp. 73-105.

Warman, M. 2004. Using near infrared spectroscopy to unlock the pharmaceutical blending process. *American Pharmaceutical Review*, vol. 7, no. 2, pp. 54-57.

Workman, J. J. 2001. "Ch. 6: NIR spectroscopy calibration basics" in *Handbook of near infrared analysis*, 2nd edn., D. A. Burns and E. W. Ciurczak, eds., Marcel Dekker, New York, pp. 91-128.

APPENDIX A
RAW MATERIAL ANALYSIS

This appendix contains:

- A.1 Spectral library validation report
- A.2 Positive challenge – starch maize
- A.3 Positive challenge – lactose monohydrate
- A.4 Negative challenge – pregelatinised starch
- A.5 Negative challenge – tablettose

A.1 Spectral Library Validation Report

General Information				Global Library Methods				
Library:	powderlibb	Samples:		Develop	Method	Threshold	Type	
Products:	6	208		CLUSTER	No			
Author/Operator:	krishel			IDENTIFY	RV	3.000	MV	
Date:	2006/04/26			Math Pre-Treatments Used				
Time:	14:52:46							
Summary Results by Set				Description	CLUSTER	IDENTIFY		
Measurement	Set Type				Order	Order		
	Training	Acceptance	Reject	1st derivative:	N/A			
Total Validated:	208	0	0	2nd derivative:	N/A	1		
Total Failed:	0	0	0	3rd derivative:	N/A			
Percent Failed:	0.00	0.00	0.00	4th derivative:	N/A			
Library Development Method Keys				Std Normal Variate:	N/A			
				Baseline Correction:	N/A			
				Detrend:	N/A			
				Savitzky-Golay:	N/A			
				Development Method				Threshold Type Keys
Mahalanobis Distance on PC scores:			Key	Threshold Type				Key
Residual Variance after PC analysis:			MD	Matching Value:				MV
Wavelength Correlation:			RV	Probability Level:				PL
Wavelength Distance:			WC					
			WD					

A.2 Positive challenge - starch maize

Acquired:

Date: 2005/11/21
 Time: 14:53:48
 Author/Operator: krishel
 Instrument Model: NIRSystems XDS
 Serial number: 3010-0231

Library: powders3lib
 Output Project: powdersout

Date	Time	Sample ID	Selected	ID as	ID Result	P/F	Qual Rslt	P/F
2005/11/21	14:18:09	X062397	Starch Maize EP 2002 Supp (4.8)	Starch Maize EP 2002 Supp (4.8)	0.160	Pass	0.999	Pass
2005/11/21	14:21:02	X060386	Starch Maize EP 2002 Supp (4.8)	Starch Maize EP 2002 Supp (4.8)	0.073	Pass	1.000	Pass
2005/11/21	14:22:00	X060338	Starch Maize EP 2002 Supp (4.8)	Starch Maize EP 2002 Supp (4.8)	0.066	Pass	0.999	Pass
2005/11/21	14:23:01	X059594	Starch Maize EP 2002 Supp (4.8)	Starch Maize EP 2002 Supp (4.8)	0.039	Pass	1.000	Pass
2005/11/21	14:24:02	X059597	Starch Maize EP 2002 Supp (4.8)	Starch Maize EP 2002 Supp (4.8)	0.028	Pass	0.999	Pass
2005/11/21	14:24:55	X062396	Starch Maize EP 2002 Supp (4.8)	Starch Maize EP 2002 Supp (4.8)	0.193	Pass	0.999	Pass
2005/11/21	14:25:42	X060364	Starch Maize EP 2002 Supp (4.8)	Starch Maize EP 2002 Supp (4.8)	0.038	Pass	1.000	Pass
2005/11/21	14:26:38	X059593	Starch Maize EP 2002 Supp (4.8)	Starch Maize EP 2002 Supp (4.8)	0.028	Pass	0.999	Pass
2005/11/21	14:27:23	X060473	Starch Maize EP 2002 Supp (4.8)	Starch Maize EP 2002 Supp (4.8)	0.033	Pass	1.000	Pass
2005/11/21	14:28:22	X061614	Starch Maize EP 2002 Supp (4.8)	Starch Maize EP 2002 Supp (4.8)	0.168	Pass	0.999	Pass

A.3 Positive challenge - lactose monohydrate

Acquired:

Date: 2006/05/16
 Time: 14:48:15
 Author/Operator: krishel
 Instrument Model: NIRSystems XDS
 Serial number: 3010-0231

Re-analyzed:

Date: 2006/05/18
 Time: 15:10:37
 Author/Operator: krishel

Library: powderlibb

Output Project: powderout

Date	Time	Sample ID	Selected	ID as	ID Result	P/F	Qual Rslt	P/F
2006/05/16	14:41:53	X064023	Lactose Monohydrate EP	Lactose Monohydrate EP	0.130	Pass	1.000	Pass
2006/05/16	14:44:45	X061787	Lactose Monohydrate EP	Lactose Monohydrate EP	0.117	Pass	0.999	Pass
2006/05/16	14:45:35	X059557	Lactose Monohydrate EP	Lactose Monohydrate EP	0.136	Pass	1.000	Pass
2006/05/16	14:46:25	X066759	Lactose Monohydrate EP	Lactose Monohydrate EP	0.133	Pass	1.000	Pass
2006/05/16	14:47:12	X064836	Lactose Monohydrate EP	Lactose Monohydrate EP	0.123	Pass	0.999	Pass
2006/05/16	14:48:15	X067199	Lactose Monohydrate EP	Lactose Monohydrate EP	0.192	Pass	0.999	Pass

A.4 Negative challenge - pregelatinized starch

Acquired:

Date: 2005/11/21
Time: 14:11:35
Author/Operator: krishel
Instrument Model: NIRSystems XDS
Serial number: 3010-0231

Re-analyzed:

Date: 2006/05/18
Time: 15:12:09
Author/Operator: krishel

Library: powderlibb
Output Project: powderout

Date	Time	Sample ID	Selected	ID as	ID Result	P/F	Qual Rslt
2005/11/21	13:57:46	X062008	unknown	No Match	7.107	Fail	0.000
2005/11/21	14:02:48	X064104	unknown	No Match	7.146	Fail	0.000
2005/11/21	14:05:32	X059601	unknown	No Match	6.774	Fail	0.000
2005/11/21	14:11:35	X059041	unknown	No Match	7.956	Fail	0.000

A.5 Negative challenge – tablettose

Acquired:

Date: 2006/05/16
Time: 13:06:35
Author/Operator: krishel
Instrument Model: NIRSystems XDS
Serial number: 3010-0231

Re-analyzed:

Date: 2006/05/18
Time: 15:13:35
Author/Operator: krishel

Library: powderlibb

Output Project: powderout

Date	Time	Sample ID	Selected	ID as	ID Result	P/F	Qual Rslt
2006/05/16	13:01:36	sample 1	unknown	No Match	0.302	Fail	0.000
2006/05/16	13:05:50	sample 2	unknown	No Match	0.444	Fail	0.000
2006/05/16	13:06:35	sample 3	unknown	No Match	0.350	Fail	0.000

APPENDIX B
MOISTURE DETERMINATION IN THE FLUID BED DRYER

This annexure contains:

- B.1 Moisture values for Product A used for the retrospective process capability study
- B.2 Moisture values for Product B used for the retrospective process capability study
- B.3 Example of recipe used for the drying of product in the FBD

B.1 Moisture values for Product A

Table B.1 Moisture values for Product A

Batch number	% Moisture
A701010	2.01
A701011	2.06
A701012	1.98
A701013	1.94
A701014 A	2.03
A701014 B	1.95
A701015 A	2.09
A701015 B	1.95
A701016 A	2.33
A701016 B	2.04
A701017 A	1.93
A701017 B	2.23
A701019	2.04
A701020 A	2.15
A701020 B	2.04
A701063 A	2.01
A701063 B	2.17
A701064 A	2.19
A701064 B	2.33
A701065 A	2.11
A701065 B	1.96
A701066 A	2.26
A701066 B	1.86
A701067 A	2.28
A701067 B	2.09
A701068 A	2.28
A701068 B	1.95
A701069 A	2.00
A701069 B	1.92
A701000	2.08
A701001	2.01
A701002	2.11
A701003	2.03
A701005	2.15
A701006	2.07

B.2 Moisture values for Product B

Table B.2 Moisture values for Product B

Batch number	% Moisture
A701071	2.87
A701072	2.82
A701073	2.48
A701074	2.9
A701075	2.85
A701144	3.14
A701145	2.77
A701146	2.82
A701147	2.65
A701148	2.65
A701149	2.97
A701150	2.76
A701589	2.55
A701590	2.69
A701591	2.74
A701592	2.76
A701593	3.01
A701594	2.82
A701595	2.17
A701596	2.92
A701597	3.05
A701598	2.73
A701599	3.12
A701600	2.69
A700674	3.04
A700676	2.79
A700682	2.86
A700342	3.22
A700343	2.82
A700344	2.75
A700345	3.1
A700346	2.73
A700642	2.80
A700644	2.74
A700643	2.57

B.3 Example of recipe used for the drying of product in the FBD

phase no.	1	2
set phase type	heating	charging
min FBD inlet air flow [m ³ /h]	0	---
set FBD inlet air flow [m ³ /h]	3000	---
max FBD inlet air flow [m ³ /h]	6000	---
min FBD inlet air temperature [°C]	0	0
set FBD inlet air temperature [°C]	60	50
max FBD inlet air temperature [°C]	100	100
min FBD product temperature [°C]	0	---
max FBD product temperature [°C]	100	---
tripp. FBD product temperature [°C]	0	---
min FBD exhaust air temperature [°C]	0	---
max FBD exhaust air temperature [°C]	100	---
tripp. FBD exhaust air temperature [°C]	0	---
set FBD inlet air flap position [%]	---	45
set FBD exhaust air flap [%]	---	60
set FBD filter shaking pause [sec]	0	30
min FBD atomising air pressure [bar(g)]	---	---
set FBD atomising air pressure [bar(g)]	---	---
max FBD atomising air pressure [bar(g)]	---	---
set delay time after blow out [sec]	---	---
set delay time discharging [min]	---	---
set delay time air flow [sec]	---	---
set process pause mode	process parameter	process interrupt
set phase text trip mode	close window to acknowledge	automatic close message window
set phase text 1	THE FBD IS HEATING UP PRE-CHARGING	
tripp. phase time [min:sec]	30	---

phase no.	3	4
set phase type	heating	heating
set phase name		
min FBD inlet air flow [m³/h]	0	0
set FBD inlet air flow [m³/h]	3500	2500
max FBD inlet air flow [m³/h]	6000	6000
min FBD inlet air temperature [°C]	0	0
set FBD inlet air temperature [°C]	70	70
max FBD inlet air temperature [°C]	100	100
min FBD product temperature [°C]	0	0
max FBD product temperature [°C]	100	100
trip. FBD product temperature [°C]	45	45
min FBD exhaust air temperature [°C]	0	0
max FBD exhaust air temperature [°C]	100	100
trip. FBD exhaust air temperature [°C]	100	100
set FBD inlet air flap position [%]	---	---
set FBD exhaust air flap [%]	---	---
set FBD filter shaking pause [sec]	30	30
min FBD atomising air pressure [bar(g)]	---	---
set FBD atomising air pressure [bar(g)]	---	---
max FBD atomising air pressure [bar(g)]	---	---
set delay time after blow out [sec]	---	---
set delay time discharging [min]	---	---
set delay time air flow [sec]	---	---
set process pause mode	process interrupt	process interrupt
set phase text trip mode	automatic close message window	automatic close message window
set phase text 1		
set phase text 2		
set phase text 3		
set phase text 4		
trip. phase time [min:sec]	12	12

phase no.	5	6
set phase type	heating	heating
set phase name		
min FBD inlet air flow [m³/h]	0	0
set FBD inlet air flow [m³/h]	2500	2500
max FBD inlet air flow [m³/h]	6000	6000
min FBD inlet air temperature [°C]	0	0
set FBD inlet air temperature [°C]	65	60
max FBD inlet air temperature [°C]	100	100
min FBD product temperature [°C]	0	0
max FBD product temperature [°C]	100	100
trip. FBD product temperature [°C]	35	35
min FBD exhaust air temperature [°C]	0	0
max FBD exhaust air temperature [°C]	100	100
trip. FBD exhaust air temperature [°C]	100	100
set FBD inlet air flap position [%]	---	---
set FBD exhaust air flap [%]	---	---
set FBD filter shaking pause [sec]	30	30
min FBD atomising air pressure [bar(g)]	---	---
set FBD atomising air pressure [bar(g)]	---	---
max FBD atomising air pressure [bar(g)]	---	---
set delay time after blow out [sec]	---	---
set delay time discharging [min]	---	---
set delay time air flow [sec]	---	---
set process pause mode	process interrupt	process interrupt
set phase text trip mode	automatic close message window	automatic close message window
set phase text 1		
set phase text 2		
set phase text 3		
set phase text 4		
trip. phase time [min:sec]	15	60

phase no.	7	8
set phase type	cooling	message
set phase name		
min FBD inlet air flow [m³/h]	0	---
set FBD inlet air flow [m³/h]	2500	---
max FBD inlet air flow [m³/h]	6000	---
min FBD inlet air temperature [°C]	0	---
set FBD inlet air temperature [°C]	0	---
max FBD inlet air temperature [°C]	100	---
min FBD product temperature [°C]	0	---
max FBD product temperature [°C]	100	---
trip. FBD product temperature [°C]	26	---
min FBD exhaust air temperature [°C]	0	---
max FBD exhaust air temperature [°C]	100	---
trip. FBD exhaust air temperature [°C]	0	---
set FBD inlet air flap position [%]	---	---
set FBD exhaust air flap [%]	---	---
set FBD filter shaking pause [sec]	30	---
min FBD atomising air pressure [bar(g)]	---	---
set FBD atomising air pressure [bar(g)]	---	---
max FBD atomising air pressure [bar(g)]	---	---
set delay time after blow out [sec]	---	---
set delay time discharging [min]	---	---
set delay time air flow [sec]	---	---
set process pause mode	process interrupt	process interrupt
set phase text trip mode	automatic close message window	close window to acknowledge
set phase text 1		ENSURE IBC IN PLACE
set phase text 2		ENSURE IBC FILTER IS IN PLACE
set phase text 3		ENSURE IBC OUTLET IS CLOSED!!
set phase text 4		ENSURE DRY SIEVE SEAL INFLATED
trip. phase time [min:sec]	30	---

phase no.	9	10
set phase type	discharge	cooling
set phase name		
min FBD inlet air flow [m³/h]	0	0
set FBD inlet air flow [m³/h]	6000	6000
max FBD inlet air flow [m³/h]	6000	6000
min FBD inlet air temperature [°C]	0	0
set FBD inlet air temperature [°C]	0	0
max FBD inlet air temperature [°C]	100	100
min FBD product temperature [°C]	---	0
max FBD product temperature [°C]	---	100
trip. FBD product temperature [°C]	---	10
min FBD exhaust air temperature [°C]	---	0
max FBD exhaust air temperature [°C]	---	100
trip. FBD exhaust air temperature [°C]	---	0
set FBD inlet air flap position [%]	---	---
set FBD exhaust air flap [%]	---	---
set FBD filter shaking pause [sec]	---	5
min FBD atomising air pressure [bar(g)]	---	---
set FBD atomising air pressure [bar(g)]	---	---
max FBD atomising air pressure [bar(g)]	---	---
set delay time after blow out [sec]	20	---
set delay time discharging [min]	25	---
set delay time air flow [sec]	90	---
set process pause mode	process interrupt	process interrupt
set phase text trip mode	automatic close message window	automatic close message window
set phase text 1		
set phase text 2		
set phase text 3		
set phase text 4		
trip. phase time [min:sec]	---	3

phase no.	11	12
set phase type	discharge	message
set phase name		
min FBD inlet air flow [m³/h]	0	---
set FBD inlet air flow [m³/h]	6000	---
max FBD inlet air flow [m³/h]	6000	---
min FBD inlet air temperature [°C]	0	---
set FBD inlet air temperature [°C]	0	---
max FBD inlet air temperature [°C]	100	---
min FBD product temperature [°C]	---	---
max FBD product temperature [°C]	---	---
trip. FBD product temperature [°C]	---	---
min FBD exhaust air temperature [°C]	---	---
max FBD exhaust air temperature [°C]	---	---
trip. FBD exhaust air temperature [°C]	---	---
set FBD inlet air flap position [%]	---	---
set FBD exhaust air flap [%]	---	---
set FBD filter shaking pause [sec]	---	---
min FBD atomising air pressure [bar(g)]	---	---
set FBD atomising air pressure [bar(g)]	---	---
max FBD atomising air pressure [bar(g)]	---	---
set delay time after blow out [sec]	20	---
set delay time discharging [min]	2	---
set delay time air flow [sec]	20	---
set process pause mode	process interrupt	process interrupt
set phase text trip mode	automatic close message window	automatic close message window
set phase text 1		OVER AND OUT
set phase text 2		
set phase text 3		
set phase text 4		
trip. phase time [min:sec]	---	---

APPENDIX C
CONCEPT ARTICLE

**THE INTRODUCTION OF PROCESS ANALYTICAL
TECHNOLOGY, USING NEAR INFRARED ANALYSIS, TO A
PHARMACEUTICAL BLENDING PROCESS**

Krishel Naicker ^a, Gareth Kilian ^{a*} and Johan Olivier ^b

^a *Nelson Mandela Metropolitan University, Department of Pharmacy, Faculty of Health Sciences, P. O. Box 77000, Port Elizabeth, 6031, South Africa*

^b *Aspen Pharmacare, 7 Fairclough Road, Korsten, Port Elizabeth, 6014*

* *E-mail: gareth.kilian@nmmu.ac.za*

ABSTRACT

This study investigates the use of a laboratory scale blender fitted with a near infrared probe to monitor lubricant uniformity in a granule blend. A software method was developed to monitor the change in absorbance at significant wavelengths for the granule and lubricant (magnesium stearate) as the blend proceeded in real-time. The standard deviation of the absorbance was plotted as a function of time to monitor the change in the blend. With near infrared spectra, when a process is complete, the spectra will not change, therefore the standard deviation will be small [6]. To verify this, the blend was sampled using a standard sampling method and analyzed with an atomic absorption method for magnesium stearate to ascertain the distribution in the blend. Blends sampled at the predetermined time intervals were well blended when the standard deviation of the absorbance was low and poorly blended when the standard deviation of the absorbance was high, thus verifying the near infrared prediction on the state of the blend in terms of lubricant uniformity.

Key Words: Process analytical technology (PAT), near infrared, blend uniformity, magnesium stearate and granule.

INTRODUCTION

Process analytical technologies are systems for the analysis and control of manufacturing processes to assure acceptable end-product quality [11]. This is achieved by timely measurements of critical parameters and performance attributes of raw material and in-process

material and processes [11]. The desired goal of process analytical technology (PAT) is to design and develop processes that can consistently ensure a predefined quality at the end of the manufacturing process [1]. To “build quality” into a product requires the manufacturing process to be monitored and controlled as opposed to only testing the product at the end of the manufacturing process to assure quality [1].

The blending of solids is a critical step in the production of many pharmaceutical products [4, 7]. Traditional methods for blend uniformity determination involve sampling of the blend using a sample thief and laboratory analysis of the samples using chemical methods [2]. In addition, blend uniformity in the “traditional sense” focuses on the distribution of the active pharmaceutical ingredient in the blend as opposed to distribution of the excipients in the blend, which can influence the desired performance of the pharmaceutical product [2].

Magnesium stearate is a commonly used tablet lubricant that forms a film of low shear strength around the granule thereby reducing the friction at the die wall during tablet ejection [8]. Blending for longer durations than is necessary could result in the incorporation of magnesium stearate intra-granularly, which can influence the bioavailability by decreasing the dissolution rate of the product, due to the hydrophobic nature of magnesium stearate [9]. In addition, over-mixing could lead to the physical destruction of the granule leading to poor compression profiles [9]. The common problems associated with poor lubrication are binding where tablets have vertically scratched edges, lack smoothness or gloss and are often fractured at the top edges; sticking where tablet faces appear dull; filming which is the early stages of sticking; picking which represents the advanced stages of sticking and capping and lamination which is normally associated with poor bonding and can also be a result of a system that is over lubricated [5].

Due to the competitive nature of the pharmaceutical industry and the continuous emphasis on quality from the regulatory authorities, pharmaceutical manufactures require a system to monitor all materials in a blend with little or no sample preparation and the ability to “build” quality into the product and predict end-points in real-time. PAT offers these advantages and near infrared (NIR) spectroscopy is one such tool that is commonly employed [3].

The majority of active pharmaceutical ingredients and excipients absorb NIR radiation, therefore NIR has the ability to provide information of all the components in the blend and is

non-invasive, speedy and requires no sample preparation [2]. In this study, NIR spectroscopy was used for the on-line monitoring of magnesium stearate in a granule blend.

EXPERIMENTAL

Materials

Magnesium stearate (EP 5.02) from approved suppliers to the pharmaceutical manufacturer was used as the lubricant. A proprietary granule was chosen to mix with the magnesium stearate.

Equipment

The study utilized a laboratory scale blender fitted with a NIR probe, operated by equipment specific software programmes. During the intermediate bulk container (IBC) inversion, the NIR probe measured the NIR spectrum of the material in the IBC. Therefore, every rotation captured a NIR spectrum.

Method

Obtaining fingerprint spectrum

The pure spectrum was obtained by placing approximately 50 g of each material on the Corona head and measuring the NIR spectrum. The NIR spectra of four random samples of magnesium stearate and six random samples of the granule were measured and the mean spectrum of each material was calculated to obtain a fingerprint spectrum. The fingerprint spectrum of magnesium stearate and the granule were superimposed.

The significant wavelengths for blend monitoring for the materials were obtained by examining the spectra in the second derivative. The software was used to highlight the peaks on the spectra (as seen in Figure 1). Preliminary blends were conducted using the wavelengths obtained from the software. The criteria used to choose the most suitable wavelengths was that the standard deviation of the absorbance at the wavelength representing the magnesium stearate and the granule should increase when the magnesium stearate was added to the blend and level off after a period of time. Following the preliminary blends using the wavelengths isolated by the software, 1213 nm was chosen to represent magnesium stearate and 1591 nm was chosen to represent the granule as highlighted in Figure 1.

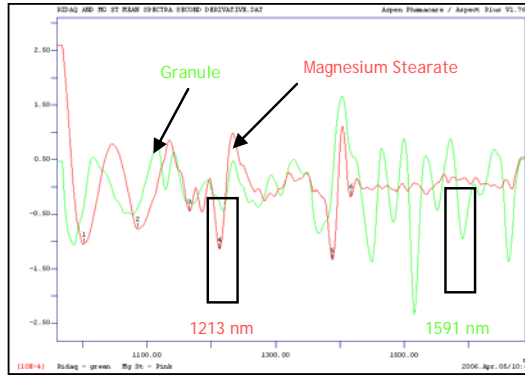


Figure 1 : Spectra of granule and magnesium stearate superimposed showing significant wavelengths

Following the determination of the significant wavelengths for blend monitoring, a method was created on the software to interpret the spectral data in terms of the rate of change in the blend. The second derivative was used for spectral pre-processing and the results were evaluated at the wavelengths of significance. The software was set to evaluate the standard deviation of the absorbance at the wavelengths of significance in a “moving block of eight” as outlined below.

Figure 2 shows a schematic of the variance calculation. Spectra are added to the block until eight spectra obtained (seen in block 1). Then for every spectrum that moves out of the block, one spectrum is added to the block (seen in block 2 and block 3). As the spectral difference decreases so too does the moving block difference. The standard deviation is calculated over the block and plotted over time to monitor the rate of change in the blend. With NIR spectra, once a process is complete, the spectra will not change, therefore the standard deviation will be small [6].

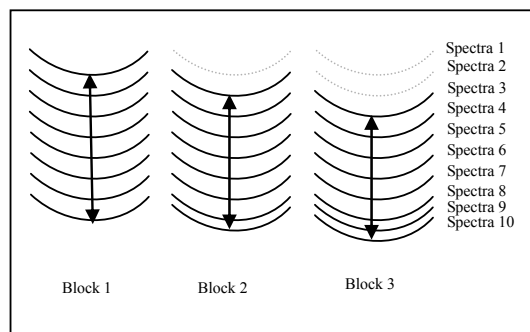


Figure 2: Moving block of eight variance calculation (adapted [6])

Spectral data from blends

During blending, spectral data were collected by the NIR probe during every rotation of the IBC. The IBC was set to rotate at 10 rotations per minute (rpm). The data were mathematically treated with the algorithms available on the software created during the method development. The blend was monitored by the standard deviation versus time plot that was generated. To confirm the prediction of end-point using NIR, the blends were sampled using a sample thief when the NIR spectrum showed no more change with respect to time at the wavelengths of significance (when a plateau level was reached) and at selected time intervals.

In order to determine the time intervals at which to sample, preliminary blends were conducted. A series of blends were run for approximately 20 minutes each. The standard deviation was plotted as a function of time and examined to identify three time intervals in the blend to predict three states namely before end-point, end-point and after end-point. The first time interval chosen was when the standard deviation had not levelled out and was high (depicting before end-point). The second time interval chosen was when the standard deviation was lower than the first time interval (depicting end-point) and the third time interval chosen was when the standard deviation maintained a low value for a longer period of time (depicting after end-point). Following these preliminary experiments the times for sampling as stated below were obtained.

The intervals for sampling of the granule blend were 1 minute and 30 seconds (before end-point), 6 minutes (at end-point) and 17 minutes (after end-point). The blends were carried out in triplicate at the predetermined time intervals. Five point samples were taken from the blender according to a sampling plan and were analysed using an atomic absorption (AA) spectroscopic method for magnesium stearate to ascertain the distribution of the magnesium stearate in the blend. One sample per point was taken due to the decreased capacity of the blender.

The standard deviation that predicted a uniform blend was obtained from the blends conducted to the selected time intervals. A further six blends were run and stopped when the standard deviation that predicted a uniform blend at the selected wavelengths was reached.

Blend preparation

Granule (3 kg) was loaded into the IBC. The IBC was rotated for 8 rotations. Thereafter the blender was stopped and 22.18 g of magnesium stearate was added to the granule. Care was taken to ensure that the magnesium stearate was evenly spread over the top of the granule. The IBC was then closed and blended for the predetermined time intervals. The blend was then sampled using a sample thief and the stated sampling plan.

Limits for AA results

A unit dose sample is 102.2 mg of which 0.75 mg is magnesium stearate. The United States Pharmacopoeial limit of content uniformity was used to calculate the acceptable limits for magnesium stearate [10]. The criteria for a uniform blend was a magnesium stearate assay of 0.6375 mg – 0.8625 mg and the relative standard deviation (RSD) less than or equal to 6.0 %.

RESULTS AND DISCUSSION

As the wavelength of significance for magnesium stearate was shown to be 1213 nm, the change in absorbance at this wavelength is presented. The standard deviation versus the number of rotations at the magnesium stearate wavelength for blends conducted for 1 minute and 30 seconds depicting before end-point can be seen in Figure 3.

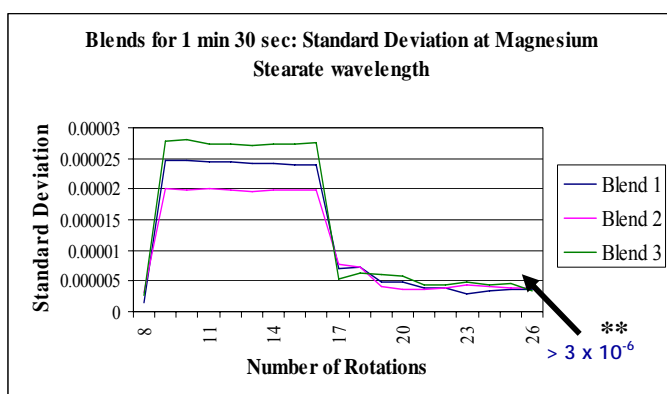


Figure 3: Standard deviation vs. number of rotations (before end-point) [** Standard deviation at the end of the blend]

An increase in the standard deviation was noted when magnesium stearate was added to the blend. At the end of the blend duration, the standard deviation was above 3×10^{-6} . The AA results revealed a non-uniform distribution of magnesium stearate.

Figure 4 reflects the blends carried out for 6 minutes, depicting end-point.

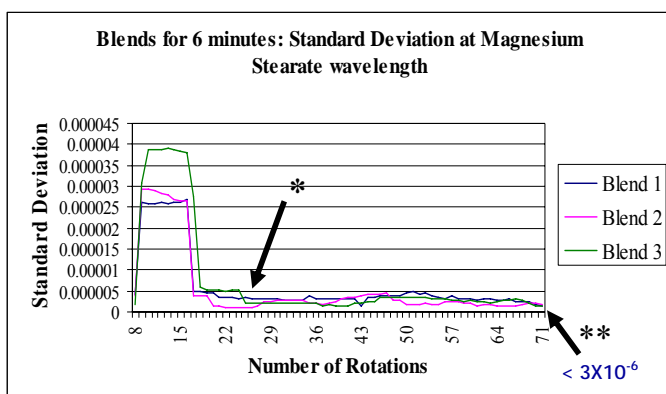


Figure 4: Standard deviation vs. number of rotations (end-point) [* Leveling out of the standard deviation, ** Standard deviation at the end of the blend]

A levelling out of the standard deviation could be seen at the 28th rotation. The standard deviation at the magnesium stearate wavelength was less than 3×10^{-6} at the end of the blend duration and the AA results revealed uniform distribution of magnesium stearate in the blend.

Figure 5 represents the blends conducted for 17 minutes depicting after end-point.

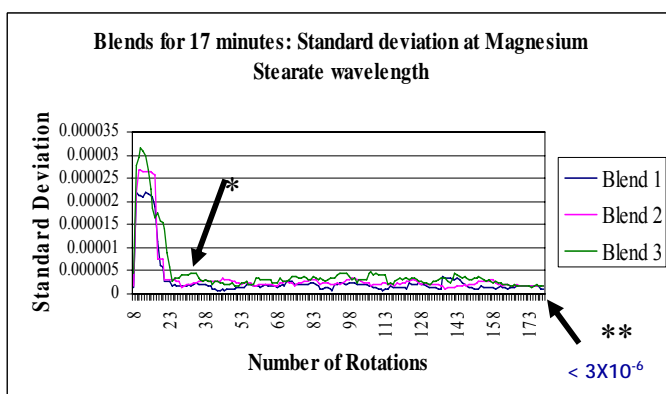


Figure 5: Standard deviation vs. number of rotations (after end-point) [* Leveling out of the standard deviation, ** Standard deviation at the end of the blend]

A leveling out of the standard deviation was noted at the 28th rotation. At the end of the blend duration, the standard deviation at the magnesium stearate wavelength was less than 3×10^{-6} . The AA results revealed uniform distribution of magnesium stearate in the blend.

Table 1 shows a summary of the relationship between the standard deviation and the uniformity of the blend for blends conducted to predetermined time intervals.

Table 1: Relationship between standard deviation and AA results of the blends.

Blend duration	Standard deviation	AA Results
Before end-point (1 min 30 sec)	$> 3 \times 10^{-6}$	Non-uniform
End-point (6 min)	$< 3 \times 10^{-6}$	Uniform blend
After end-point (17 min)	$< 3 \times 10^{-6}$	Uniform blend

The distribution of the magnesium stearate in the blends for 17 minutes and 6 minutes show a relationship, in that both sets of blends are uniform and the standard deviation of the absorbance was below 3×10^{-6} . It was noted that a decrease in blend time of 11 minutes still resulted in a uniform blend. The blends for 1 minute and 30 seconds had a higher standard deviation (greater than 3×10^{-6}) and the AA results revealed an uneven distribution of magnesium stearate.

Based on the blends conducted above, the criteria selected to predict a uniform blend in “real-time” was a standard deviation value below 3×10^{-6} at 1213 nm (wavelength for magnesium stearate) at four consecutive data points. Figure 6 shows the standard deviation versus number of rotations for six blends conducted to an end-point as predicted by NIR and Table 2 shows the AA results.

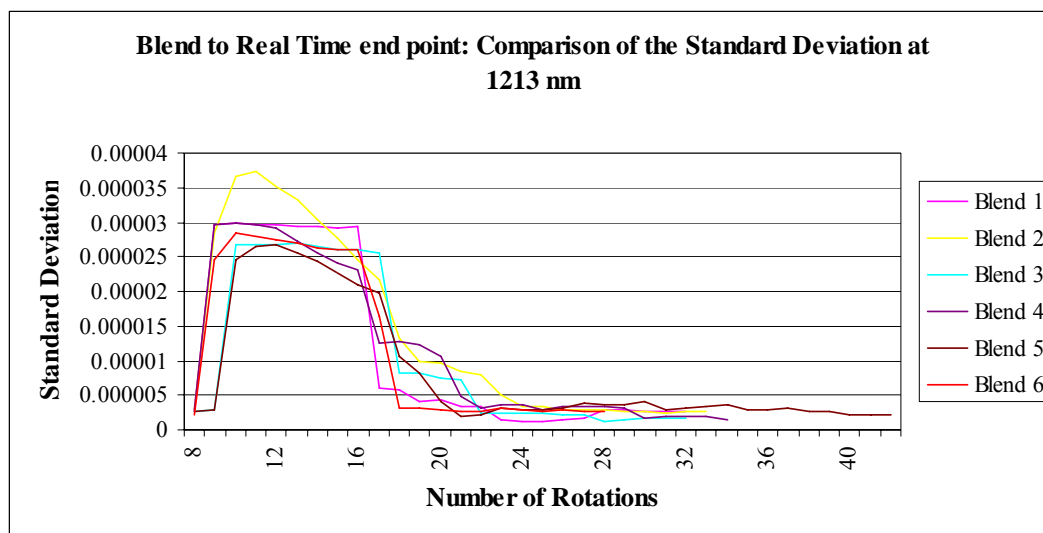


Figure 6: Blends conducted to end-point as predicted by NIR

Table 2: AA results for magnesium stearate per 102.2 mg sample mass (values shown in red represent out of specification results)

End-point	Blend 1	Blend 2	Blend 3	Blend 4	Blend 5	Blend 6
Actual Blend Time	3 min 18 sec	2 min 23 sec	2 min 10 sec	2 min 27 sec	3 min 9 sec	1 min 52 sec
Point 1	0.678 mg	0.781 mg	0.686 mg	0.655 mg	0.697 mg	0.630 mg
Point 2	0.701 mg	0.680 mg	0.706 mg	0.726 mg	0.675 mg	0.655 mg
Point 3	0.684 mg	0.743 mg	0.706 mg	0.744 mg	0.718 mg	0.649 mg
Point 4	0.717 mg	0.744 mg	0.697 mg	0.682 mg	0.710 mg	0.627 mg
Point 5	0.694 mg	0.715 mg	0.736 mg	0.706 mg	0.701 mg	0.687 mg
Mean	0.695 mg	0.732 mg	0.706 mg	0.703 mg	0.700 mg	0.650 mg
RSD	2.24 %	5.17 %	2.62 %	5.00 %	2.34 %	3.71 %

The results show that all blends were uniform with the exception of blend 6 where the amount of magnesium stearate was marginally out of specification. Blend 6 also represents the shortest blend duration. It was noted that the standard deviation at the 1591 nm (wavelength for granule monitoring) wavelength at the end of the blend was the highest for blend 6.

At present, the blend duration for this granule is set at 10 minutes, which was determined by standard validation techniques. With NIR, blend durations range from 2 min 10 sec to 3 min

18 sec. It was noted that the time durations are significantly lower than the standard blend durations.

CONCLUSION

A relationship exists between the uniformity of the blend and the standard deviation of the absorbance at the significant wavelength. Blends were found to be poorly blended when the standard deviation of the absorbance was high and well blended when the standard deviation of the absorbance was low. It is evident that more information regarding the uniformity of the blend could be obtained from the 1591 nm wavelength to aid an accurate prediction of endpoint using NIR. The standard deviation value selected should be on a product-by-product basis and optimised in conjunction with standard blend uniformity methods.

ACKNOWLEDGEMENT

The authors would like to thank Aspen Pharmacare for the supply of all materials and the sponsorship of equipment utilized for the study.

REFERENCES

1. Afnan, A.M. 2004. PAT: What's in a Name? *The Journal of Process Analytical Technology* [online], 1(1), pp. 8-9. Available: <http://www.patjournal.com/article.aspx?article=8> [Accessed: 6/07/2005].
2. Ciurczak, E. W. and Drennen III, J. K. 2002a. "Ch. 3: Blend uniformity Analysis", in *Pharmaceutical and medical applications of near infrared spectroscopy*, vol. 31, E. W. Ciurczak and J. K. Drennen III, eds., Marcel Dekker Inc, New York, pp. 33-54.
3. Ciurczak, E. W. 2006. Near infrared spectroscopy: Why is it still the number one technique in PAT? *The Journal of Process Analytical Technology*, vol. 3, no. 1, pp. 19-22.
4. El-Hagrasy, A. S., Morris, H. R., Damico, F., Lodder, R. A. and Drennen III, J. K. 2001. Near-infrared spectroscopy and imaging for the monitoring of powder blend homogeneity. *Journal of Pharmaceutical Sciences*, vol. 90, no. 9, pp. 1298-1307.

5. Gilbert, S. B. and Anderson, N. R. 1986. "Tablets", in *The theory and practice of industrial pharmacy*, 3rd edn., L. Lachman, H. A. Liberman and H. L. Kanig, eds., Lea and Febiger, Philadelphia
6. Hammond, S. 2005. *PAT strategies for identifying, measuring and controlling process risk: Process to measurement interface issues- Set up and remote triggering* [online]. Available: www.fda.com [Accessed: 20 September 2005].
7. Lantz, J. and Schwartz J.B. 1989. "Ch. 1: Mixing", in *Pharmaceutical Dosage Forms: Tablet*, 2nd edn., H.A. Liberman and J.B. Schwartz, eds., New York: Marcel Dekker Inc, pp 1-71.
8. Marshall, K. 1986. "Compression and consolidation of powdered solids", in *The theory and practice of industrial pharmacy*, 3rd edn., L. Lachman, H. A. Liberman and H. L. Kanig, eds., Lea & Febiger, Philadelphia, pp. 66-99.
9. Muzzio, F. J., Alexander, A., Goodridge, C., Shen, E. and Shinbrot, T. 2003. "Solids mixing", in *Handbook of industrial mixing: Science and practice*, E. L. Paul, V. Atiemo-Oheng and S. M. Kresta, eds., Wiley & Sons Inc., New York, pp. 906-907.
10. Pharmacopeial Forum. 2006. "Ch. 905: Uniformity of dosage forms", in *USP29-NF24*. USPC, Inc. Official.
11. United States Food and Drug Administration, United States Department of Health and Human Services, Centre for Drug Evaluation and Research, Centre for Veterinary Medicine and Office of Regulatory Affairs. 2004. Guidance for industry PAT: A Framework for Innovative Pharmaceutical Development, Manufacturing, and Quality Assurance. Available: <http://www.fda.gov/cder/guidance/index.htm>. [Accessed: 10/07/2005].